kOMUNIKÁCIE
COMMUNICATIONS

OPERATION AND ECONOMICS

MECHANICAL ENGINEERING

CIVIL ENGINEERING

KOMUNIKÁCIE
COMMUNICATIONS

SAFETY AND SECURITY ENGINEERING

Daria Gunina - Vladislav Bina - Michal Novak*

STRATEGIC ADVERTISING MANAGEMENT: THE CASE OF THE TRANSPORTATION AND STORAGE MARKET IN THE CZECH REPUBLIC

The aim of this study is to analyse the advertising strategy on the transportation and storage market in the Czech Republic. The study provides information and knowledge of seasonal advertising scheduling by answering three research questions. The statistical analysis is based on a research sample of 840,204 advertisements aired in 2013-2017. The results of the study show different scheduling patterns of subcategories in the transportation and storage market. They also point out that subcategories in the transportation and storage NACE category are different. Therefore, marketing researchers should take this knowledge into account in their generalisations.

Keywords: *commercials, mass media, communication strategy, transport*

1. Introduction

Strategic advertising management includes such activities as advertising planning, organising and decision-making for achieving the set strategic goals [1], [2], [3]. It attempts to solve the problem of how to effectively deliver the message to potential consumers through media [4]. Thus, the media plan should provide a clear schedule of what (product) to advertise, when (date, hour) and where (media type, medium). Media plan suitability can significantly influence advertising effectiveness as it can influence companies' brand image, brand attitude, sales, and other indicators of success such as company performance [5], [6]. Hence, the media plan is an important pillar of advertising success and this issue deserves more in-depth attention and should not be underestimated.

The motivation of this study is to contribute to the debate on marketing in the transport industry and to analyse advertising strategy on the transportation and storage market in the Czech Republic. As the transportation market provides services, so transport marketing differs from manufacturing marketing [7]. Companies on this market should deploy a marketing campaign to gain a competitive advantage, attract potential customers, and retain regular customers [8]. The transportation market targets many different consumer segments [8] according to their age, economic situation, and lifestyle.

This study focuses on different subcategories of the transportation and storage market as consumer behaviour [8] and advertising activity in subcategories may differ. The transportation and storage market in the Czech Republic is divided into subcategories: Air transport; Other post and courier services; Post and courier services; Land and pipeline transport; Land and personal transport; Road freight transport; Storage; Storage and subsidiary transport; Subsidiary transport activities; Inland shipping; Railroad transport; Sea and seashore shipping; Shipping; Pipeline transport. Different types of transport tend to compete. For example, with the rise of private cars, the demand for public transport decreases [9]. Such circumstances force the transportation market not only to optimise the supply [10] or search for non-traditional solutions [11] but also to study its consumers' behaviour [9], [12], [13], to promote its offer [8], [14], [15], to improve communication between consumers and service providers [16], [17], [18], and to be market-oriented [19]. For example, advertising (along with other marketing activities) in Perth (Scotland) helped public transport to increase the number of passengers [8].

Forms of media plans and general advertising activities differ depending on the industries or product categories [20]. In particular, these stem from the nature of the product. For example, low-involvement and high-involvement products require using different media types and diverse timing [2]. This is also related to different seasonality [21], [22]. Some products (e.g. groceries) tend to be bought at the end of a workweek; some products (e.g. gym membership) sell more at the beginning of a year [5]. Also, some products (e.g. flight tickets, shoes) have a higher demand in the middle of the month following payday. Advertising seasonal patterns precede the industry peak in one or two months to reach the consumer in time [2]. Seasonal patterns can also be found in dayparts as different shows in different daytimes can reach different audiences [5]. This is one the reasons why some advertisements tend to be aired in different dayparts. This all reveals the background for posing the following research questions regarding the transportation industry in order to find such patterns:

- RQ1: "Is there a seasonal component in the advertising activity (during the year) on the Czech transportation market?"
- RQ2: "Is there a correlation between the advertising activity of different categories of transportation and storage on the Czech market?"
- RQ3: "Is there a seasonal component in the advertising activity (during the day) on the Czech transportation market?"

* **Daria Gunina, Vladislav Bina, Michal Novak**
Faculty of Management, University of Economics in Prague, Jindrichuv Hradec, Czech Republic
E-mail: daria.gunina@vse.cz

Table 1 *Research sample: number of ads on TV, radio, and print in particular subcategories*

	2013	2014	2015	2016	2017
Air transport	41,035	31,732	45,647	45,963	45,603
Other post and courier services	677	10,244	2,975	5,055	2,114
Post and courier services	4,240	2,850	1,423	2,363	1,021
Land and pipeline transport	15	450	464	130	2,793
Land and personal transport	22,160	27,582	21,222	20,942	26,504
Road freight transport	2,136	3,833	8,118	4,852	5,559
Storage	24	5	21	14	113
Storage and subsidiary transport	521	558	734	1,730	1,817
Subsidiary transport activities	52,360	92,088	103,699	79,096	50,075
Inland shipping	837	584	1,347	896	928
Railroad transport	10,004	7,335	7,410	14,882	22,256
Sea and seashore shipping	14	287	53	25	17
Shipping	5	39	166	267	294
Pipeline transport	1	0	0	0	0

2. Research design and methodology

This research analyses the mass media market data for the Czech Republic obtained by media monitoring by the Nielsen Admosphere research agency in the NACE "Transportation and Storage" category. The research sample contains data on all advertising messages on television (174,503), radio (620,797), and print (44,904) in 2013-2017. The analysis does not include online media as the volumes of Internet advertising and investment in it are difficult to measure. The research is based primarily on quantitative quasi-experiment methods. The whole research sample contains 840,204 advertisements aired in the years 2013-2017. The research sample divided into NACE subcategories is shown in Table 1.

Since the data file contains data concerning all advertising messages on television, radio and print, it is sufficient to use the descriptive means of statistics. There is no straightforward possibility to generalise the results within the scope of the Czech Republic and the analysed timeframe. Therefore, it is not reasonable to employ means of mathematical statistics such as hypothesis testing or interval estimates.

The statistical software R 3.4.3 [23] was used for statistical analysis and the depiction of data. Various statistical methods were used for the data analysis. The methods used are introduced in the following text according to the research questions.

To answer the first research question (RQ1), the seasonal components of the monthly time series of the advertisement count in different categories are computed using the seasonal decomposition of the time series by LOESS smoothing [24] (a locally weighted polynomial regression). In this procedure, the seasonal values are removed and the remainder is smoothed to find the trend. The overall level is removed from the seasonal component and added to the trend component. This process is iterated a few times.

To answer the second research question (RQ2), the seasonal components calculated by the LOESS smoothing procedure are further analysed using a correlation matrix containing Pearson correlation coefficients. The graphical display approach of Murdoch and Chow [25] is used for the graphical representation.

To answer the third research question (RQ3), the time of advertisement broadcasting (hour-minute-second) was categorised into a daypart. Katz [5] defines nine dayparts for the American market. As the Czech media market differs from the American market, we defined the dayparts according to media habits in the Czech Republic using the following categories: Late night (23:00:00-00:59:59), Dead time (1:00:00-5:59:59), Early morning (6:00:00-8:59:59), Daytime (9:00:00-11:59:59), Early fringe (12:00:00-16:59:59), Evening (17:00:00-18:59:59) and Primetime (19:00:00-22:59:59). Since we are analysing the time of the day, we use only data concerning advertisements on TV and Radio. Therefore, the analysis is based on a two-dimensional contingency table of the counts of advertisements, in particular, the categories according to the categorised time of the day.

3. Findings and discussion

The findings are divided into three sections according to the formulated research questions.

3.1 RQ1 - Seasonal components in advertising activity (during the year)

Figure 1 shows the seasonal components of a monthly series of advertisement counts in 14 NACE categories. According to the visualised graphs, one can conclude that there are seasonal components in the advertising activity (during the year) on the Czech transportation market. It is evident that a substantial difference in the particular month counts exists in all the categories. A decrease can be frequently observed in the summer period or an increase during autumn - as in the subcategories Air transport, Post and courier services, and Land personal transport. Contrary to these observations, a rise can be observed in advertising activity during the summer in the subcategories

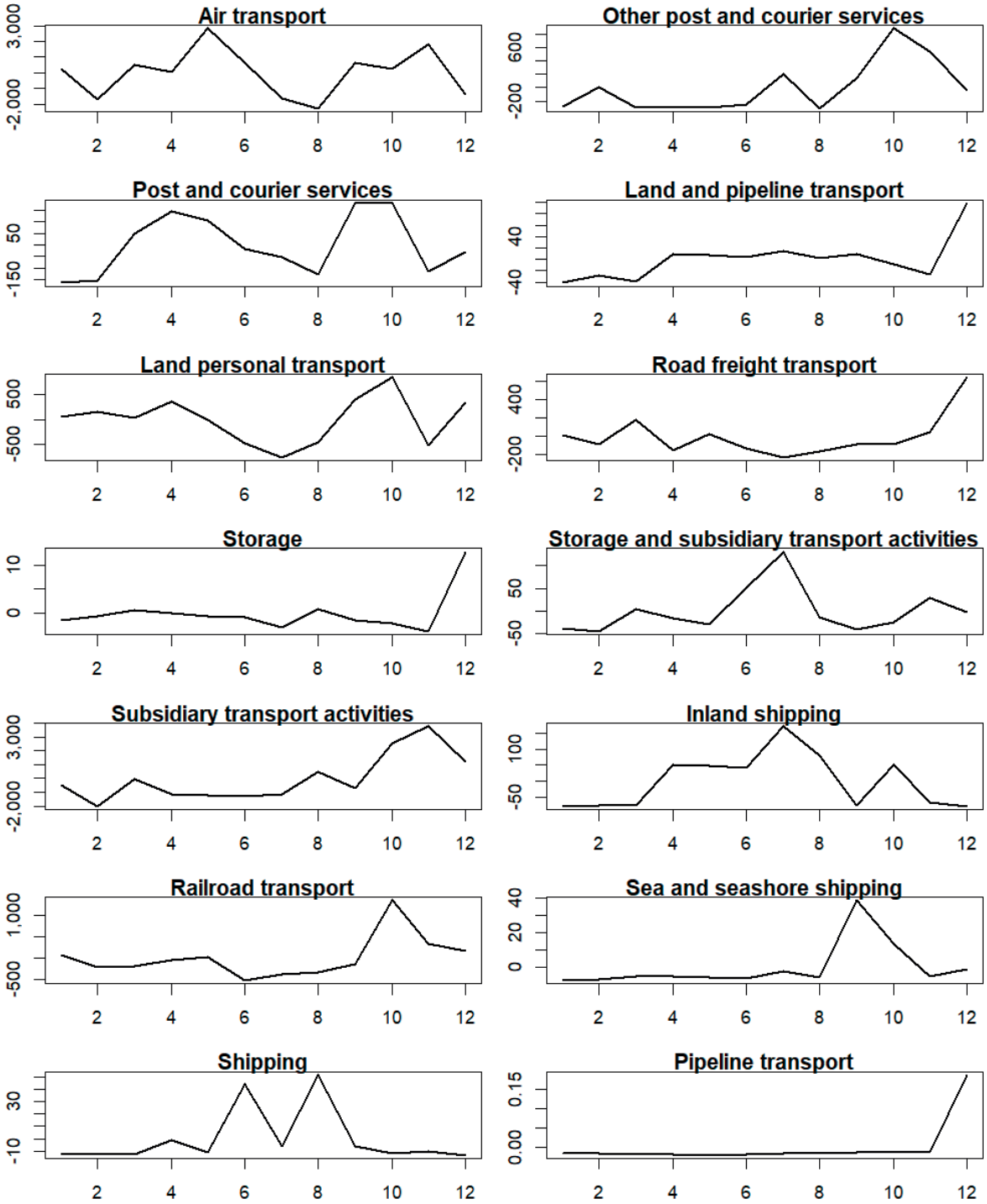

Figure 1 *Seasonal components of the monthly series of advertisement counts in different categories*

Shipping, Other post and courier services, Inland shipping and Storage and subsidiary transport activities. Some subcategories also have a strong seasonal component for a few months before the end of a year - e.g. Other post and courier services, Road freight transport, Storage, and Subsidiary transport activities. In terms of the transportation of people - Air transport, Land personal transport and Railroad transport, it can be observed that these three subcategories have different seasonal advertising trends.

3.2 RQ2 - Advertising activity of different transportation and storage categories

As can be seen in Figure 1, the advertising activity in some categories of transportation and storage branches show common patterns. Therefore, it is reasonable to conduct a correlation analysis to find which categories show related behaviour. This is in the correlation plot of the seasonal components of the monthly time series (Figure 2).

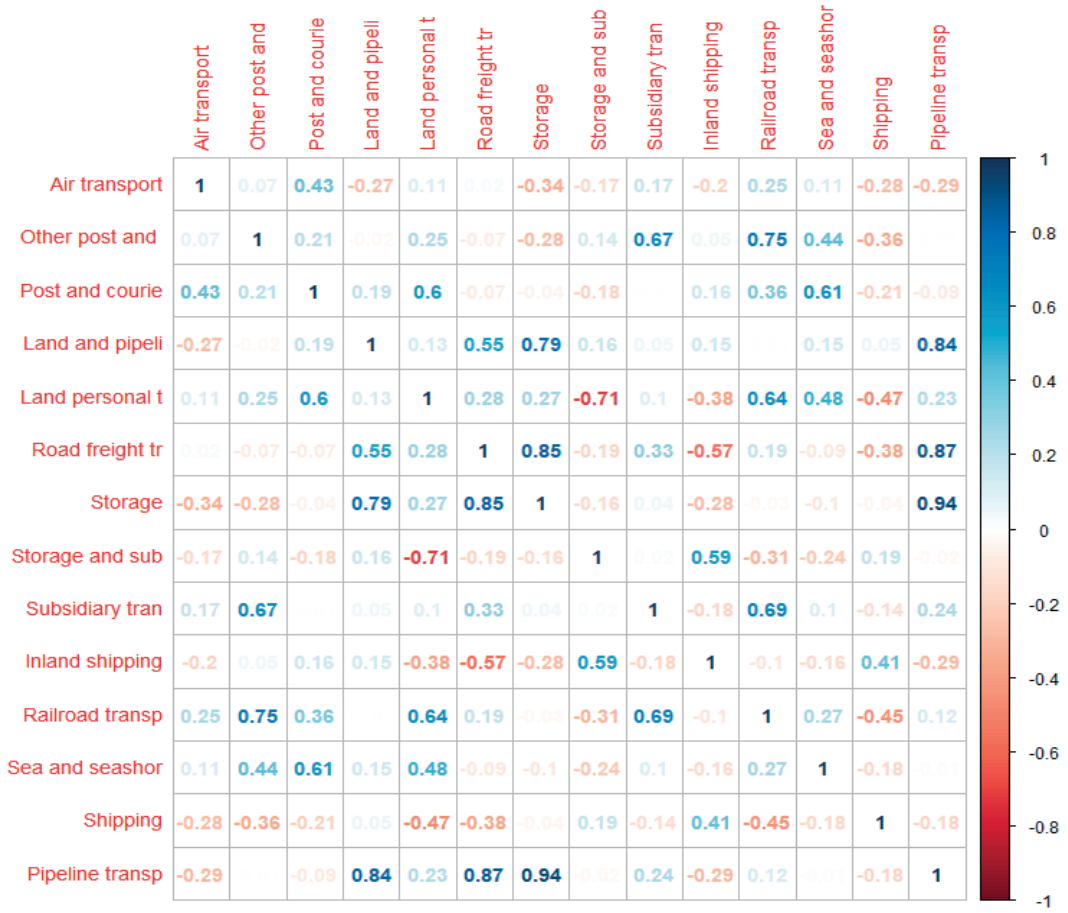

Figure 2 *Correlation plot of seasonal components of the monthly time series in the transport branches*

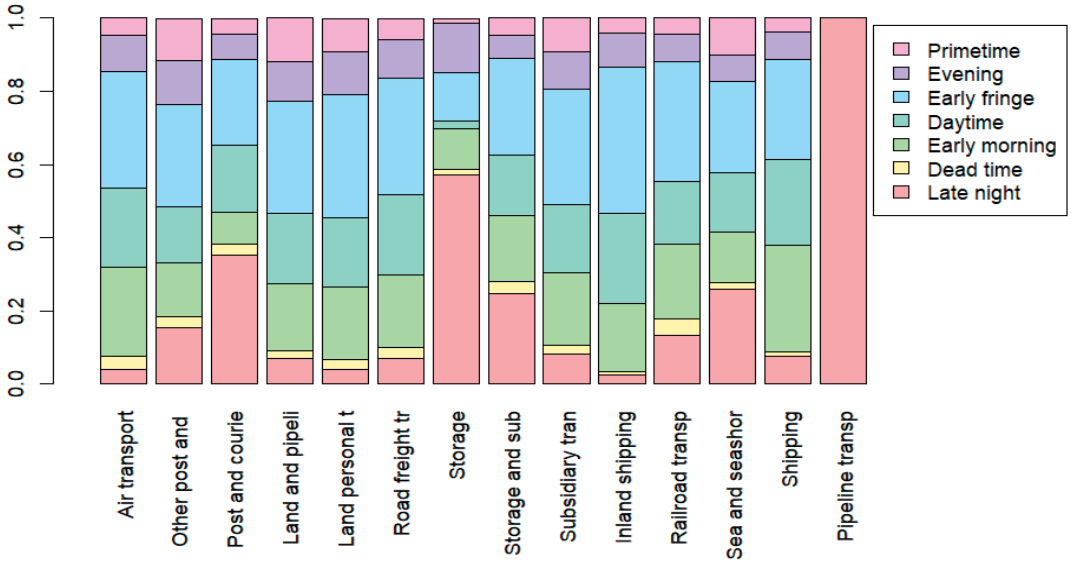

Figure 3 *Frequencies of advertisements in particular NACE categories during the day from Monday to Friday*

It can be observed that the Air transportation somehow has a unique seasonal component. It has a weak correlation (0.11) with the Land personal transportation and Railroad transportation (0.25). However, the correlation between the Land personal transportation and Railroad transportation has a stronger correlation (0.64). One can conclude that the air transport segment on the Czech market has a different seasonality than the railroad and land transportation segments.

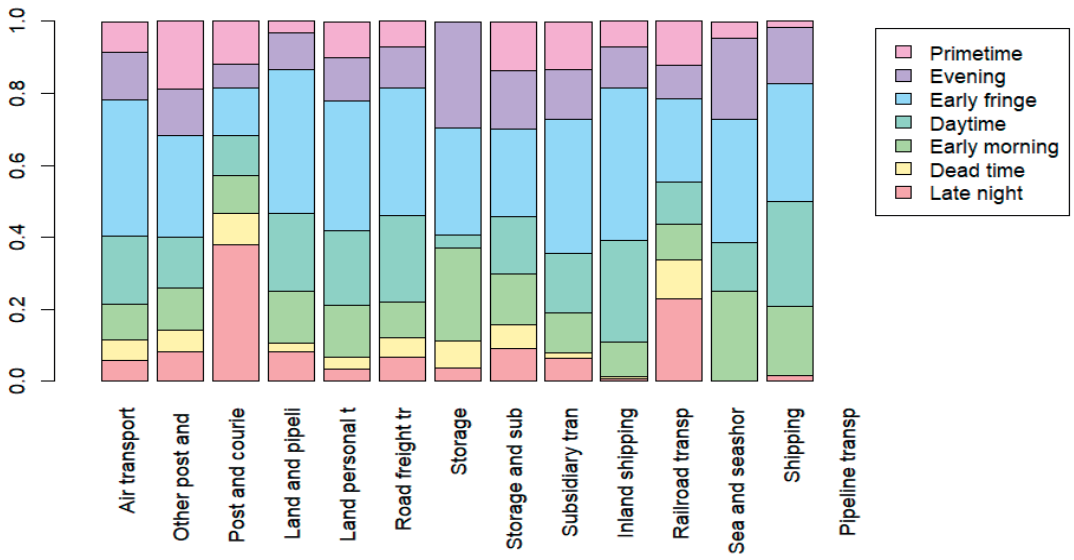

Figure 4 *Frequencies of advertisements in particular NACE categories during the day during the weekends*

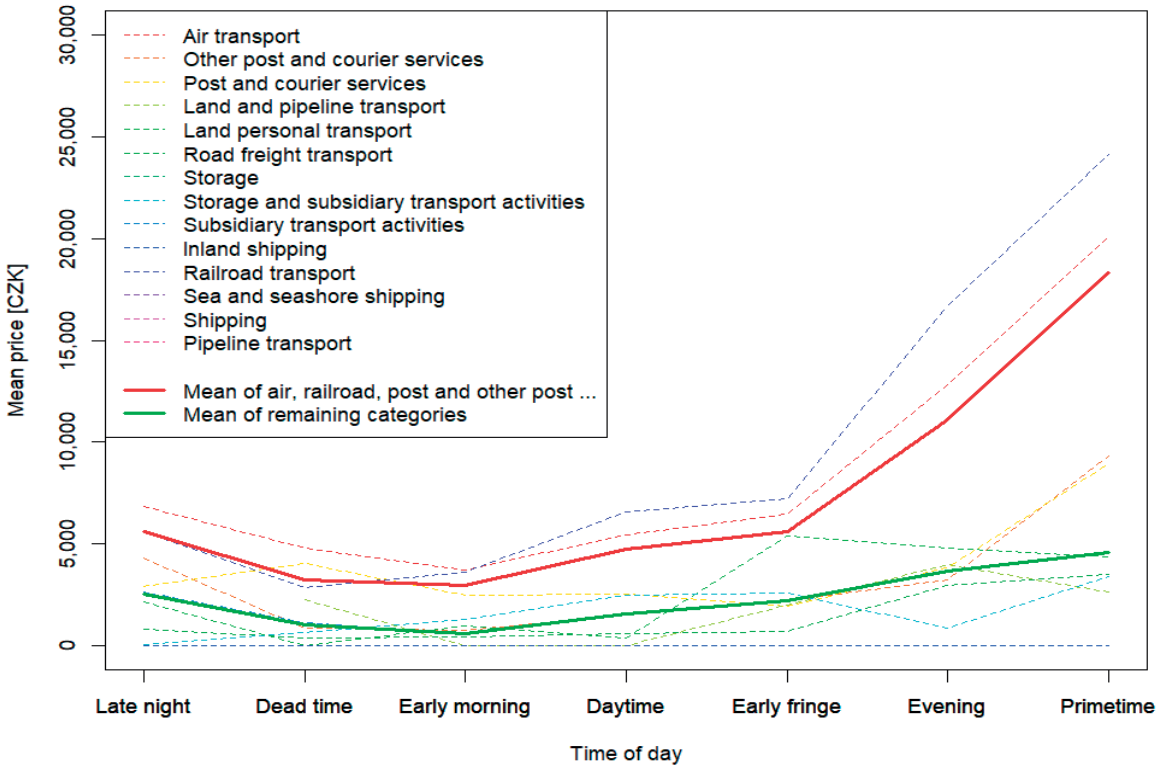

Figure 5 *Mean prices of TV advertisements during the daytime*

3.3 RQ3 - Seasonal components in advertising activity (during the day)

The frequency of appearance of advertisements on TV and radio during the day appears to be different for some subcategories. In Figure 3 and Figure 4, one can see that advertising during the daytime differs not only in particular subcategories but during the working days and weekends, as well. In terms of personal transportation, the Land personal transport uses more primetime advertising on weekdays than Air transport or Railroad transport. However, during the weekends it is the Railroad transport which uses most primetime in terms of personal transportation.

The strategy concerning advertising also substantially differs in different media. In Figure 5 and Figure 6, one can see different mean prices of advertisements during the daytime. It is quite understandable that the highest prices appear in the case of TV during the evening and in primetime, although there are categories for which this effect is stronger - namely those

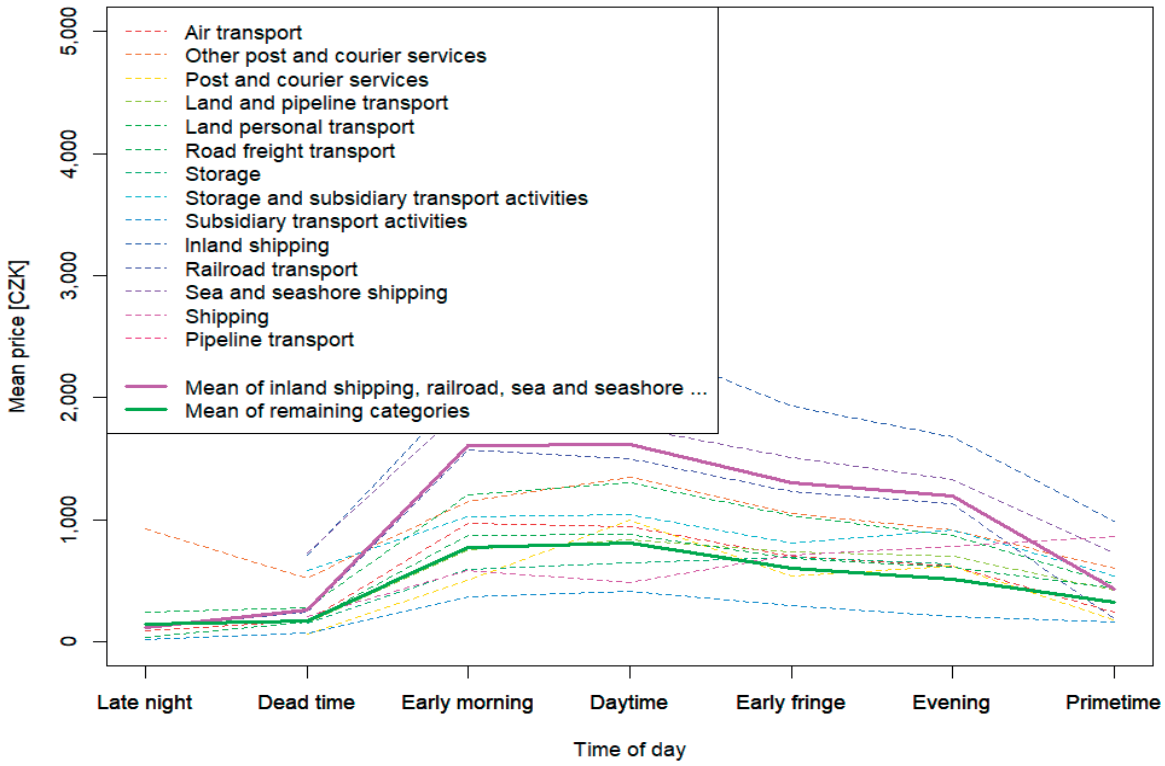

Figure 6 *Mean prices of radio advertisements during the daytime*

categories concerning air and railroad transport together with post and related services. On the contrary, in the case of the radio advertisements, a peak during the early morning and daytime (i.e., working hours) can be observed. Again, the peak is more substantial in the case of the shipping and railroad transport categories.

4. Conclusion

This study aimed to analyse advertising strategy on the transportation and storage market in the Czech Republic. The research sample was 840,204 advertisements aired in the Czech Republic in 2013-2017. Results show that particular NACE subcategories in the transportation and storage market evince a difference in advertising strategy. Naturally, different transportation types (i.e. NACE subcategories) compete with each other [8], [9], [19]. Nevertheless, on the advertising market, they appear to follow diverse goals, target different audiences, and deploy different advertising strategies. The analysis revealed the expected [5] advertising seasonality on the transportation and storage market either in months or parts of the day.

Such a conclusion contributes to the debate on marketing in the transport industry. The study also provides various managerial implications. It provides useful information and knowledge about seasonal advertising scheduling not only for media practitioners but also for managers in the transportation market. Ultimately, this study provides an overview of the transportation and storage market in the Czech Republic and emphasises the role of advertising competition in subcategories. The recommendation for advertisers is to monitor the competitors advertising strategy only in a particular subcategory rather than the entire transportation market.

This study has several research limitations. It analyses only one industry (transportation) and generalisations on other industries cannot be made. In addition, the study focused only on traditional media types: the research sample consists only of commercials in the TV, radio and print media. The Internet as a decentralised medium is not taken into account. In this case, non-studied new and alternative media provide a gap for further research extension.

Moreover, possible delays in reactions between variables are not considered. This presents significant opportunities for further research. The study could be extended by comparing different industries on the first NACE level or by comparing the results from the Czech Republic with those of different countries.

Acknowledgements

This study was supported by the Internal Grant Agency project of the University of Economics, Prague IGS F6/01/2018.

References

[1] ARENS, W. F., BOVEE, C. L.: Contemporary Advertising. McGraw-Hill Education, 1994.

[2] PERCY, L., ROSENBAUM-ELLIOTT, R.: Strategic Advertising Management, 5th ed. Oxford University Press, 2016.

[3] GOLOB, U., PODNAR, K.: Advertising Decision Makers' and Consumers' Perceptions of Media Substitutability. Journal of Promotion Management, 21(6), 798-816, 2015. https://doi.org/10.1080/10496491.2015.1088923

[4] AAKER, D. A., MYERS, J. G., BATRA, R.: Advertising Management. Englewood Cliffs, N.J Prentice Hall, 1992.

[5] KATZ, H.: The Media Handbook: A Complete Guide to Advertising Media Selection, Planning, Research, and Buying, 6th ed. New York: Taylor & Francis, 2017.

[6] TELLIS, G. J.: Effective Advertising: Understanding When, How, and Why Advertising Works. SAGE Publications, Marketing for a New Century, 2003.

[7] KRIZANOVA, A., HRIVNAK, M.: Supply in Marketing Process of Road Transport. Communications - Scientific Letters of the University of Zilina, 7(2), 13-16, 2005.

[8] IBRAEVA, A., DE SOUSA, J. F.: Marketing of Public Transport and Public Transport Information Provision. Procedia-Social and Behavioral Sciences, 162, 121-128, 2014. https://doi.org/10.1016/j.sbspro.2014.12.192

[9] KAMPF, R., LIZBETIN, J., LIZBETINOVA, L.: Requirements of a Transport System User. Communications - Scientific Letters of the University of Zilina, 14(4), 106-108, 2012.

[10] CERNY, J., CERNA, A., LINDA, B.: Support of Decision-Making on Economic and Social Sustainability of Public Transport. Transport, 29(1), 59-68, 2014. https://doi.org/10.3846/16484142.2014.897645

[11] CERNA, A., CERNY, J.: A Note to Non-Traditional Systems of Public Transport. Communications - Scientific Letters of the University of Zilina, 7(1), 64-66, 2006.

[12] CANTWELL, M., CAULFIELD, B., O'MAHONY, M.: Examining the Factors that Impact Public Transport Commuting Satisfaction. Journal of Public Transportation, 12(2), 1-21, 2009. http://doi.org/10.5038/2375-0901.12.2.1

[13] URBANEK, A.: Big Data - A Challenge for Urban Transport Managers. Communications - Scientific Letters of the University of Zilina, 19(2), 36-42, 2017.

[14] FRAMPTON, N.: Changing the Image of Public Transport through Marketing. Logistics & Transport Focus, 9(8), 15-18, 2007.

[15] KLEMENTSCHITZ, R., ROIDER, O.: Active Measures as Part of Dialogue Marketing Promoting the Use of Public Transport in Rural Areas. Transport Problems: An International Scientific Journal, 10(4), 57-74, 2015. http://doi.org/10.21307/tp-2015-048

[16] DRDLA, P., HRABACEK, J.: Website Contents of Municipal Transport Undertaking as a Modern Communication Tool for Enhancing Quality of Transport Services. Communications - Scientific Letters of the University of Zilina, 7(2), 46-48, 2005.

[17] MCGOVERN, E.: Transport Behavior: A Role for Social Marketing. Journal of Nonprofit & Public Sector Marketing, 17(1-2), 121-134, 2007. https://doi.org/10.1300/J054v17n01_06

[18] PENDER, B., CURRIE, G., DELBOSC, A., SHIWAKOTI, N.: Social Media Use during Unplanned Transit Network Disruptions: a Review of Literature. Transport Reviews, 34(4), 501-521, 2014. https://doi.org/10.1080/01441647.2014.915442

[19] MOLANDER, S., FELLESSON, M., FRIMAN, M., SKÅLEN, P.: Market Orientation in Public Transport Research - A Review. Transport Reviews, 32(2), 155-180, 2012. https://doi.org/10.1080/01441647.2011.633248

[20] GUNINA, D., KINCL, T., SULDOVA, S.: Usage of Colors in TV Commercials: Cross-Industry Analysis of Mass Media Communications. Communications - Scientific Letters of the University of Zilina, 19(4), 64-71, 2017.

[21] GENESOVE, D., SIMHON, A.: Seasonality and the Effect of Advertising on Price. The Journal of Industrial Economics, 63(1), 199-222, 2015. https://doi.org/10.1111/joie.12067

[22] KIYGI-CALLI, M., WEVERBERGH, M., FRANSES, P. H.: Modeling Intra-Seasonal Heterogeneity in Hourly Advertising-Response Models: Do Forecasts Improve? International Journal of Forecasting, 33(1), 90-101, 2017. https://doi.org/10.1016/j.ijforecast.2016.06.005

[23] R CORE TEAM: R: A Language and Environment for Statistical Computing [online]. R Foundation for Statistical Computing, 2017. Available: https://www.r-project.org/ [accessed 2018-05-26].

[24] CLEVELAND, W. S., DEVLIN, S. J.: Locally Weighted Regression: An Approach to Regression Analysis by Local Fitting. Journal of the American Statistical Association, 83(403), 596-610, 1988. https://doi.org/10.1080/01621459.1988.10478639

[25] MURDOCH, D. J., CHOW, E. D.: A Graphical Display of Large Correlation Matrices. The American Statistician, 50(2), 178-180, 1996. https://doi.org/10.1080/00031305.1996.10474371

Marjan Sternad - Tomas Skrucany - Borut Jereb*

INTERNATIONAL LOGISTICS PERFORMANCE BASED ON THE DEA ANALYSIS

Logistics is a very important service, which can influence the international trade. However, the rates in the development of international activities vary by country. In developing countries, the share of the logistics services is increasing, while the share of manufacturing activities, especially those with the lower added value, is declining due to the relocation of production to other countries. In order to achieve competitive advantages in the logistics sector, the development of logistics services with the higher added value is required. The effectiveness of logistics processes is very important for international competitiveness. In the paper, is presented the literature review on logistics performance. After presenting relevant research, the effectiveness of logistics is compared using the logistics performance index based on the Data Envelopment Analysis (DEA). The DEA analysis is a benchmarking technique which is useful for a multi-criteria comparison. Values of the international logistics performance index for 2016, for selected European countries, were used for the input and output variables of the DEA model. European countries rank high in the international comparison of the logistics performance index. In the paper, it was found out that the compared countries are competitive in international business, but not all the countries are considered as efficient. Germany achieves the highest points in the international comparison of the LPI but, does not achieve efficiency. We also found out that Austria, Serbia, Russian Federation and Bosnia and Herzegovina were efficient, while other compared countries did not.

Keywords: *international logistics performance, logistics performance index, DEA analyses, logistics efficiency*

1. Introduction

In a globalizing economy, countries and companies are competing in the international environment. For an economy such as the Slovenian economy, openness and the ability to integrate into international business are the most important factors. By participating in markets, the country becomes well known and improves its international position. Competition in the international trade has become one of the very important factors of the state economy, which is reflected in the export efficiency and import profile [1].

Different authors suggest the primary forms of measurement for capturing the performance of transformational processes [2], [3], [4]:

- utilization (spending metrics, financial and nonfinancial performance, inventory measures),
- productivity (total factor productivity and financial productivity measures),
- effectiveness (quality of the process output by comparing the actual output to the standards).

The effectiveness of logistics processes is very important for international competitiveness. Logistics is a part of the supply chain that plans, introduces and manages an efficient storage of goods, services and relevant information from their sources to their use, in order to cater for the requirements of buyers and sellers [5]. The meeting customer needs is one of the most important characteristics of the logistics process. Efficiency of this act is evaluated by the customer satisfaction. Stopka describes different methods [6]. The analysis of movements of goods in space and time has recently become increasingly important. Nowadays, there is an increasing demand for full tracking of the complete physical flow of goods; in other words, monitoring the flow of goods in time and space. New computational technologies and hardware are used for measuring, evaluating and customer information. Kubasakova and Krajcovic studied some of these technologies [7], [8]. According to Gnap, logistics is very important service, which can influence the international trade and the national GDP [9]. However, the rates in the development of international activities vary by country. In developing countries, the share of the logistics services is increasing, while the share of manufacturing activities, especially those with the lower added value, is declining due to the relocation of production to other countries. In order to achieve the competitive advantages in the logistics sector, development of logistics services with the higher added value is required. Javalgi and Martin [10] emphasize the importance of the logistics services in the international economy, as the internationalization of services affects the competitiveness of companies and increases comparative advantages of individual countries. Saez et al. [11] note that services also logistics are a source of diversification of exports of each country. Services with the higher added value, which include logistics services, are at the forefront. Even in a broader view, transport services can often be seen as a primary tool in the improvement of the value chain of traded goods, not only services [1]. Winsted and Patterson [12] warn about legislative restrictions, international competition, knowledge and resource constraints in terms of infrastructure and superstructure when considering exports of services.

* **[1]Marjan Sternad, [2]Tomas Skrucany, [1]Borut Jereb**
[1]Faculty of Logistics, University of Maribor, Slovenia
[2]Faculty of Operation and Economics of Transport and Communications, University of Zilina, Slovakia
E-mail: tomas.skrucany@fpedas.uniza.sk

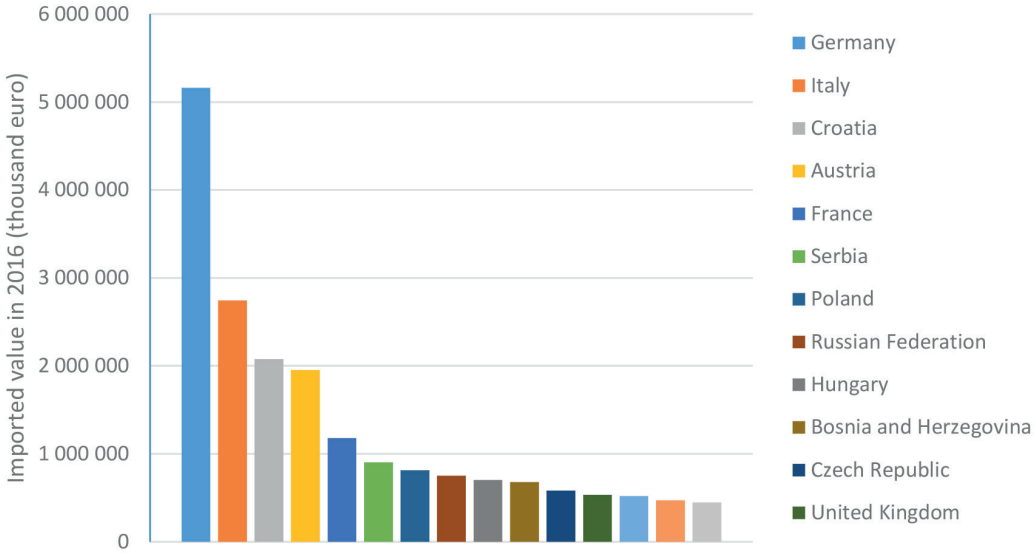

Figure 1 *The most important trading partners [1]*

Many authors compare the effectiveness of logistics by using different methods. Sternad et al. [13] compare the import and export efficiency of transport services by using a modified RCA (revealed comparative advantages) index, which then focuses only on services and it does not take into account the total exports of each country. They found that Slovenia has achieved a comparative advantage measured by the RCA index. In order to preserve its strength in the transport sector, it will be necessary to increase the added value of transport services along with the services that enhance the value of the transport process in the future.

Hilmola [14] compared the efficiency of transport chains by using a data envelopment analysis (DEA). He found out that the DEA analysis is an appropriate method for analyzing the transport chains. Petrovic et al. [15] used the DEA approach for a cross-country evaluation of rail freight transport. The authors (ibd.) recognized the DEA as a method of great potential for measuring the efficiency of the logistics sector. Marti et al. [16] used the DEA approach to compare logistics performance index for different countries. The authors used the input-oriented DEA efficiency model. They found out that the logistics performance depends largely on the income and geographical area.

Effectiveness of logistics using the logistics performance index based on the DEA analysis is compared in this paper. The logistics performance index (LPI) is a benchmarking tool created to help countries to identify the challenges and opportunities they face in their performance in trade logistics and what they can do to improve their performance [17]. Data for international LPI, which provide qualitative evaluations of the country in six areas by its trading partners, were used in this paper.

The DEA analysis is a benchmarking technique, which is useful for a multi-criteria comparison. For each individual observation with an objective of calculating, the DEA optimizes a discrete piecewise frontier determined by a set of Pareto-efficient decision-making units [18].

Based on the presented issues, the following research question was answered:

RQ: Are the top performer countries based on international LPI also effective?

2. Methodology

The international logistics performance by using a Data Envelopment Analysis (DEA), which is a linear mathematical programming approach that evaluates the efficiency of homogeneous decision-making units (DMUs), was analyzed. Efficiency is the ratio between the outputs produced and the number of inputs used. DEA optimizes the performance measure of each DMU [18]. The DMUs that are not on the efficiency frontier are inefficient. An inefficient unit must reach the efficiency frontier in order to become efficient. There are three options to become efficient [19]:

- by reduction of the inputs with constant outputs (input-oriented approach),
- by increasing the outputs with constant inputs (output-oriented approach),
- to increase outputs and reduce the inputs.

Based on characteristics of the DMUs and relevant research [16], the logistics performance is going to be based on a CCR (Charnes, Cooper and Rhodes model) input-oriented model with constant return to scale (CRS). The mathematical programming problem for the CCR input-oriented is [18]:

$$\max \frac{\sum_r u_r y_{ro}}{\sum_i v_i x_{io}} \tag{1}$$

$$\frac{\sum_r u_r y_{rj}}{\sum_i v_i x_{io}} \leq 1, \; for \; j = 0, 1, \ldots, n \tag{2}$$

$$\frac{u_r}{\sum_i v_i x_{io}} \geq \varepsilon, \; for \; r = 1, \ldots, s \tag{3}$$

$$\frac{v_i}{\sum_i v_i x_{io}} \geq \varepsilon, \; for \; r = 1, \ldots, m \tag{4}$$

where:

- x and y are the input and output vectors,
- v and u are the input and output weights.

Table 1 *Descriptive statistics of logistics performance components*

Components	Mean	Median	Max.	Country	Min.	Country	Standard Deviation
Inputs							
X_1 Customs	3.33	3.37	4.12	Germany	2.01	Russian Federation	0.61
X_2 Infrastructure	3.50	3.42	4.44	Germany	2.43	Russian Federation	0.66
X_3 International shipments	3.37	3.54	3.94	Netherlands	2.28	Bosnia and Herzegovina	0.52
Outputs							
Y_1 Logistics competence	3.53	3.52	4.28	Germany	2.52	Bosnia and Herzegovina	0.56
Y_2 Tracking & tracing	3.59	3.65	4.36	Austria	2.56	Bosnia and Herzegovina	0.60
Y_3 Timeliness	3.86	3.91	4.45	Germany	2.94	Bosnia and Herzegovina	0.49

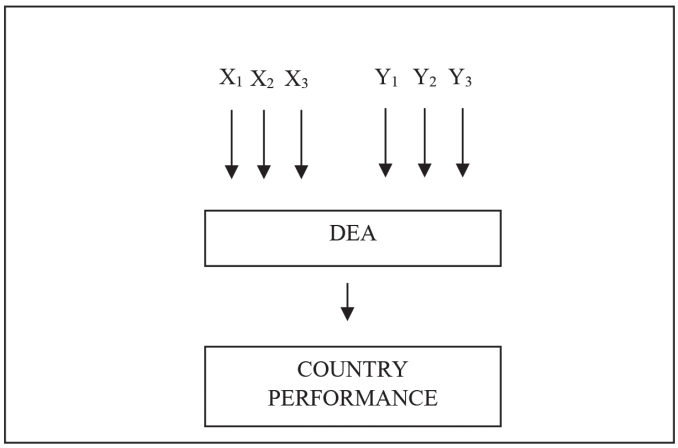

Figure 2 *The research model*

For the input and output variables of the model, values of the international logistics performance index for 2016 [20] for Slovenia and the ten most important trading partners by the value of import from Slovenia (see Figure 1), were used [1].

The international logistics performance index provides qualitative evaluations of a country in six areas by its trading partners. The six core components are [17]: the efficiency of customs and border clearance, the quality of trade and transport infrastructure, the ease of arranging competitively priced shipments, the competence and quality of logistics services, the ability to track and trace consignments and the frequency with which shipments reach consignees within scheduled or expected delivery times. Table 1 presents the descriptive statistics of logistics performance components.

Data were analysed by using the Open Source DEA software [19]. Figure 2 presents the research model.

3. Results

The efficiency of the logistics sector is becoming an increasingly important factor for competitive success in international business [21]. The largest logistics market in the EU is Germany [22]. Slovenia is affiliated with Germany through the international trade, and it is important that Slovenia works more effectively on the logistics market. Slovenia reaches higher LPI than Croatia, Serbia, Russian Federation and Bosnia and Herzegovina, but far behind Germany, Austria and France [17].

Table 2 shows the results of the DEA analysis for the CCR input-oriented model. The ratio between the outputs produced and the number of inputs used presents efficiency. Austria, Serbia, Russian Federation and Bosnia and Herzegovina received score 1 and they are considered as efficient. Other countries are inefficient. Hungary gets the lowest score.

The slacks exist only for those countries, which are identified as inefficient. The slacks present only the leftover portions of inefficiencies and they are needed to push the DMU to the frontier. Table 3 presents the results of slacks for the inefficient countries. Slovenia cannot reduce any inputs but it must augment logistics competence and timeliness. Italy represents the same case. Similarly, Slovakia must augment logistics competence and tracking. Germany and France have the very good quality of trade and transport infrastructure. They can reduce these inputs and they can also augment the timeliness. Hungary must improve the competence and quality of logistics services. Croatia, Poland and Czech Republic can reduce the efficiency of customs and border clearance or augment the timeliness if they want to be efficient.

Efficiency targets for inputs and outputs are presented in Table 4. Targets are the results of respective slack values added to proportional reduction amounts. To calculate the target values for an input, the input value is multiplied with an optimal efficiency score [18]. Projection describes the path of inefficient DMUs towards the efficient frontier. The target values for efficient countries are equivalent to their original input and output values.

Comparison between international LPI and efficiency for compared countries (Table 5) shows that the country which is

Table 2 *Results of CCR input-oriented model solution*

DMUs	Value	Efficient
Slovenia	0.950	
Germany	0.997	
Italy	0.947	
Croatia	0.950	
Austria	1	Yes
France	0.976	
Serbia	1	Yes
Poland	0.951	
Russian Federation	1	Yes
Hungary	0.906	
Bosnia and Herzegovina	1	Yes
Czech Republic	0.975	
United Kingdom	0.971	
Unites States of America	1	Yes
Slovakia	0.907	
Netherlands	0.960	

Table 3 *Input and output slacks*

DMUs	Customs	Infrastructure	International shipments	Logistics competence	Tracking & tracing	Timeliness
Slovenia	0.000	0.000	0.000	0.030	0.000	0.037
Germany	0.552	0.331	0.000	0.000	0.000	0.263
Italy	0.000	0.000	0.000	0.010	0.000	0.028
Croatia	0.384	0.000	0.050	0.000	0.000	0.293
Austria	0.000	0.000	0.000	0.000	0.000	0.000
France	0.108	0.000	0.000	0.000	0.000	0.000
Serbia	0.000	0.000	0.000	0.000	0.000	0.000
Poland	0.224	0.000	0.125	0.000	0.000	0.110
Russian Federation	0.000	0.000	0.000	0.000	0.000	0.000
Hungary	0.000	0.000	0.000	0.114	0.000	0.000
Bosnia and Herzegovina	0.000	0.000	0.000	0.000	0.000	0.000
Czech Republic	0.201	0.000	0.099	0.019	0.000	0.308
United Kingdom	0.313	0.073	0.000	0.000	0.000	0.055
Unites States of America	0.000	0.000	0.000	0.000	0.000	0.000
Slovakia	0.065	0.000	0.000	0.175	0.303	0.000
Netherlands	0.537	0.146	0.000	0.000	0.000	0.270

a top performer in logistics (Germany) is not efficient. Germany has a good quality of trade and transport related infrastructure, but it must improve timeliness in terms of infrastructure quality. European countries with the higher LPI ranking have a similar problem (Netherlands and France).

4. Conclusion

Logistics is becoming the most important factor in achieving competitive advantages in international business. Smaller economies than Slovenia depend on competitiveness in the international environment, so they need to improve their processes in international trade. The quality of logistics processes depends on various factors.

In this paper, the effectiveness of logistics processes was analyzed using the DEA analysis, which makes it possible to compare performance across countries. As the input data, were used the logistics performance index for 2016: the efficiency of the clearance process, the quality of trade and transport related infrastructure and assessment of the simplicity of arranging competitive price pricing. Output data of the DEA model are

Table 4 *Projections*

DMUs	Customs	Infrastructure	International shipments	Logistics competence	Tracking & tracing	Timeliness
Slovenia	2.736	3.030	2.945	3.230	3.270	3.507
Germany	3.554	4.094	3.842	4.280	4.270	4.713
Italy	3.267	3.589	3.456	3.780	3.860	4.058
Croatia	2.532	2.840	2.913	3.210	3.160	3.683
Austria	3.790	4.080	3.850	4.180	4.360	4.370
France	3.513	3.914	3.552	3.920	4.020	4.250
Serbia	2.500	2.490	2.630	2.790	2.920	3.230
Poland	2.886	3.015	3.146	3.390	3.360	3.910
Russian Federation	2.010	2.430	2.450	2.760	2.620	3.150
Hungary	2.739	3.114	3.120	3.451	3.400	3.880
Bosnia and Herzegovina	2.690	2.610	2.280	2.520	2.560	2.940
Czech Republic	3.288	3.275	3.459	3.669	3.840	4.218
United Kingdom	3.551	4.015	3.661	4.050	4.130	4.385
Unites States of America	3.750	4.150	3.650	4.010	4.200	4.250
Slovakia	2.908	2.937	3.091	3.295	3.423	3.810
Netherlands	3.419	3.974	3.784	4.220	4.170	4.680

Table 5 *Comparison between international LPI and efficiency*

DMUs	Rank International LPI	Efficient
Slovenia	50	
Germany	1	
Italy	21	
Croatia	51	
Austria	7	Yes
France	16	
Serbia	76	Yes
Poland	33	
Russian Federation	99	Yes
Hungary	31	
Bosnia and Herzegovina	97	Yes
Czech Republic	26	
United Kingdom	8	
Unites States of America	10	Yes
Slovakia	41	
Netherlands	4	

competence and quality of logistics services, the ability to track and trace consignments and timeliness. For the comparative analysis, the efficiency of Slovenia was compared to the ten most important trading partners by the value of import from Slovenia.

Within the international comparison, Slovenia is not efficient regarding logistics. Slovenia cannot reduce any inputs but it must augment logistics competence and timeliness.

In this paper, it was also found out that Austria, Serbia, Russian Federation and Bosnia and Herzegovina were efficient, while other compared countries were not. Germany and France are ineffective due to the good quality trade and transport infrastructure, as they need to improve timeliness.

The logistics market is developing rapidly in the European Union. European countries rank high in the international comparison of the logistics performance index. Compared countries are competitive in international business, but not all the countries are considered as efficient. Germany achieves the highest points in the international comparison of the LPI but it does not achieve efficiency, as often high investments in the logistics sector are visible only in a few years. The economy cannot often follow the rapid technological changes in logistics.

References

[1] ITC: International Trade Centre [online]. Available: http://www.intracen.org/.

[2] MCKINNON, A. C.: Benchmarking Road Freight Transport: Review of a Government-Sponsored Programme. Benchmarking: An International Journal, 16(5), 640-656, 2009. https://doi.org/10.1108/14635770910987850

[3] GUNASEKARAN, A., PATEL, C., TIRTIROGLU, E.: Performance Measures and Metrics in a Supply Chain Environment. International Journal of Operations & Production Management, 21(½), 71-87, 2001. https://doi.org/10.1108/01443570110358468

[4] CAPLICE, C., SHEFFI, Y.: A Review and Evaluation of Logistics Metrics. The International Journal of Logistics Management, 5(2), 11-28, 1994.

[5] Council of Logistics Management [online]. Available: https://cscmp.org/ [accessed 2018-04-02].

[6] STOPKA, O., CERNA, L., ZITRICKY, V.P.: Methodology for Measuring the Customer Satisfaction with the Logistics Services. Nase More/Our Sea, 63(3), 189-194, 2016. https://doi.org/10.17818/NM/2016/Sl21

[7] KUBASAKOVA, I., KAMPF, R., STOPKA, O: Logistics Information and Communication Technology. Communications - Scientific Letters of the University of Zilina, 16(2), 9-13, 2014.

[8] KRAJCOVIC, M., STEFANIK, A., DULINA, L.: Logistics Processes and Systems Design Using Computer Simulation. Communications - Scientific Letters of the University of Zilina, 18(1A), 87-94, 2016.

[9] GNAP, J., KONECNY, V., VARJAN, P.: Research on Relationship between Freight Transport Performance and GDP in Slovakia and EU Countries. Nase More/Our Sea, 65(1), 32-39, 2018. https://doi.org/10.17818/NM/2018/1.5

[10] JAVALGI, R., MARTIN, C.: Internationalization of Services: Identifying the Building-Blocks for Future Research. Journal of Services Marketing, 21(6), 391-397, 2007. https://doi.org/10.1108/08876040710818886

[11] SAEZ, S., TAGLIONI, D., VAN DER MAREL, E., ZAVACKA, V.: Valuing Services in Trade: A Toolkit for Competitiveness Diagnostics. The World Bank, Washington DC, 2014.

[12] WINSTED, K. F., PATTERSON, P.: Internationalization of Services: The Service Exporting Decision. Journal of Services Marketing, 12(4), 294-311, 1998.

[13] STERNAD, M., JUSTINEK, G., CVAHTE OJSTERSEK, T.: International Comparison of Import and Export Efficiency of Transport Services. International Journal of Diplomacy and Economy, 3(1), 75-84, 2016. https://doi.org/10.1504/IJDIPE.2016.079167

[14] HILMOLA, O. P.: European Railway Freight Transportation and Adaptation to Demand Decline: Efficiency and Partial Productivity Analysis from the Period of 1980-2003'. International Journal of Productivity and Performance Management, 56(3), 205-225, 2007. https://doi.org/10.1108/17410400710731428

[15] PETROVIC, M., PEJCIC-TARLE, S., VUJICIC, M., BOJKOVIC, N.: A DEA Based Approach for Cross-Country Evaluation of Rail Freight Transport. Proceedings of the conference Building a Smarter Future, Bulgaria, 152-156, 2012.

[16] MARTI, L., MARTIN, J.C., PUERTAS, R.: A DEA-Logistics Performance Index. Journal of Applied Economics, 20(1), 169-192, 2017. https://doi.org/10.1016/S1514-0326(17)30008-9

[17] World Bank [online]. Available: https://lpi.worldbank.org/.

[18] CHARNES, A., COOPER, W., LEWIN, A. Y., SEIFORD, L. M.: Data Envelopment Analysis: Theory, Methodology and Applications. Springer Science+Business, New York, 1994.

[19] VIRTOS, H.: Open Source DEA [online]. Available: http://opensourcedea.org/.

[20] ARVIS, J. F., SASLAVSKY, D., OJALA, L., SHEPHERD, B., BUSCH, C., RAJ, A., NAULA, T.: Connecting to Compete 2016: Trade Logistics in the Global Economy [online]. World Bank, 2016. Available: https://wb-lpi-media.s3.amazonaws.com/LPI_Report_2016.pdf.

[21] CERNA, L., MASEK, J.: The Proposal the Methodology of the Supply Chain Management in Transport and Logistic Company. Proceedings of the International Scientific Conference Transport Means, Lithuania, 567-570, 2015.

[22] European Commission: Fact-Finding Studies in Support of the Development of an EU Strategy for Freight Transport Logistics: Analysis of the EU Logistics Sector, 2015.

Martin Krajcovic - Patrik Grznar - Miroslav Fusko - Radovan Skokan*

INTELLIGENT LOGISTICS FOR INTELLIGENT PRODUCTION SYSTEMS

The main topic of the submitted paper is intelligent logistics and its integration into production systems. In the beginning, the problem that lies in the inadequate knowledge of the internal state has been defined. The new society-wide trends that will originate in a few years are also outlined. Those trends will affect factories and their logistics systems on a large scale. Therefore, it is necessary to have a strategy that takes these new trends into consideration. In this manuscript, is described a strategy for intelligent production systems, as well as technologies for different types of production-logistic strategies. Many of these technologies can be applied together with the Digital Twin. The Digital Twin is a new concept in the field of designing production and logistics systems in the factory. Finally, we provide a description of the implementation of the Digital Twin into the production and logistics system.

Keywords: *logistics, strategy, new trends, digital twin, intelligent logistics, production systems*

1. Introduction

Logistics is becoming a very powerful engine for the success of industrial organizations in the global markets. Globalization has brought a potential of the global market, an abolition of market barriers and a free capital movement on one hand, but at the same time, on the other hand, the global competition and a so-far unknown rate at which the market turbulence appears. The present effort of designers of modern production and logistics systems is to implement an ability of quick adaptability to constantly changing market requirements as a solid part of their features. Those systems are now called the adaptive logistics systems. They implement new types of technologies to provide adaptability based on computer simulation and emulation. One of those methods, that can be defined as a part of those systems is the Digital Twin. The Digital Twin is a digital image of the production or logistics process, by means of which one can optimize production or logistics process in the factory. With the assistance of the CAx systems and simulation software, one can create the Digital Twin and then apply the Digital Twin into the real world of the factory. That results in an increase in the production and logistics process efficiency. The submitted paper is based on a case study for a medium-sized factory operating in the automotive industry. To maintain competitiveness, the factory cannot be named and detailed results cannot be published. Stated chapters reflect the research that was carried out for the factory and it is possible to implement the selected technologies in the following years.

2. Formulation of the problem

The success in business is nowadays determined more by the brain than by hands. The latest massive wave of innovations is referred to as the fourth industrial revolution, and it is built upon the use of the most advanced information and communication technologies (ICTs), automation, and robotization of all areas of the industry [1]. Modern factories, utilizing the most advanced technologies, are termed as Smart Factories. This paper responds to the growing need to design intelligent factories with reconfigurable logistics systems and logistics systems testing in real conditions in the case of extending production before the installation of a new production equipment. As the production, delivery and installation of complex production and assembly equipment can take several months, the opportunity to test logistics processes before and during installation can provide, in a dynamic global market, the necessary competitive advantage to the factories [2]. The problem with such implementations of innovative solutions is that factories do not prepare audits of logistics systems, logistics strategy, production systems and technical service in advance and do not know the real technical state of machines and equipment. In most cases, factory authorities do not provide ideas about new tendencies and development in a selected area. Thus, a lack of knowledge of the current state can cause a problem with the level of implementation of the new strategies or solutions. Furthermore, this may result in a sharp increase of financing the implementation of such solutions. In the end, it will affect negatively the schedule of the whole implementation. Therefore, it is necessary to deal with a complex logistics strategy including new trends in this area first, e.g. digitization, robotization, reconfigurable manufacturing systems, a lack of skilled workers, sustainability of production systems, green energy, and others [3], [4].

3. New trends and logistics strategy

There are several megatrends that are fundamentally reshaping the entire industry for the next 10 years. These include increased oil price volatility that creates investment challenges,

* **Martin Krajcovic, Patrik Grznar, Miroslav Fusko, Radovan Skokan**
Department of Industrial Engineering, Faculty of Mechanical Engineering, University of Zilina, Slovakia
E-mail: martin.krajcovic@fstroj.uniza.sk

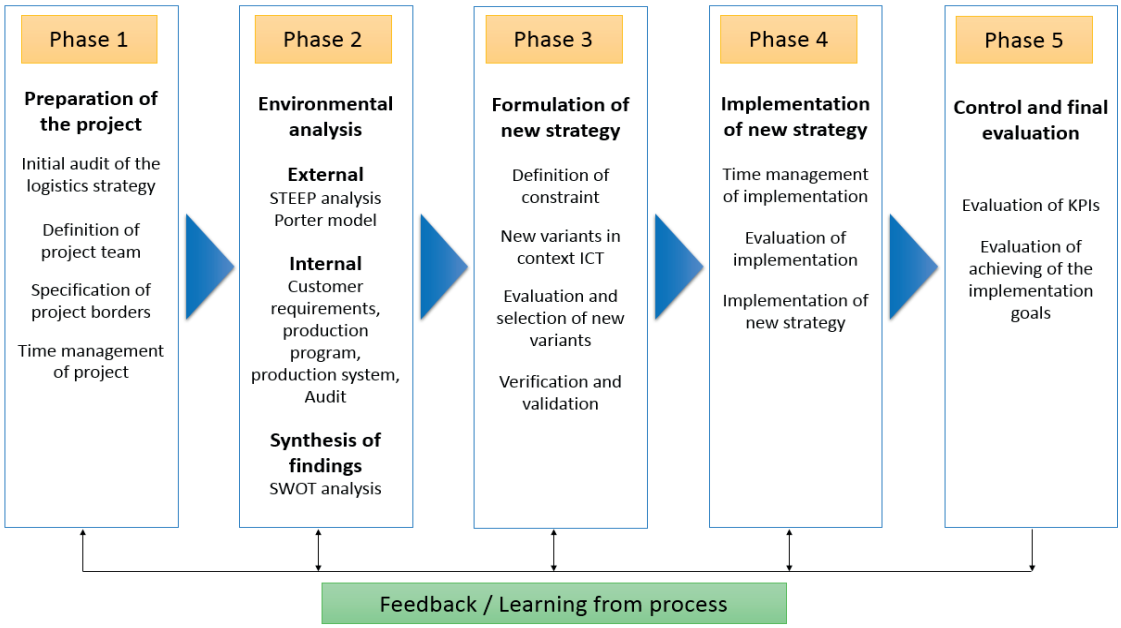

Figure 1 *The proposed procedure for making the logistics strategy*

energy consumers that are driving the transition to a low carbon and efficient energy world, supply constraints that are triggered and controlled by the government and geopolitical events, while also stimulating demands for green energy. The most important area will be the Internet of Things. Internet of Things is a novel paradigm that is based on the pervasive presence of numerous things or objects. [5].

3.1 Industry 4.0

The achievement of a stable economic development of an economic entity and growth of its competitiveness make it necessary to increase the level of its business activity based on improvement of the strategic management process [6]. Currently, everyone talks about Industry 4.0, but it is a topic where directions are indicated, solutions are prepared, but one still cannot imagine all the impacts. The phrase “Internet of Things” is the most widely used in this context, from which only a few of us can put together a clear idea. For this reason, we will use the word SMART. Intelligent and flexible processes and things will define production factories of the future. When the building components of one product communicate independently with the production equipment and if it is necessary, they become self-repair. Furthermore, when people, equipment and industrial processes will be intelligently networked, only then we can talk about complete Industry 4.0. A factory of the future enables mass production of products according to individual requirements and customer wishes - not too costly but of a high quality. Therefore, it cannot be denied that especially for small and medium-sized factories the smart and digital production brings great competitiveness.

3.2 Logistics strategy

Logistics is increasingly becoming a motor of success of industrial organisations on global markets. Resources play a decisive role in the functioning of economy [7]. Globalisation brought not only the potential of global market, disturbance of market barriers and free movement of capital, but also the global competition and so far, unknown speed by which the market turbulences appear [8]. Nowadays, internal logistics is the key to most businesses. Different products from many imported components are often finalized on one production line. Efficient and operation technologies together with auxiliary and service procedures secure whether they reach the line in time in the right version, in quantity and order. In this research, the focus was set on the development of a methodology for the formation of a logistics strategy for a selected medium-sized factory. No similar sequence (methodology) was found in literature by this authors. Relevance of a research subject is caused by the need for economic growth of the enterprise due to increase of its business activity based on improvement of strategic management by the managing subject [6]. The proposed methodology (shown in Figure 1) will provide instructions to develop its own logistics strategy considering an application of progressive tools and the inclusion of new trends in ICT (information and communication technologies) to a factory. The new trends for the factory are developed in the following sections. The first phase provides recommendations for the project preparation of a creation of logistics strategy, such as creating a project team, defining the limits of the strategy, creating a timeline for strategy creation. The second phase demonstrates the analyses that are suitable to be performed before the formulation of the logistics strategy and by the strategic synthesis of the acquired knowledge from the analyses. The third phase focuses on the process of formulating variants of a strategy based on information about the current

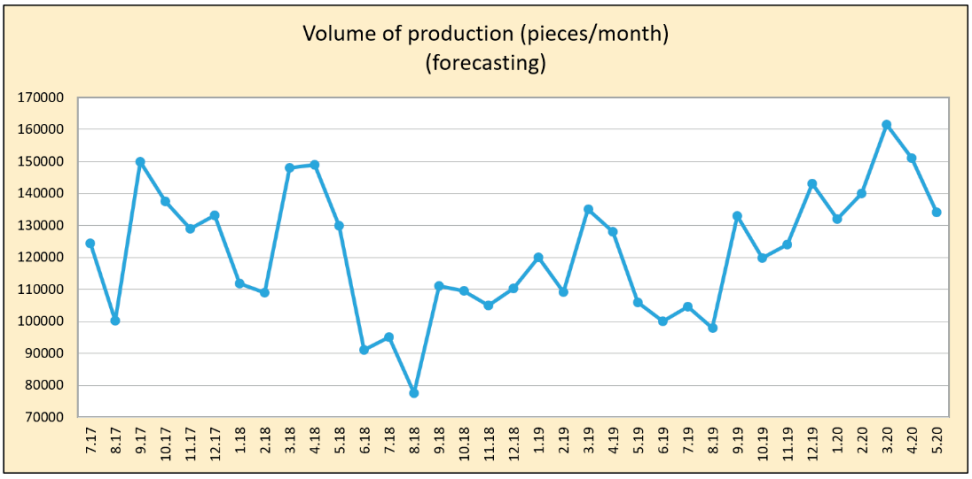

Figure 2 *The forecasting of the produced quantities*

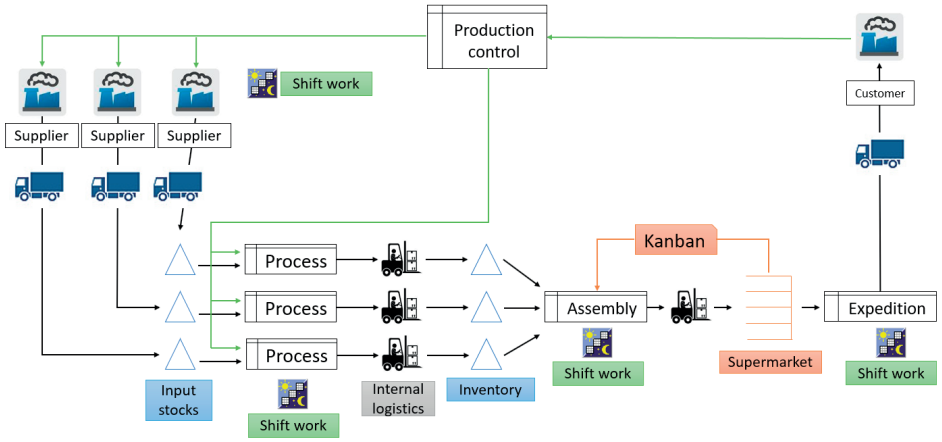

Figure 3 *The simulation of the value flow for the selected representative item*

state, objectives set and possible constraints. The fourth phase shortly demonstrates how the strategy is implemented since it represents the common project management activities. The final - fifth phase demonstrates the proposal evaluation during and after the implementation of the strategy.

The proposed methodology cannot be verified in a short time. The new strategy is usually implemented within 3 - 5 years. Therefore, only a selected part of the methodology, which describes interesting results, was verified. The methodology was experimentally verified in the automotive industry. Only some of the outputs are selected for this manuscript because several factory data are top secret (factory competitiveness information).

3.2.1 Verification results

This part of the section 3.2 contains some results from an analysis of the factory's internal environment.

Production program: The factory provided historical data based on which d the forecast of production quantities for the planned period implementation of the logistics strategy was prepared. The estimated production quantities are shown in Figure 2.

From the forecasting, it is possible to see that the trend of the quantity produced is increasing. Therefore, logistics must expect a growth of manipulated quantities. It is about a 10% increase over three years.

Analysis of the production system: The analysis of the production system was performed by the Value Stream Mapping (VSM). The output of the simulation of the value flow for the selected representative item is illustrated in Figure 3.

By use of mapping, it has been found out that in the production area, in front of assembly, there are disproportionately high inventories of work in process. The simulation also shows that the value of inventories demonstrates an increasing tendency in recent years.

Evaluation of logistics areas: From the point of view of the competitive advantage of the factory, one cannot describe the exact values of the logistics area. It consists of distribution logistics, shopping logistics, warehouse logistics, green and reverse logistics, organization of logistics processes, documentation - layouts, safety and ergonomic, KPI, production logistics, lean logistics, information flows and data, Industry 4.0 and engineering and technology. The overall result of evaluation of various logistics areas, before the implementation of the new strategy in the factory, is shown in Figure 4. There is presented that after the implementation of the new strategy in the selected factory the results is that the factory reached the area of the efficient logistics system.

Category	%	Symbol
Efficient logistics system	100 – 85	
Average logistics system	84 – 60	
Inconvenient logistics system	59 - 0	

Factory score 60 % Before implementation of the new strategy

Factory score 86 % After implementation of the new strategy

Figure 4 *The initial and the new valuation of the logistics system*

Logistics 4.0

Factory logistics	Phase 0	Phase 1	Phase 2	Phase 3	Phase 4
Shopping logistics	Push system	Pull system	Inventory managed by the supplier	Autonomous inventory management	Prediktion in intralogistics
Factory logistics	Manually guided castor cart	Manually guided vehicle	AGV – fixed ways	AGV – open space	AGV – open space managed by machines
Warehouses logistics	Without automatization	Automatic warehouse system	Automatic warehouse network	Supply chain warehose network	Without warehouse in supply chain
Distribution logistics	Push system	Manage supplies by order	Active manage of supplies	Automatic manage of supplies	Predictive manage of supplies
Identification	Without label	Numeric label	Barco des / Barco des	QR codes	RFID
Supply chain logistics	Structure of local plant	Structure of global plant	Partial planning / controlling of global resources	Fully planning / controlling global resources	Open and flexible operation
Logistics way	Decentralized vehicles	Centralized vehicles	Planned and centralized fleet	Ways in real time and linking navigation	Autonomous vehicle

Figure 5 *Moving of the logistics development in the selected production factory*

By means of single phases of the methodology, it was possible to exactly specify areas of logistics, which were needed to be focused on in the creation of a logistics strategy. Based on the SWOT analysis, the individual aspects of the factory logistics system that operates in the automotive industry were identified. Based on the analyses, the goals that factory planned to achieve in the next 3 - 5 years were set. Finally, y the necessary indicators that the company should monitor and evaluate had to be identified.

The industrial environment is characterized by a permanent change. As a result, the production requirements and their processes are constantly changing [9]. From Figure 5, one may observe how the factory will develop in the coming years - green coloured cells. The further set phases were defined and established for the factory. The phases should motivate the factory to reach Phase 4 which means Logistics 4.0. The factory was set out on the journey already and it has realistic preconditions from an average factory to become a Factory of the Future.

4. Logistics 4.0 (Smart logistics)

Logistic systems have to become more adaptive as well. One can see the growing trend of employing the concept of Factories of the Future (FoF) and Intelligent Manufacturing Systems (IMS), which In Slovakia are being supported by the Smart Industry, a movement that is gaining momentum under the auspices of the Ministry of Economy of the Slovak Republic and the German industry program Industry 4.0. The topic of the smart logistics systems (Smart Logistics) is becoming very popular [10]. The fourth industrial revolution has far-reaching

Table 1 *The relations between production, logistics strategy and technologies*

Usability of the individual technologies for the specific strategies						
Technology/ Strategy	Intelligent systems in pre-production phases	Design to order	Shopping service to order	Production to order	Assembly to order	Make to stock
CAX - Computer-Aided Technologies	4	2	2	2	1	1
Simulation	4	3	2	2	2	2
Virtual Commissioning	4	2	2	2	1	1
Virtual prototyping, Virtual and Augmented Reality	4	1	1	1	1	1
3D Printing	3	4	3	1	1	1
Reconfigurable Production System	0	1	1	4	4	1
Adaptive logistics systems	0	2	4	4	4	4
Advanced Planning and Scheduling Systems	0	4	4	4	4	4
Internet of Things	0	4	4	4	4	4
Real-Time Location System (RTLS)	0	4	4	4	4	4

4 - Full usability 3 - Partially limited usability 2 - Limited usability 1 - Currently difficult to use technology for a strategy 0 - Unusable technology

consequences for logistics and its self-image. Last, but not the least, the consumption behaviour of society leads to the new logistical requirements, for which the concept of an "Internet of Things and Services" is emerging as a probable solution [11]. Logistics 4.0 (Smart Logistics) is the key to the future. Digitization provides new ways of creating networks together with automation of their supply chains to factories. Nowadays, a whole range of advanced technologies is available for the new logistics strategies to optimize the logistics processes. The degree of impact of selected technologies is described in Table 1, where those technologies totally change business models, not only in industry but in services, as well.

At present, in the area of design of production and logistics systems beginning, authorities and professionals start to talk about the Digital Twin. The above-mentioned methods for formation of the physical twin of the real logistic system, as presented in Table 1, were used. These are the specific methods of CAx, simulation, Internet of Things and RTLS systems. Those systems make up a basic structure to create a physical object or system.

5. The Digital Twin

The Digital Twin can be defined as an evolving profile of the history of current behaviour of a physical object or a process. That helps to optimize the performance of a production factory [12]. The Digital Twin creates an environment in which one can optimize a factory operation directly within the production chain. One can modify the relevant production parameters and production processes and tailor a product or a process to meet the market requirements. All the generated data in this production process create a complete picture of a product or production. The Digital Twin gathers necessary information and permanently evaluates it. This has the effect of shortening and making the production cycle more efficient, shortening of the start-up time of new products and one can easily detect ineffective settings of production processes [13].

5.1 The factory management development

The production factory strategies can be classified as four types of strategies. In the past, the production factory operated on a reactive strategy. That strategy solved different types of problems only after something had happened. Then the second type of strategy followed, a real-time strategy, and it managed to solve production problems in real-time. The future of production factories is a predictive strategy that involves the Digital Twins and the Big Data. Finally, in a proactive strategy, Artificial Intelligence operates hand-in-hand with the Digital Twin. In Figure 6, one can see the production management scheme of the selected production factory.

5.2 Implementation of the Digital Twin in manufacturing factory

The concept of the Digital Twin calls for virtual replicas of the real world products. Achieving this requires a sophisticated network of models that have a level of interconnectivity, [14]. In the first step of implementation of the Digital Twin, one needs to obtain the required data, the so-called Big Data, about a product or a system for which one intends to create the Digital Twin. These data are collected from a production process and

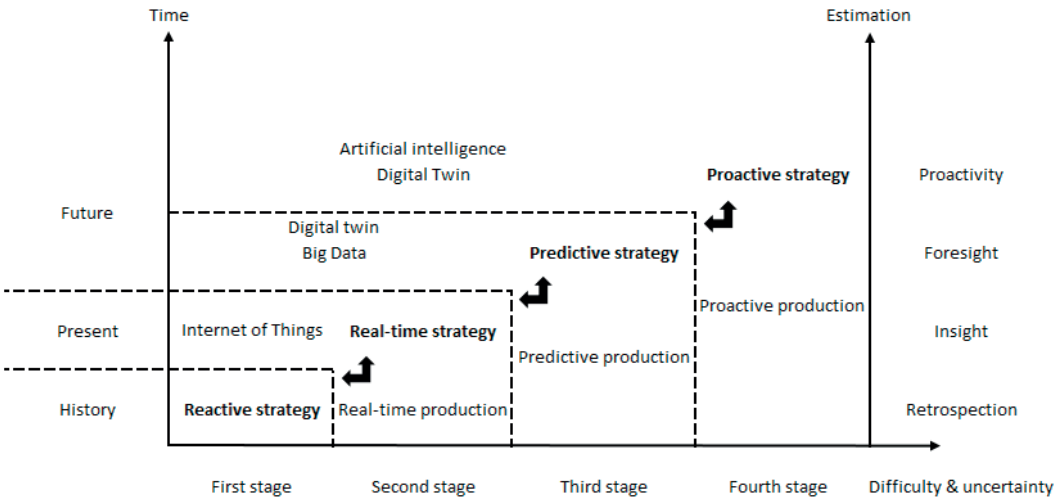

Figure 6 *The factory management development*

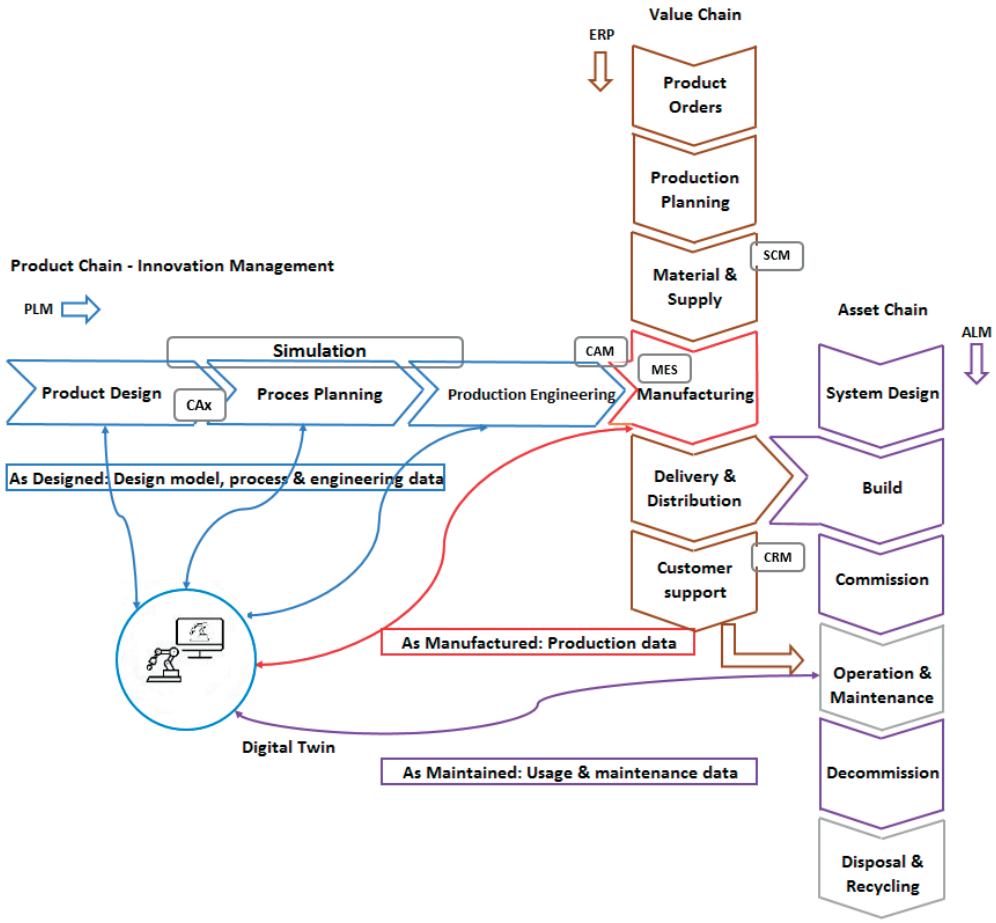

Figure 7 *The proposal of the Digital Twin in the selected production factory*

transformed by different methods. One can use several types of monitoring units to gather and process data from the production process to monitor the movement of objects. All the data are stored in Cloud. Consequently, collected data are implemented into the simulation software, where the process is simulated. After obtaining the results from the simulation software, optimization results follow and, finally, improvements are implemented to the real product or process. To collect data within Industry 4.0 concept allows to transfer and apply them in a variety of ways. One needs to consider the distance at which he intends to collect data and the speed of data processing. One can use technology such as Bluetooth, Wi-Fi and UWB (Ultra-Wide Band) for a specific intended operation as these methods can collect data up to a distance of 100 m. However, if one needs to acquire data from a larger production factory or from a whole production factory, then one must apply technology such as Lora, Sigfox, etc.

5.3 The Digital Twin and life cycle of the product

Many of product lifecycle processes, from design, to process planning and engineering, manufacturing is siloed because different software tools, models, and data representations are used and often by many different teams across different organizations and geographic locations. To achieve the goals of smart manufacturing, these product lifecycle processes and manufacturing functions need to be connected and integrated to increase process automation, responsiveness and efficiency and to reduce human errors. In Figure 7, one can see the flowchart about the Digital Twin, where its capabilities and performance can be more readily assessed and deficiencies discovered through analytics and simulation.

One can optimize the manufacturing and operations processes including the better fault detection and diagnostics and predictive maintenance, and thus can improve product design and process engineering and can even precisely determine the product recall scope to reduce the recall cost since the quality factors for each product can be traced back. Within the value, the product and asset chains described previously, the manufacturing, the operation and maintenance and the supply chain management functions deal with physical objects directly and are natural areas that IIoT will bring the most impact. By applying the IIoT technologies to the manufacturing environment, one can collect large amount of data in near-the-real-time covering machine operational states, performance indicators, process parameters, environmental data, quality measurements, all of which reflect the real-time state and performance of the machines and the quality of the products that are being made. Through analytics, one can optimize the manufacturing processes through the real-time monitoring, fault detection and diagnostics, predictive maintenance, precise OEE, online quality assurance, energy efficiency management and worker safety monitoring.

6. Conclusions

The submitted paper includes a survey focused on a medium-sized factory from the automotive industry. The survey focuses on the possibility for implementation of new technologies for the selected factory. Authors in the paper describe the intelligent logistics for the intelligent manufacturing systems. Global developments provide indicators that the main goal is to build intelligent factories that are characterized by capabilities of rapid changes, resource efficiency and ergonomics, as well as the integration of customers and the factory partners into business and value-making processes. Technological bases are Cyber-Physical Systems (CPS) and the Internet of Things (IoT) [15]. Manufacturing factories are economic units that are built for profit. If factory owners want their factories to succeed in a strong competitive environment, it is necessary that they solve their strategy from the perspective of the new trends and the geopolitical and social situation, as well. Factories should consider areas such as digitization, robotization, reconfigurable manufacturing systems and a lack of skilled workers, sustainability of production systems, green energy and others. Technologies that interfere into single strategies in the factory strongly affect the competitiveness of the factory. Therefore, those methods play an important role in different types of strategies for the factory. To improve the efficiency of logistics and production systems in the factory, the Digital Twin starts to be utilized to optimize production systems in the factory. With help of the Digital Twin implementation the factory can increase the efficiency of its production system, minimize costs and times that originate in these production systems.

Acknowledgment

This work was supported by the Slovak Research and Development Agency under the contract No. APVV-16-0488.

References

[1] GREGOR, M., MEDVECKY, S., GRZNAR, P., GREGOR, T.: Smart Industry Requires Fast Response from Research to Innovation. Communications - Scientific Letters of the University of Zilina, 19(2A), 3-9, 2017.

[2] CEE, J., DIEIEV, O., HOLMAN, D., LENORT, R., STAS, D., WICHER, P.: System Oriented Sustainable Supply Chain Management Innovations in Automotive Industry - Skoda Auto Case Study. Communications - Scientific Letters of the University of Zilina, 18(3), 54-59, 2016.

[3] VODAK, J., KUBINA, M., SOVIAR, J., ZRAKOVÁ, D., FERENC, P.: Online Reputation in Automotive [online]. Proceedings of the 18th International Scientific Conference (LOGI 2017), Czech Republic, 134(00060), 6, 2017. Available: https://www.matec-conferences.org/articles/matecconf/pdf/2017/48/matecconf_logi2017_00060.pdf. https://doi.org/10.1051/matecconf/201713400060

[4] DULINA, L., BARTANUSOVA, M.: Cave Design Using in Digital Factory [online]. Procedia Engineering: International Symposium on Intelligent Manufacturing and Automation (DAAAM 2014), Austria, 100, 291-298, 2014. Available: http://www.sciencedirect.com/science/article/pii/S1877705815003975/pdf?md5=d5565dbdf901ae3c0cd55794fae70483&pid=1-s2.0-S1877705815003975-main.pdf. https://doi.org/10.1016/j.proeng.2015.01.370

[5] KOWSHALYA, A. M., VALARMATHI, M. L.: Think Smart, Think Social! The Road Map from Smarter Objects to Social Objects in Social Internet of Things - A Survey. Journal of Applied Engineering Science, 15(2), 149-154, 2017. https://doi.org/10.5937/jaes15-12161

[6] LJEVCENKO, A. S., RUDICEV, A. A., KUZNECOVA, I. A., NIKITINA, J. A.: Competitive Strategy as Instrument of Increase of Business Activity of the Industrial Enterprise. Journal of Applied Engineering Science, 13(1), 19-24, 2015. https://doi.org/10.5937/jaes13-7859

[7] TROJAHN, S.: Logistics Strategies for Resource Supply Chains. Transport and Telecommunication Journal, 19(3), 244-252, 2018. https://doi.org/10.2478/ttj-2018-0021

[8] FURMANN, R., FURMANNOVA, B., WIECEK, D.: Interactive Design of Reconfigurable Logistics System. Proceedings of 12th International scientific conference on sustainable, modern and safe transport (TRASCOM 2017), Slovakia, 192, 207-212, 2017. https://doi.org/10.1016/j.proeng.2017.06.036

[9] SCHMIDTKE, N., BEHRENDT, F., THATER, L., MEIXNER, S.: Technical Potentials and Challenges within Internal Logistics 4.0. Proceedings of 4th IEEE International Conference on Logistics Operations Management (GOL 2018), 1-10, 2018. https://doi.org/10.1109/GOL.2018.8378072

[10] MICIETA, B., STASZEWSKA, J., BINASOVA, V., HERCKO, J.: Adaptive Logistics Management and Optimization through Artificial Intelligence. Communications - Scientific Letters of the University of Zilina, 19(2A), 10-14, 2017.

[11] HOMPEL, M., KERNER, S.: Logistics 4.0: The Vision of the Internet of Autonomous Things (in German). Informatik-Spektrum, 38(3), 176-182, 2015. https://doi.org/10.1007/s00287-015-0876-y

[12] Industry 4.0 and the Digital Twin, Manufacturing Meets its Match [online]. 2018. Available: https://www2.deloitte.com/content/dam/insights/us/articles/3833_Industry4-0_digital-twin-technology/DUP_Industry-4.0_digital-twin-technology.pdf.

[13] Creating a Digital Twin of a Production Line in the Industry 4.0 concept (in Slovak) [on-line]. 2018. Available: https://www.atpjournal.sk/rubriky/prehladove-clanky/tvorba-digitalneho-dvojcata-vyrobnej-linky-v-ramci-konceptu-industry-4.0.html?page_id=24830

[14] MILLER, A. M., ALVAREZ, R., HARTMAN, N.: Towards an Extended Model-Based Definition for the Digital Twin. Computer-Aided Design and Applications, 15(6), 880-891, 2018. https://doi.org/10.1080/16864360.2018.1462569

[15] GASOVA, M., GASO, M., STEFANIK, A.: Advanced Industrial Tools of Ergonomics Based on Industry 4.0 Concept. Proceedings of 12th International scientific conference on sustainable, modern and safe transport (TRASCOM 2017), Slovakia, 192, 219-224, 2017. https://doi.org/ 10.1016/j.proeng.2017.06.038

https://doi.org/10.26552/com.C.2018.4.24-28

Jaroslav Smutny - Viktor Nohal - Daniela Vukusicova - Herbert Seelmann*

VIBRATION ANALYSIS BY THE WIGNER-VILLE TRANSFORMATION METHOD

This paper deals with description and application of the Wigner-Ville transformation for vibration analysis. This transformation belongs to the group of non-linear time-frequency processes. Thanks to its properties, it may be successfully used in the area of non-stationary and transitional signals describing various natural processes. The use in the field of the railway constructions testing represents a quite an interesting application area of the transformation. This paper contains mathematical analysis of the transformation, a case study and practical experience obtained and recommendations for its practical use.

Keywords: *non-linear time-frequency transform, cross-component, Heisenberg uncertainty principle, vibration, railway fastening*

1. Introduction

The information on any engineering, physical, or other phenomenon, is represented in the signal by changes over time of the current value of the quantity described by the signal. A large number of methods can be applied to the measured signal in the time domain.

In many applications, direct evaluation of the time-amplitude representation is neither easy nor advantageous. For this reason, the signal can be transformed from the time-domain into another one. In some cases, important information can be obtained from the frequency domain. Fourier transform-based methods are the most frequently used ones. Thus, Fourier transform, its modifications and some of the parametric methods are the well suited techniques for processing stationary (at best ergodic or periodic) signals. They can even be used to analyse the non-stationary signals if it is important to know only the frequency components contained in the entire signal. This, of course, gives no information on the time at which they occur. To localise such frequency components in time, some other transforming methods and other computational techniques have to be used. If the information sources from the time and frequency domains are combined one can use so called time-frequency transformations [1], [2]. This enables determination of the frequency as a function of time. The time-frequency transformations can be divided in two basic groups [3], [4]:

- Linear (including mainly short Time Fourier Transformation, Wavelet Transformation, etc.)
- Non-linear (including mainly Wigner-Ville transformation, quadratic Cohen transformations, affine and hyperbolic transformations, eventually some further special proceedings).

Advantages of the linear transformations are mainly the speed of calculation and satisfactory time-frequency distribution. The main disadvantage of the linear transformation is the fact that resulting differentiation in time and frequency is limited by the so-called Heisenberg principle of uncertainty. Hence, the component of the signal cannot be presented as a point in time-frequency space. It is therefore possible to state only its position inside the rectangle $\Delta t \cdot \Delta f$ in a given time-frequency area [5].

A characteristic feature of non-linear transformations is the fact that their resulting differentiation in time and frequency is not limited by the Heisenberg principle of uncertainty. This fact includes the high distinguishing ability in the time-frequency level that gives rise to "precise" localisation of important frequency components in time.

2. The Wigner-Villa's transformation

The Wigner´s distribution was proposed in 1932 by Professor Wigner in the field of quantum physics and about 15 years later, it was adapted for the area of signal analysis by the French scientist Ville. The Wigner-Ville transformation is defined for the time-frequency domain by relation [6], [7]

$$\mathrm{WVT_x(t,f)} = \int_{-\infty}^{\infty} \mathrm{x}\left(t+\frac{\tau}{2}\right)\cdot \mathrm{x}^{*}\left(\mathrm{t}-\frac{\tau}{2}\right)\cdot \mathrm{e}^{(-\mathrm{j}\cdot 2\cdot\pi\cdot \mathrm{f}\cdot\tau)}\cdot \mathrm{d}\tau \qquad (1)$$

where '*' represents a complex conjunction, t is time, τ is shift along the time axis, x is time representation of the signal x(t) and $\mathrm{WVT_x(t,f)}$ is a time-frequency representation of the input signal. Equation (1) shows that it is essentially the Fourier transformation of relation $x(t+\tau/2)\cdot x^{*}(t-\tau/2)$, so the functions $x(\tau/2)$ and the complex conjugate of $x^{*}(-\tau/2)$ at some point in time *t*. From Equation (1) it is also apparent that the Wigner-Ville transformation is a complex function in the time-frequency space. Similarly, one gets the equation for the calculation in the frequency domain. If the discrete data sequence is processed, it is necessary to modify the integral equation mentioned above (1) in the form of summation.

Unlike the other linear methods (for example the short time Fourier transformation), in which the resolution is limited by a window function, the Wigner-Ville spectrum provides a good

* [1]Jaroslav Smutny, [1]Viktor Nohal, [1]Daniela Vukusicova, [2]Herbert Seelmann
[1]Institute of Railway Structures and Constructions, Faculty of Civil Engineering, Brno University of Technology, Czech republic
[2]Rail Data Services Austria GmbH & Co KG, Wien, Austria
E-mail: smutny.j@fce.vutbr.cz

resolution both in the frequency and in time domain. The important feature here is that the calculation is not limited by Heisenberg uncertainty principle. The Wigner-Ville distribution satisfies the time-frequency marginal according to Equation (2) [6], [8].

$$\int \mathrm{WVT}(t,\omega)\mathrm{d}\omega = \left| x(t)^2 \right|$$

$$\text{and} \int \mathrm{WVT}(t,\omega)\mathrm{d}\omega = \left| X(\omega)^2 \right| \tag{2}$$

where WVT(t,ω) is the Wigner-Ville transformation, x(t) is time signal, X(ω) is Fourier transformation of a time signal x(t), t is time and ω is angular frequency. Other properties of the Wigner-Ville distribution are - time shift invariant, frequency modulation invariant, synchronous invariant time shift and frequency modulation, time scaling.

Although the calculation of the coefficients of the Wigner-Ville transformation is not limited by the Heisenberg's uncertainty principle, certain problems may arise in calculating multicomponent signal, which is generated by the sum of two or more signals. The signal, which arises from additive combination (sum) of signals x_1 and x_2, is now considered according to equation

$$x(t) = x_1(t) + x_2(t) \tag{3}$$

For the Wigner Ville transformation subsequently applies the following relation

$$\begin{aligned} &\mathrm{WVT}(t,\omega) = W_{11}(t,\omega) + W_{22}(t,\omega) + W_{12}(t,\omega) + \\ &+ W_{21}(t,\omega) = W_{11}(t,\omega) + W_{22}(t,\omega) + \\ &+ 2 \cdot \mathrm{Re}\{W_{12}(t,\omega)\} \end{aligned} \tag{4}$$

where the symbol "Re" stands for the real part and with keeping equality $W_{12} = W_{21}$ one obtains:

$$W_{12}(t,\omega) = \int_{-\infty}^{\infty} x_2\left(t+\frac{\tau}{2}\right) \cdot x_1^*\left(t-\frac{\tau}{2}\right) \cdot e^{(-j\cdot 2\cdot \pi \cdot f \cdot t)} \cdot \mathrm{d}\tau \tag{5}$$

It is obvious that the Wigner-Ville transformation of the sum of the signals is not equal to the sum of the Wigner-Ville transformation of signals. There is an additional term 2·Re{W12(t,ω)}. This addition may be called interference or contribution to the cross-component. Based on the fact that the autocorrelation function is a bilinear operation on the processed signal and when it is formed, there are "false" contributions from the aforementioned cross-component in the final calculation of the time-frequency spectrum display, which then deteriorate the reproducibility of the view. For a better explanation of the problem defined above, consider now the signal composed of the two sine waves of frequencies f_1 = 5 Hz and f_2 = 20 Hz according to the equation

$$X(t) = A_1 \cdot e^{j\cdot\omega_1\cdot t} + A_2 \cdot e^{j\cdot\omega_2\cdot t} \tag{6}$$

The Wigner-Ville transformation of such a signal can be analytically expressed as

$$\begin{aligned} &\mathrm{WVT}(t,\omega) = 2\cdot\pi\cdot\sum_{i=1}^{2} A_i^2 \cdot \delta\cdot(\omega-\omega_i) + \\ &+ 4\cdot A_1\cdot A_2\cdot\pi\cdot\delta\cdot(\omega-\omega_\mu)\cdot\cos(\omega_d\cdot t) \end{aligned} \tag{7}$$

where the symbol δ represents delta function, ω_μ and ω_d are the geometric center, or the distance between the two sinusoidal functions in the frequency plane, respectively, given by:

$$\omega_\mu = \frac{\omega_1+\omega_2}{2} \qquad \omega_d = \omega_2 - \omega_1 \tag{8}$$

Equation (7) fully corresponds to Equation (4) and it means that in the time-frequency plane the contributions of the examined signal are concentrated at the frequency ω_1, ω_2 and also to nonzero frequency ω_μ.

With the number of individual frequency components N, contained in the analyzed signal, one gets the total number of contributions from interference $N\cdot\frac{(N-1)}{2}$. To eliminate this effect certain adjustments of the Wigner-Ville transformation can be used for certain types of signals.

In principle, there are two reasons to modify the basic properties of the Wigner-Ville transformation. The first reason is that in practice it is not possible to integrate from -∞ to +∞, but the calculation can be carried out only for limited signals. The second reason is to try to eliminate the effect of the cross-components, which often oscillate heavily. Restrictions of both problems can be achieved by calculating the modified Wigner-Ville transformation (often called pseudo or smoothed) by equation [7], [9]

$$\begin{aligned} &\mathrm{PWVT}_X(t,f) = \int_{-\infty}^{\infty} h(\tau)\cdot x\left(t+\frac{\tau}{2}\right)\cdot \\ &\cdot x^*\left(t-\frac{\tau}{2}\right)\cdot e^{(-j\cdot 2\cdot\pi\cdot f\cdot\tau)}\cdot \mathrm{d}\tau \end{aligned} \tag{9}$$

where the function h(τ) is a window function with maximum at τ = 0. Such a solution quite effectively suppresses interference (smoothed), but deteriorates the resolution. The smoothed Wigner-Ville transformation is therefore a certain compromise between smoothing and resolution. For the better explanation, consider a signal composed of the two sine waves according to the Equation (3). Suppose that, parameter α is set by expansion of function h(τ). The smoothed Wigner-Ville transformation of such a signal can be analytically expressed by the following relation:

$$\begin{aligned} &\mathrm{PWVT}_x(t,\omega) = \frac{1}{\sqrt{2\cdot\pi\cdot\alpha}}\cdot \\ &\cdot\left[A_1^2\cdot e^{-\frac{(\omega-\omega_1)}{2\cdot\alpha}} + A_2^2\cdot e^{-\frac{(\omega-\omega_2)}{2\cdot\alpha}}\right] + \\ &+ \frac{2\cdot A_1\cdot A_2}{\sqrt{2\cdot\pi\cdot\alpha}}\cdot\cos\left[(\omega_2-\omega_1)\cdot t\right]\cdot e^{-\frac{(\omega-(\omega-\omega_2))^2}{8\cdot\alpha}} \end{aligned} \tag{10}$$

For the practical presentation of these conclusions, a simulated signal, composed of the two sine waves of frequencies f_1 = 5 Hz and f_2 = 20 Hz and amplitude 0.5 V, based on equation (3), was used. It should be noted that the signal is technically stationary. Significant frequency components in the signal occur throughout the implementation.

At this signal the classical Wigner-Ville transformation was first applied, later the smoothed version ones. For the analysis, pictures (Figure 1 and Figure 2) were used, which consist of a trio of graphs. The top graph shows the time course of amplitude of changes in a physical quantity (in this case the voltage). The lower

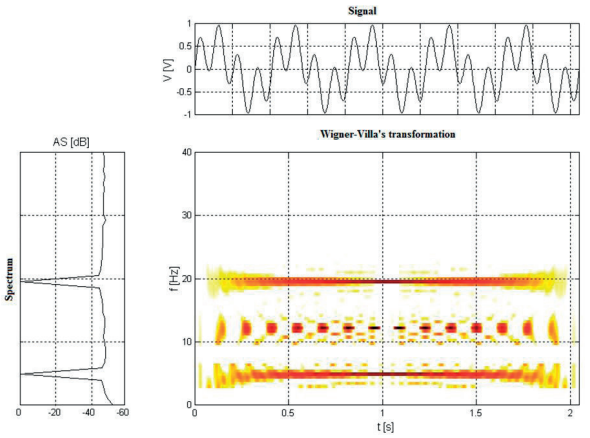

Figure 1 *The classical Wigner-Ville transformation of a simulated signal*

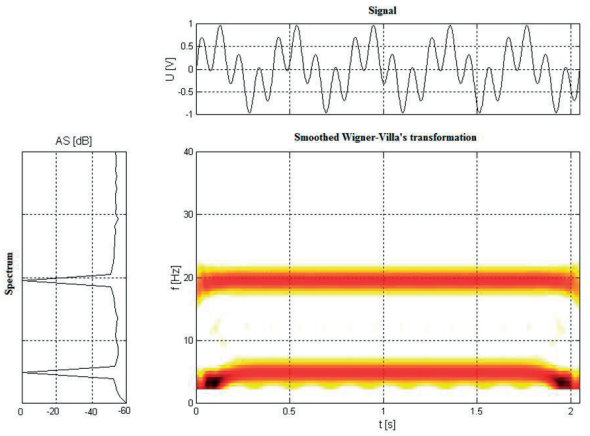

Figure 2 *The smoothed Wigner-Ville transformation of a simulated signal*

left graph shows the amplitude spectrum calculated by direct application of the Fourier transformation of the signal.

In the middle graph there is a 3D representation of the time-frequency course of amplitude spectrum computed by application of the Wigner-Ville transformation. The spectral data are shown in different colours. Note that the maximum value is marked as black. Figure 1 shows calculation results of classical the Wigner-Ville transformation signal according to Equation (7).

From the representation, it is evident that in the time-frequency spectrum in addition to the two basic frequencies of 5 Hz and 20 Hz, a cross component occurs also at the frequency of 12.5 Hz. Components are found in the spectrum, above that other interfering frequency, resulting from the finite length of the signal (sharp start and stop of the signal), or other discontinuities. From the middle graph of Figure 1, an extremely accurate localization of the two fundamental frequencies is particularly visible.

Figure 2 shows calculation results of the smoothed Wigner-Ville transformation from the signal according to Equation (10). As seen from the presented view, the influence of the cross component is suppressed by selecting an appropriate small parameter α in the function.

On the other hand, the middle graph in Figure 2 clearly shows that the localization of the two basic frequency components, in the frequency domain, is obviously worse. This is due to the higher blur on the frequency axis.

3. Case study

The measurements were made on a test sample of a rail fastening. This sample was composed of UIC60 structural rail with elastic fastening Vossloh Skl14, mounted on a B91P concrete sleeper. For the experimental investigation of the dynamic properties of the test sample, a method based on the measurement of a mechanical shock response was used. The mechanical shock was excited by a special hammer, which had a force transducer, in the radial direction to the rail head. The response was measured by acceleration sensors on the foot of the rail and the sleeper seat, as shown in Figure 3.

Figure 3 *View of the rail fastening sample*

Frequency response functions were calculated from the response signals due to normalization to the excitation signal. Those were recalculated by the inverse Fourier Transform into the time domain. In this way, the normalized time course of oscillation acceleration was obtained. This method, including instrumentation, is described in detail in the literature [8], [10]. Analysis in time, frequency and time-frequency domain was used to evaluate the measured data. The Fourier transform was used for the analysis in the frequency domain. A procedure, based on application of the Wigner-Ville transformation, was used for analysis in the time-frequency domain.

Time histories of the impulse response function, recorded by accelerometers, located on the rail foot, are depicted in the upper graph of Figure 4. The left graph of Figure 4 shows the amplitude spectrum calculated by applying the Fourier transform. There are six distinct frequencies (200 Hz, 600 Hz, 1.7 kHz, 1.9 kHz, 3.2 kHz and 3.3 kHz).

The time-frequency amplitude spectrum, estimated by application of the Wigner-Ville transformation from the impulse response function, is depicted in the middle graph in Figure 4. As shown in this graph, the time history of important frequency components essentially differs. As can be seen from this graph, the time occurrence of significant frequency components varies considerably. The 1.9 kHz frequency component acquires the highest values for a relatively long time (relative to other

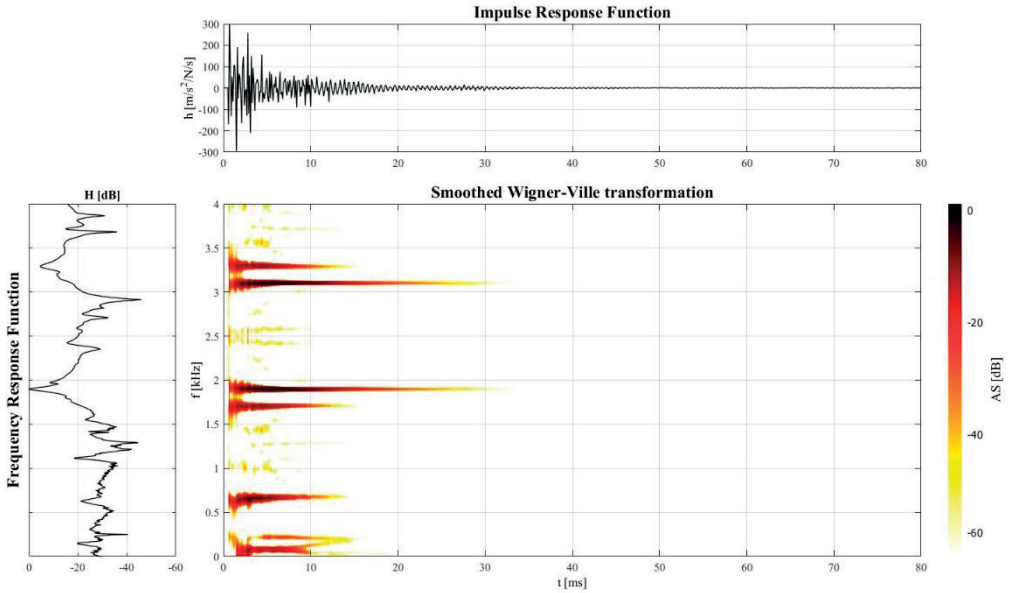

Figure 4 *Sensor located on the rail foot, time-frequency analysis by the Wigner-Ville transformation method*

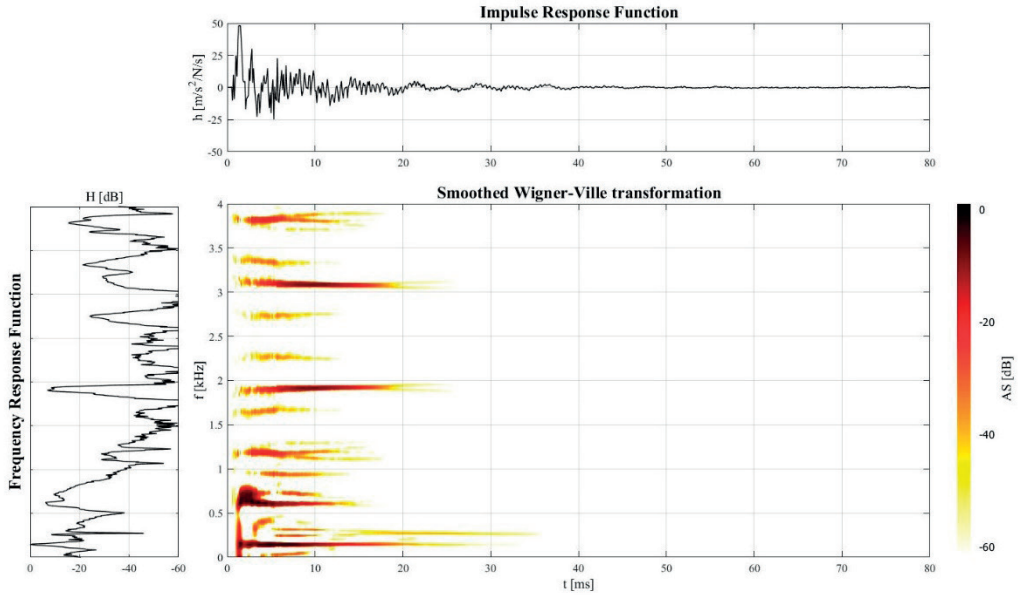

Figure 5 *Sensor located on concrete sleeper, time-frequency analysis by the Wigner-Ville transformation method*

frequency components). It occurs in the signal almost in its entirety, i.e. about 32 ms (at attenuation of up to 40 dB). The second most important component is the frequency 3.2 kHz with a duration of 30 ms. Others no,le frequencies of 1.7 kHz and 3.3 kHz are in the signal for the time of 2 ms up to 15 ms.

The signal taken by the second sensor, located on the concrete sleeper seat, has a different character. From the time recording (see the upper graph of Figure 5), it is clear that the maximum acceleration amplitude is lower than the signal from the sensor on the foot of the rail (Figure 4), due to the waving process via the fastening rail, rail pad and sleeper to the accelerometer sensor.

The course of the amplitude spectrum (left graph of Figure 5) differs significantly from the characteristics measured by the sensor located on the foot of the rail. The most significant components occur at the lower frequencies than those captured by the sensor at the foot of the rail, i.e. in the range of 200 Hz to 2 kHz, and there is a higher number of them in this interval. The same conclusion is provided in the middle graph of Figure 5, which presents the time-frequency representation of the Wigner-Ville coefficients. The longest component is 200 Hz with a duration of up to 34 ms. The highest values are on frequencies 600 Hz and 700 Hz with a duration of about 15 ms. A very interesting waveform has a frequency of 1.9 kHz, which occurs in the time interval of 2 ms to 24 ms. It is the same with the frequency of 400 Hz, which occurs between 5 ms and 35 ms.

4. Conclusion

The Wigner-Ville transformation offers a comprehensive tool for analysing the non-stationary signals, in particular. Characteristic feature of presented transformation is the fact that

its resulting distinguishing in time and frequency is not limited by the Heisenberg uncertainty principle. This fact includes the high distinguishing ability in the time-frequency plane that gives rise to a "precise" localisation of important frequency components in time. This method gives a fast and accurate localisation of frequency components included in the measured signal.

The existence of the "false" interference frequency components may be a certain disadvantage of the Wigner-Ville transformation. However, their influence can be effectively defused by using the so-called smoothed version, when the properties of a given transformation are affected by the use of suitable local window function. The result is a compromise solution where one obtains the reasonable time and frequency resolution when interferences are suppressed.

From this point of view, the Wigner-Ville transformation is highly applicable in the area of railway construction upon noise, vibration and strain analyses. It is possible to apply this method successfully not only on samples of several constructions of railway and tramway superstructure, but directly in the field on real tracks, as well.

Acknowledgments

This research has been supported by the research project FAST-S-18-5216, The dynamic response analysis of the railway line to the load using selected nonlinear time-frequency procedures.

References

[1] RIHACZEK, A. W.: Signal Energy Distribution in Time and Frequency. IEEE Transaction on Information Theory, 14(5), 369 – 374, 1968. https://doi.org/10.1109/TIT.1968.1054157

[2] SMUTNY, J., SADLEKOVA, D.: The Vibration Analysis by Margenau-Hill Transformation Method. Communications - Scientific Letters of the University of Zilina, 16(4), 123-127, 2014.

[3] HAMMOND, J. K., WHITE, P. R.: The Analysis of Non-Stationary Signals Using Time-Frequency Methods. Journal of Sound and Vibration, 190(3), 419-447, 1996. https://doi.org/10.1006/jsvi.1996.0072

[4] ZHENG, G. T., MCFADDEN, P. D.: A Time-frequency Distribution for Analysis of Signals with Transient Components and Its Application to Vibration Analysis. Journal of Vibration and Acoustic, 121(3), 328-333, 1999.

[5] SMUTNY, J., VUKUSICOVA, D., NOHAL, V., SEELMANN, H.: Vibration Analysis by Gabor Transformation Method. Communications - Scientific Letters of the University of Zilina, 19(4), 24-29, 2017.

[6] MARTIN, W., FLANDRIN, P.: Wigner-Ville Spectral Analysis of Non-stationary Processes. IEEE Transactions on Acoustics, Speech, and Signal Processing, ASSP-33(6), 1461-1470, 1985.

[7] KAKOFENGITIS, D., STEUERNAGEL, O.: Wigner's Quantum Phase Space Current in Weakly Anharmonic Weakly Excited Two-State Systems. European Physical Journal Plus 132(381), 2017. https://doi.org/10.1140/epjp/i2017-11634-2

[8] SMUTNY, J.: Measurement and Analysis of Dynamic and Acoustic Parameters of Rail Fastening. NDT & E International - Independent Nondestructive Testing and Evaluation, 37(2), 119-129, 2004. https://doi.org/10.1016/j.ndteint.2003.08.003

[9] SHARMA, R. R. PACHORI, R. B.: Improved Eigenvalue Decomposition-Based Approach for Reducing Cross-Terms in Wigner-Ville Distribution. Circuits, Systems, and Signal Processing, Elsevier, 37(8), 3330-3350, 2018. https://doi.org/10.1007/s00034-018-0868-7

[10] MORAVCIK, M.: Analysis of Vehicle Bogie Effects on Track Structure-Nonstationary Analysis of Dynamic Response. Communications - Scientific Letters of the University of Zilina, 13(3), 33-40, 2011.

https://doi.org/10.26552/com.C.2018.4.29-35

Michal Jambor - Frantisek Novy - Milos Mician - Libor Trsko - Otakar Bokuvka - Filip Pastorek
Daniel Harmaniak*

GAS METAL ARC WELDING OF THERMO-MECHANICALLY CONTROLLED PROCESSED S960MC STEEL THIN SHEETS WITH DIFFERENT WELDING PARAMETERS

In this paper are presented results of mechanical properties evaluation of the thin sheets welds made of the S960MC TMCP steel, which were executed using the GMAW procedure with different process parameters. The microstructural changes in the heat affected zone (HAZ) were evaluated, as well. The microstructural observation revealed significant changes in the HAZ and the three main zones, coarse grain, fine grain and intercritical (CGHAZ, FGHAZ and ICHAZ) were identified in the HAZ for both sets of tested welding parameters. Evaluation of the micro-hardness showed significant reduction of the micro-hardness in the ICHAZ, for both tested states, and the ICHAZ was identified as the most critical area of the whole welded joint. Results of the tensile tests revealed significant reduction of mechanical properties regardless of the welding parameters.

Keywords: *gas metal arc welding, S960MC steel, heat affected zone, mechanical properties, microstructural changes*

1. Introduction

The thermo-mechanically controlled processed (TMCP) steels belong to the group of ultra-high strength steels, which exhibit exceptional combination of high tensile and yield strength, toughness and ductility. The ultra-high strength steels exhibit also high abrasion resistance, when comparing to the carbon steels [1]. These properties are obtained by the combination of alloying by small addition of V, Ti, Cr, Ni, Si, Mn, Mo, and properly chosen processing, which allows to achieve the high strength properties while the amount of C is maintained low [2]. Nowadays, in the many industrial applications, the usage of the high strength steels is increasing [3]. Those steels were introduced in the heavy machinery constructions as heavy mobile cranes, where exist requirements for the high UTS with combination with the high damage tolerance [4], [5], [6], [7]. Exceptional properties led to expansion to other applications like the construction of military vehicles, offshore constructions, shipbuilding industry, high pressure pipes for oil/gas transportation and nowadays also to a construction of commercial vehicles [1], [7], [8], [9]. The only drawback that prevented the wider introducing of the high strength steels to constructions is the higher price of those steels; thus their price must be compensated by introducing other advantages [10]. Application of the high strength steels in constructions enables application of small thickness profiles and consequently reduction of the construction mass [11]. The weight savings in the construction, reached by the substitute of standard mill steels (S355) by the high strength steel S960MC, can be up to 60 % [12]. Efforts to decrease the air pollution is another strong reason to introduce the high strength steels to the construction of transport vehicles, where the reduction of the weight can bring really significant increase of the fuel efficiency and thus the lower the air pollution level [10], [13].

The high strength steels have worse forming properties than conventional mild steels, so their usage in the constructions is restricted to the profiles, which can be easily fabricated (mostly sheets); thus for manufacturing more complicated shapes, welding is the most common technology, which can be used for producing joints of these steels. Using the high strength steels in the construction leads to reduction of the cross section, which also reduces the time required for the welding and the consumption of the filler metal [14]. The high tensile and yield strength of this type of steels is obtained by the combination of the chemical composition, heat treatment and the processing. The heat input into the material during the welding can thus significantly affect properties of the steel and the whole joint. The main problem of the welded structures of high strength steels is the softening in the heat affected zone (HAZ) [8], [15], [16], [17], [18], [19]. In steels with the tensile strength higher than 500 MPa, due to the heat effect, occur structural changes in the HAZ, which can significantly degrade properties in those areas [20]. To allow weldability of these steels, without excessive degradation of the mechanical properties, the chemical composition is carefully arranged to meet the requirement for the high mechanical properties with high toughness and to ensure weldability and the resistance to formation of hot and cold cracks [6], [14], [21].

The majority of the recent papers, regarding welding of the high strength steels (especially S960), investigate the effect of the processing parameters and technology on the resulting properties, but those studies mostly consider the quenched-tempered steels and sheets with thickness of 8 mm and more. It is well known that the welding of the thin sheets can reveal some differences

* [1]Michal Jambor, [1]Frantisek Novy, [2]Milos Mician, [3]Libor Trsko, [1]Otakar Bokuvka, [3]Filip Pastorek, [2]Daniel Harmaniak
[1]Department of Materials Engineering, Faculty of Mechanical Engineering, University of Zilina, Slovak Republic
[2]Department of Technological Engineering, Faculty of Mechanical Engineering, University of Zilina, Slovak Republic
[3]Research Centre, University of Zilina, Slovak Republic
E-mail: michal.jambor@fstroj.uniza.sk

Table 1 *Chemical composition (in weight %) and the mechanical properties of tested material*

S960MC										
C	Si	Mn	P	S	V	Ti	Cu	Cr	Ni	Mo
0.087	0.18	1.11	0.009	0.001	0.01	0.022	0.017	1.08	0.06	0.128
YS [MPa]	1034	UTS [MPa]	1150	Elongation [%]	11.5					

Table 2 *Welding parameters used in the study*

Weld	Voltage [V]	Current [A]	Welding speed [m/min]	Wire feeding rate [m/min]	Heat input [kJ/cm]
A	19	135	0.45	4	2.7
B	17	120	0.23	4	4.3

Table 3 *Chemical composition (in weight %) and mechanical properties of the filler metal*

G 89 5 M21 Mn4Ni2.5CrMo												
C	Si	Mn	P	S	Cr	Ni	Mo	Cu	Al	V	Ti	Zr
0.11	0.66	1.77	0.009	0.007	0.41	2.43	0.46	0.17	0.007	0.007	0.069	0.0019
YS [MPa]	≥ 930	UTS [MPa]	≥ 980	Elongation [%]	≥ 14							

in the resulting properties of the welded joint when compared to the thick sheets. In this study, the high strength TMCP S960MC steel welded joints were examined. Welded joints prepared from 3 mm thick sheets were obtained by welding with different welding parameters resulting in different heat input to the material.

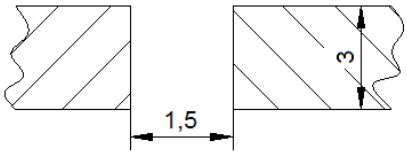

Figure 1 *Schematic view of the welding configuration.*

2. Material and experimental procedures

In this study, the S960MC thermo-mechanically processed steel sheets were used. The chemical composition and the basic mechanical properties of tested steel are shown in Table 1 and they meet the requirements for the S960MC steel according to standard EN 10149-2. Sheets with dimensions 300×300 mm and thickness of 3 mm were used. A configuration of the but welded joint without grooves was prepared by a single pass gas metal arc welding (GMAW) technique (gap width was of 1.5 mm, Figure 1). Prior to the welding process, the surface was ground and degreased by ethanol, to prevent occurrence of welding defects. To protect the mold welding pool, prevent the excessive oxidation and obtain adequate penetration, the weld was protected by M21 gas mixture (82 % Ar + 18 % CO_2). Two sets of welding parameters were used; they are shown in Table 2. The G 89 5 M21 Mn4Ni2.5CrMo filler metal (EN ISO 16834-A) in the form of a wire with ϕ = 1 mm was used. Chemical composition and mechanical properties of used welding wire are shown in Table 3. The welds were obtained without any preheating and with cooling in the air. No additional post-weld heat treatment was applied.

After the welding procedure, the specimens were cut in the transversal direction. The tensile tests were carried out, according to EN ISO 6892-1 standard to obtain the mechanical properties of the weldments. Specimens for the tensile tests were prepared according to EN ISO 4136 standard. Two specimens from the both welds were manufactured.

The microstructure evolution after the welding was characterized by the optical microscopy; specimens were prepared by the standard procedure for preparation of metallographic specimens and etched by 1 % Nital. Specimens for macroscopic and microscopic evaluation and the microhardness measurements were cut from the sheets at the minimal distance 25mm from the begining of the welds. Microhardness measurements were used for characterization of changes of the properties through the welds; the microhardness was measured in the line, from the base metal, through the weld up to the base metal on the other side. For all the micro-hardness measurements, the force F = 1kp (9.8 N) was used.

3. Results and discussion

3.1 Macro and microstructural characterization

Welds were prepared with the two different sets of welding parameters. The most significant differences were in the welding speed, which resulted in the 60 % increase of the heat input in the second weld. For simplification, the weld made with the lower heat input will be designated as ‘weld A’ and the other one as a ‘weld B’. Both welded sheets were subjected to visual control, which did not reveal presence of any defects on the welds surface and there were none visual differences between both welds, as well. The welds‘geometry was macroscopically examined (Figure 2a, Figure 2b) and it fulfills requirements according to EN ISO 17639 standard for the used type of welds. As a result of macroscopic observation, it was found that both tested joints have no cracks, no lack of penetration, no porosity, regular profile and a smooth transition to the base metal. A small angular deviation was observed, as a result of the welding process during which the sheets were not clamped. Despite the large

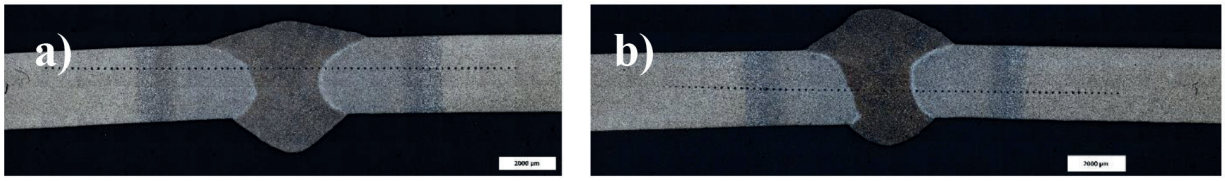

Figure 2 *Macroscopic view of the weld A (a) and weld B (b)*

differences in the heat input, no enlargement of the HAZ due to the higher heat input was observed. Due to the low thickness of the welded sheets, most of the heat is transferred rapidly to the air, and no excessive heat dissipation in the welded sheets occurs. As a result, the higher heat input does not significantly enlarge an area which is heated above the A_{C1} temperature. The greater emphasis was placed on the microstructural observation. Microstructure of the base metal is shown in Figure 3 and it is composed of a mixture of martensite and tempered martensite. This kind of structure allows obtaining the combination of high mechanical properties and high toughness. The weld metal (WM) microstructure was characterized as a mixture of martensite and tempered martensite in the large columnar grain structure (Figure 4). No significant differences were recorded in the comparison of welds A and B. The heat affected zone (HAZ) is the most problematic zone in the welds of the high strengths steels, as its properties are a result of the thermo-mechanical processing; introducing of the thermal energy during the welding process can significantly affect the structure in the HAZ and thus also the resulting properties of the whole weldedjoint. Regardless of the welding parameters, three different areas in the HAZ, were recorded, depending on the temperature to which the individual zones were exposed and the cooling rates (the similar behavior was reported by many authors [2], [9], [12], [14]). In the direction from the weld metal to the base metal, the first observed zone was the coarse grain zone (CGHAZ) (Figure 5a, Figure 5b). The CGHAZ is the area, which was heated high above the A_{c3} temperature, what resulted in the transformation of the base metal to austenite, which subsequently grew. Followed by the rapid cooling, the enlarged austenitic grains transformed back to martensite. The amount of the austenite phase growth increases with getting closer to the fusion zone, which corresponds to the temperature increase in the same direction. Coarsening of the austenitic grains in the TMCP steels at elevated temperatures is accelerated by the dissolving of NbC (and other small particles) in the matrix, and thus the pinning effect is significantly reduced [22]. The second area resolved in HAZ, is the fine grain heat affected zone (FGHAZ) (Figure 5c, Figure 5d). This area was heated slightly above the A_{c3} temperature, but the holding time above A_{c3} was very short. Exposure to heat at this zone caused thetransformation of the base metal to austenite, but due to the low temperature and very short duration of this exposure, followed by the rapid cooling, it resulted in the refinement of austenitic structure and its subsequent transformation to martensite. The last area of the HAZ is called the intercritical heat affected zone (ICHAZ) (Figure 5e, Figure 5f). This area was exposed to temperatures in the range between A_{c1} and A_{c3} where the martensite is partially transformed to austenite. This exposure resulted in formation of the mixture of martensite and austenite, which transformed, after the rapid cooling, to martensite and

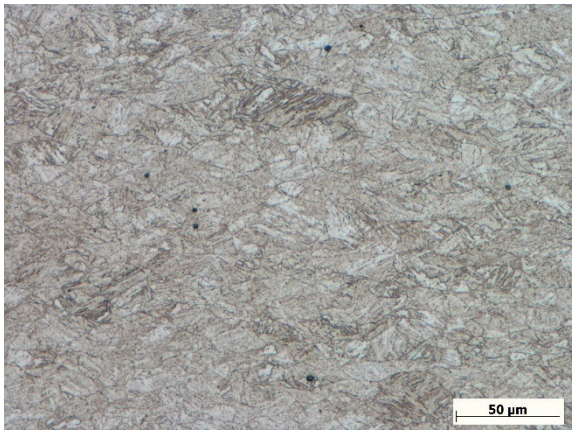

Figure 3 *Microstructure of the base metal*

ferrite, while the untransformed martensite was tempered. The resulting microstructure of this area is the mixture of martensite, ferrite and tempered martensite - similar to other studies [9], [12]. According to other authors, the ICHAZ is the weakest area in the welded quenched-tempered and TMCP steels [1]. The width of the ICHAZ was approximately 740 µm for weld A and slightly less for the weld B - approximately 680 µm, but it is unlikely, that this difference could be significant for the mechanical properties of the whole welded joint. In addition, the base metal near the HAZ was affected by the introduced heat, but heat exposure did not exceed the A_{c1} temperature, so no phase transformation occured, only a tempering of the martensite phase, which actually resulted in decrease of the mechanical properties in that area.

3.2 Microhardness measurements

Phase transformations occurred mainly in the HAZ and strongly affected the resulting mechanical properties of the whole welds. Microhardness measurements were performed by the measuring hardness profiles from the base metal, throughout the HAZs and the weld metal (WM). The microhardness profiles are shown in Figure 6.

Microhardness profiles show continual decrease of microhardness in the direction from the base metal to ICHAZ, which was similar for both welds. This decrease is related to the tempering of martensite in the base metal structure. Decrease of strength related properties is common behavior for all the high strength steels (quenched tempered and TMCP steels), when they are heated in the range 450 °C - A_{c1} temperature, due to martensite tempering [5]. The lowest values of microhardness were obtained in the ICHAZ, where only 66 % of the base metal hardness was recorded. The ICHAZs seems to be most critical areas, even the width of these zones is relatively small (≈ 0.7 mm).

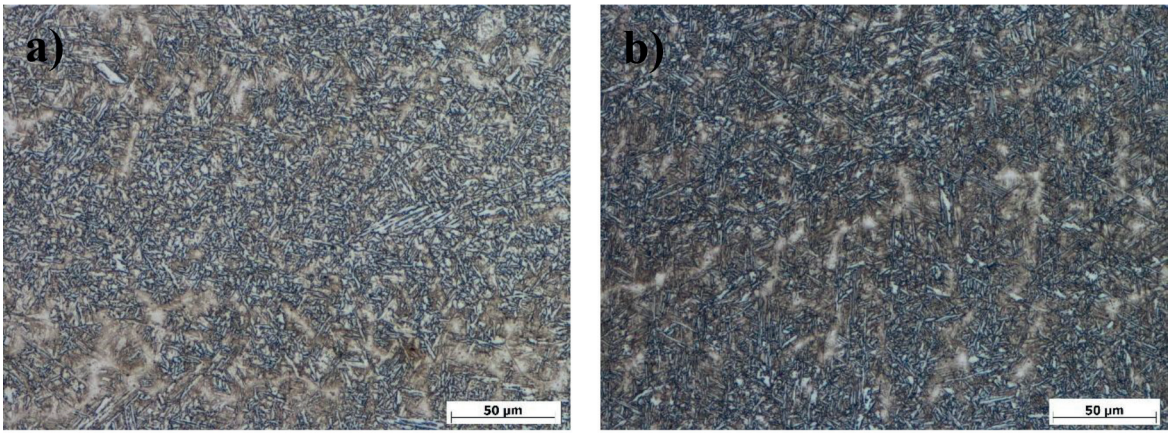

Figure 4 *Microstructures of the weld metal, weld A (a) and weld B (b)*

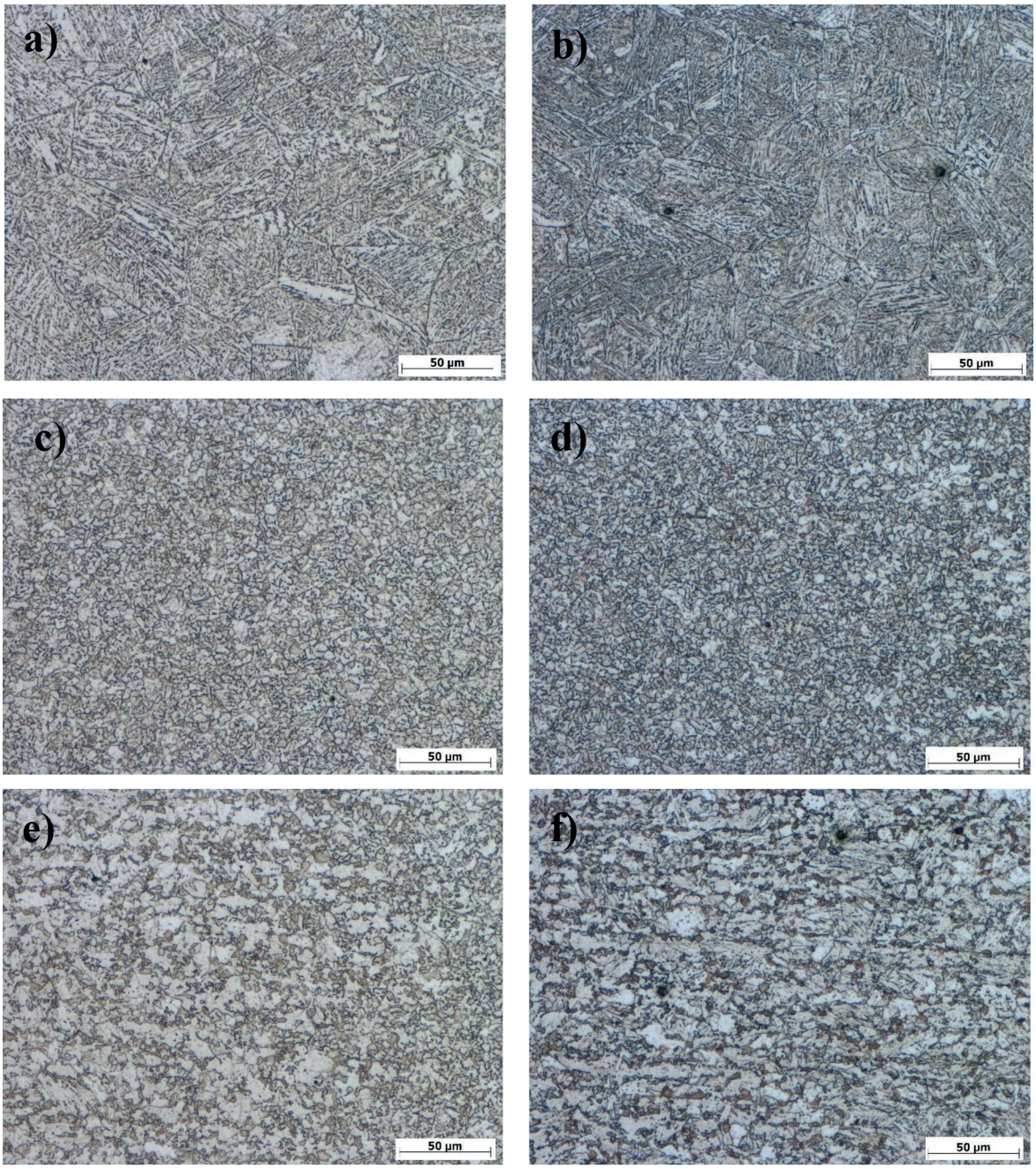

Figure 5 *Microstructures of the HAZ; a, c and e represent CGHAZ, FGHAZ, ICHAZ of weld A, respectively; b, d and f represent CGHAZ, FGHAZ and ICHAZ of weld B, respectively*

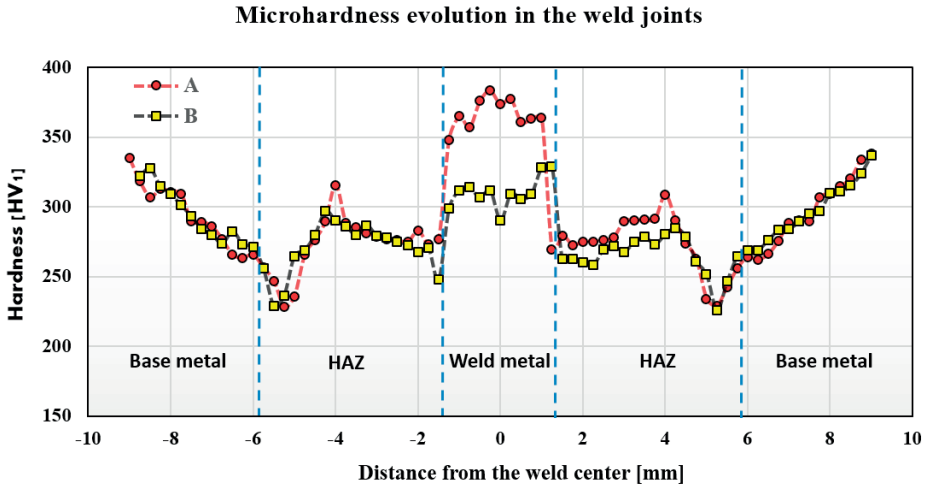

Figure 6 *Micro-hardness profile of the welds*

Table 4 *Results of the welds tensile tests*

	YS [MPa]	UTS [MPa]	Elongation [%]
A-01	794	826	5
A-02	836	858	3
Average - weld A	815	842	4
B-01	830	848	3
B-02	838	877	3
Average - weld B	834	863	3
Base metal	1034	1150	11.5

In FGHAZ, the microhardness started to increase and reached its maximum at microstructures shownin Figure 2c, Figure 2d. For the weld A, the maximum value was a little bit higher than for the weld B, which is related to the amount of heat introduced to the material during the welding. Towards the CGHAZ, a small decrease of microhardness was recorded, what is related tothe excessive grain growth in this zone. The microhardness in that area is given by the mean grain size, which is a function of the cooling rate and the holding time at elevated temperatures [22]. The weld metal microhardness values were different for the two welds. Weld A exhibits the higher microhardness in the weld metal, value of 383 HV_1 was recorded. Though this value is higher than that of the base metal, it is still lower than the considered limit value 450 HV_1 at which an embrittlement of the welded joint can occur. The weld metal in the weld B exhibited the lower microhardness, the maximum value recorded in that area was 328 HV_1. According to that, the higher heat input used in the weld B resulted in the lower hardness of the weld metal. In majority of cases, achieving of lower microhardness values in the weld metal is desirable, but in this case, these values were even lower than the base metal microhardness, thus it could be detrimental for the whole welded joint properties. Some authors suggest that the main problem during the welding of the high strength steels is an increasing hardness in the weld metal region, which causes embrittlement and lower toughness and ductility. In this study, the highest measured hardness in the weld metal region was only 383 HV_1 for weld A and 328 HV_1 for weld B. According to previously mentioned values, the most crucial for theTMCP steels is not an increase of the mechanical properties in the weld metal region but a decrease of the mechanical properties in the HAZ. This is in consistence with other authors, but in the case of thin sheet, the HAZ softening is more dramatic. The sheets with the lower thickness are more susceptible to excessive overheating and thus the degradation of the properties in HAZ is more likely to occur. Depending on the width of that HAZ, the general properties of thewelded joint can be decreased. The TMCP steels are more susceptible to the HAZ softening than thequenched-tempered steels with the similar mechanical properties, sincetheir carbon content is lower and the final mechanical properties are reachedby several strengthening mechanisms. (Precipitates of-V,Nb,Ti-CN, which can dissolve in the matrix at high temperature exposures, also influence the high mechanical properties,which can contribute to the strength reduction after the welding) [6].

3.3 Tensile tests

The tensile tests were performed according to EN ISO 6892-1 standard and two specimens of each weld were tested. Results of the tensile tests are shown in Table 4.

The tensile tests show the significant reduction of the tensile strength and yield strength. The ultimate tensile strength was reduced to 79% of the base metal value in the weld A and 81% in the weld B. Similarly, the yield strength was reduced as well, and it reached 73% of the base metal yield strength in the weld A, and 75% in the weld B. Regardless of welding parameters, the UTS and YS were significantly reduced in both welds. Even more dramatic decrease was recorded for the

tensile elongation. The tensile elongation reduction was similar in both welds and its value reached less than 40 % of the parent base material elongation. Fracture of specimens, tested by the tensile tests, occurred approximately 6 mm from the weld center in all thespecimens, what corresponds to the micro-hardness measurements and appearance of the most softened zone in that area. Thus, it can be said that the fracture occurs in the narrow area of the ICHAZ. This phenomenon is a result of changes in the ICHAZ microstructure, where the softening occurs in the narrow areas. Due to the decrease of the yield strength of these regions, the plastic deformation during the tensile testing occurs in these regions at lower stress values than the yield strength of the rest of the weld; thus the yielding occurs only in those narrow areas, which results in localization of all the plastic deformation to relatively small area causing the significant reduction of the tensile elongation. Some authors claim that the decrease of the ductility and toughness is a result of formation of the brittle martensite phases in the HAZ (especially in the CGHAZ) [22], [23], but according to result of the tensile tests, the fracture occurs in the region of ICHAZ and the reduction of tensile elongation is due to yielding localization. In the study [12], the 8 mm thick S960QL steel sheets were successfully welded by the multi pass GMAW technique, with the heat input ranging from 4.6 kJ/cm to 8.4 kJ/cm. A decrease of hardness in the HAZ was also recorded, but the decrease was only 15 % and result of the tensile tests showed the 7.1 % drop in the UTS and 1.4 % drop in elongation. The failure of the tensile specimens also occurred in the HAZ. There are many other studies where the high strength steels were successfully welded by using the GMAW with the heat input of 7-18 kJ/cm [5], [8], [12], but those studies were carried on much thicker sheets (at least 8 mm) and, in addition, the used steels were mostly of the quenched-tempered type, which has the higher carbon content. Based on the previously mentioned facts, there follow a few important conclusions. At first, the changing of welding parameters (in the range used in this study: 2.3-4.3 kJ/cm) did not significantly affect the overall properties of the welded joints. The weld made with the higher heat input showed the better mechanical properties, though the lower values of microhardness were recorded in the HAZ and WM. Comparison of those results to other studies, made on quenched tempered steels, shows that there is clearly an evident higher drop of the mechanical properties for the TMCP steels, which contain less carbon and the high mechanical properties are also obtained by other strengthening mechanisms. The last very important factor is the thickness of the welded sheets. Sheets of a smaller thickness are more susceptible to excessive overheating and thus the degradation of the properties in the HAZ is more likely to occur, which results in the severe degradation of the overall properties of whole joint.

4. Conclusions

Based on the carried out experiments, the following conclusions can be drawn:

- The S960MC TMCP steels sheets of 3 mm thickness were successfully welded with the G 895M21Mn4Ni2.5CrMo filler metal without appearance of any cracks and weld imperfections.
- The microstructure observations revealed a few different zones in the HAZ, whose evolution was similar for the both sets of welding parameters and only minor differences were recorded as a result of difference in welding parameters.
- The microhardness measurement shows that the ICHAZ is the weakest area of the whole joint, with microhardness of only 66 % of the parent material hardness. Similar values were recorded for both sets of tested welding parameters and no correlation between the ICHAZ microhardness and the heat input was found.
- The weld metal microhardness was found to be dependent on the welding parameters. In the weld A, the hardness exceeds hardness of the base metal, but that value still did not exceed 400 HV_1; thus there are no concerns for any embrittlement. The weld metal in the weld B exhibits the lower hardness than the base metal, due to excessive heat input.
- The tensile tests show the significant reduction of mechanical properties and elongation for both tested welds, where the YS reached 73 % of that of the base metal, the UTS reached 79 % and elongation less than 40 % of the base metal values.
- No significant differences were found in the welds properties after welding with the heat inputs of 2.7 and 4.3 kJ/cm, while the slightly higher mechanical properties were obtained with the latter one.
- Thin sheets of the TMCP steels are strongly susceptible to excessive overheating, so the standard GMAW procedure is not an appropriate method for welding the thin sheets made of the TMCP S960MC steel. Modern welding methods using high energy narrow beams (electron/laser) could be the solution to the problem of TMCP thin sheets welding.

Acknowledgement:

The research was supported by Scientific Grant Agency of the Ministry of Education, Science, Research and Sport of the Slovak Republic under the contract VEGA No. 1/0951/17 and Slovak Research and Development Agency under the contract no. APVV-16-0276 and APVV-14-0096.

References

[1] SHARMA, V., SHAHI, A. S.: Quenched and Tempered Steels Welded with Micro-Alloyed Based Ferritic Fillers. Journal of Materials Processing Technology, 253, 2-16. 2018. https://doi.org/10.1016/j.jmatprotec.2017.10.039

[2] BLACHA, S., WEGLOWSKI, M. S., DYMEK, S., KOPYSCIANSKI, M.: Microstructural and Mechanical Characterization of Electron Beam Welded Joints of High Strength S960QL and Weldox 1300 Steel Grades. Archives of Metallurgy and Materials, 62(2A), 627-634, 2017. https://doi.org/10.1515/amm-2017-0092

[3] BORKO, K., HADZIMA, B., NESLUSAN-JACKOVA, M.: Corrosion Resistance of Domex 700 Steel after Combined Surface Treatment in Chloride Environment. Procedia Engineering, 192, 58-63, 2017. https://doi.org/10.1016/j.proeng.2017.06.010
[4] GOSH, M., KUMAR, K., MISHRA, R. S.: Analysis of Microstructural Evolution during Friction Stir Welding of Ultrahigh-Strength Steel. Scripta Materialia, 63, 851-854, 2010. http://dx.doi.org/10.1016/j.scriptamat.2010.06.032
[5] GASPAR, M., BALOGH, A.: GMAW Experiments for Advanced (Q+T) High Strength Steels. Production Processes and Systems, 6, 9-24, 2013.
[6] WEGLOWSKI, M. S., ZEMAN, M.: Prevention of Cold Cracking in Ultra-High Strength Steel Weldox 1300. Archives of Civil and Mechanical Engineering, 14(3), 417-424, 2014. https://doi.org/10.1016/j.acme.2013.10.010
[7] NEIMITZ, A., DZIOBA, I., LIMNELL, T.: Modified Master Curve of Ultra High Strength Steel. International Journal of Pressure Vessels and Piping, 92, 19-26, 2012. https://doi.org/10.1016/j.ijpvp.2012.01.008
[8] MIN, D., XIN-HUA, T., FENG-GUI, L., SHUN, Y.: Welding of Quenched and Tempered Steels with High-Spin Are Narrow Gap MAG System. The International Journal of Advanced Manufacturing Technology, 55(5-8), 527-533, 2011.
[9] GUO, W., CROWTHER, D., FRANCIS, J. A., THOMPSON, A., LIU, Z., LI, L.: Microstructure and Mechanical Properties of Laser Welded S960 High Strength Steel. Materials and Design, 85, 534-548, 2015. https://doi.org/10.1016/j.matdes.2015.07.037
[10] SENUMA, T.: Physical Metallurgy of Modern High Strength Steel Sheets. ISIJ International, 41(6), 520-532, 2001.
[11] ARSIC, D., LAZIC, V., NIKOLIC, R., ALEKSANDROVIC, S., HADZIMA, B., DJORDJEVIC M.: Optimal Welding Technology of High Strength Steel S690QL. Materials Engineering - Materialove Inzinierstvo, 22, 33-47, 2015.
[12] GUO, W., LI, L., DONG, S., CROWTHER, D., THOMPSON, A.: Comparison of Microstructure and Mechanical Properties of Ultra-Narrow Gap Laser and Gas-Meta-Arc Welded S960 High Strength Steel. Optics and Lasers in Engineering, 91, 1-15, 2017. https://doi.org/10.1016/j.optlaseng.2016.11.011
[13] YOUN - SUK, J., YOUNG-KOOK, L., DONG-CHEOL, K., MOON-JIN, K., IN-SUNG, H., WON-BEOM, L.: Microstructural Evolution and Mechanical properties of Resistance Spot Welded Ultra High Strength Steel Containing Boron. Materials Transactions, 52(6), 1330-1333, 2011. https://doi.org/10.2320/matertrans.M2011005
[14] NOWACKI, J., SAJEK, A., MATKOWSKI, P.: The Influence of Welding Heat Input on the Microstructure of Joints of S1100QL Steel in One Pass Welding. Archives of Civil and Mechanical Engineering, 16, 777-783, 2016. https://doi.org/10.1016/j.acme.2016.05.001
[15] VALKONEN, I.: Ultimate Limit Load in Welded Joints and in Net Section of High Strength Steels with Yield Stress 960 MPa. Procedia Materials Science, 3, 720-725, 2014. https://doi.org/10.1016/j.mspro.2014.06.118
[16] LAZIC, V., ALEKSANDROVIC, S., ARSIC, D., SEDMAK, A., ILIC, A., DJORDJEVIC, M., IVANOVIC, L.: The Influence of Temperature on Mechanical Properties of the Base Metal (BM) and Welded Joint (WJ) Made of Steel S690QL. Metalurgija, 55(2), 213-216, 2016.
[17] QIANG, X., JIANG, X., BIJLAARD, F. S. K., KOLSTEIN, H.: Mechanical Properties and Design Recommendation of Very High Strength Steel S960 in Fire. Engineering Structures, 112, 60-70, 2016. https://doi.org/10.1186/s40038-017-0017-6
[18] TALAS, S.: The Assessment of Carbon Equivalent Formulas in Prediction the Properties of Steel Weld Metals. Materials and Design, 31, 2649-2653, 2010. https://doi.org/10.1016/j.matdes.2009.11.066
[19] OYYARAVELU, R., KUPPAN, P., ARIVAZHAGAN, N.: Metallurgical and Mechanical Properties of Laser Welded High Strength Low Alloy Steel. Journal of Advanced Research, 7, 463-472, 2016. https://doi.org/10.1016/j.jare.2016.03.005
[20] BARSOUM, Z., KHURSHID, M.: Ultimate Strength Capacity of Welded Joints in High Strength Steels. Procedia Structural Integrity, 5, 1401-1408, 2017. https://doi.org/10.1016/j.prostr.2017.07.204
[21] MAZUR, M., ULEWICZ, R., NOVY, F., SZATANIAK, P.: The Structure and Mechanical Properties of DOMEX 700 MC Steel. Communications - Scientific Letters of the University of Zilina, 31(4), 54-57, 2013.
[22] LAN, L., QIU, CH., ZHAO, D., GAO, X., DU, L.: Microstructural Characteristics and Toughness of Simulated Coarse Grained Heat Affected Zone of High Strength Low Carbon Bainitic Steel. Material Science and Engineering A, 529, 192-200, 2011. https://doi.org/10.1016/j.msea.2011.09.017
[23] LAN, L., QIU, CH., ZHAO, D., GAO, X., DU, L.: Analysis of Microstructural Variation and Mechanical Behaviors in Submerged Arc Welded Joint of High Strength Low Carbon Bainitic Steel. Material Science and Engineering A, 558, 592-601, 2012. https://doi.org/10.1016/j.msea.2012.08.057

Petr Hruby - Tomas Nahlik - Dana Smetanova*

MATHEMATICAL MODELLING OF SHAFTS IN DRIVES

Propeller shafts of the vehicle's drive transmit a torque to relatively large distances. The shafts are basically long and slender and must be dimensioned not only in terms of torsional stress, but it is also necessary to monitor their resistance to lateral vibration.

In the paper, a simple model (of the solved problem) is constructed by the method of physical discretization, which is evident from the nature of the centrifugal force fields' influence on the spectral properties of the shaft. An analytical solving of speed resonances prop shafts test model (whose aim is to obtain values for verification subsequently processed models based on the transfer-matrix method and the finite element method) is performed.

Keywords: *Hook's joint, shaft, vibration, mathematical and physical model, transfer matrix, Finite element method*

1. Introduction

Problem of modelling and description of propeller shafts is quite old [1]. Propeller shafts of drive vehicles are evolutionary systems. Evolutionary system means the parameters of the shaft are changing in time. The shafts are long and slender. For this reason, they are affected by torsional stress and also by lateral and transversal vibrations [2].

Due to the continuous operations, the shafts have to operate in subcritical speed. Results of previous works, which were also compared to experiments, showed that the propeller shafts represent strong evolutionary systems (increasing the angular velocity of rotation significantly reduces the spectrum of natural frequency relative lateral vibrations) and in practical calculations it is necessary to respect this influence. For that reason, it is not possible to model the shafts using procedures that are commonly reported in the literature, but it is necessary to formulate a model that allows for this effect to be respected. Due to results of previous works and experiments, it is not possible to model the shafts using procedures that are commonly reported in the literature [3], [4], but it is necessary to formulate a model that allows respecting that with increasing the angular velocity of rotation the spectrum of natural frequency relative lateral vibrations is significantly reduced.

Propeller shafts are in a steady state stressed by excitation bending moment's harmonics and their vectors are perpendicular to the rotating plane of a relevant fork Hooks joints. The drive torque mentioned in a steady state is generated due to the transmission flow through Hooks joints and causes lateral oscillations of the propeller shaft in its rotating space. In formulating a mathematical model, it is necessary to start from the assumption of existence of the relative spatial bending vibration in the shaft system 0(x,y,z), which rotates at an angular speed . If one neglects the Coriolis force and gyroscopic moments acting on the element of the shaft, one can solve the problem in the rotating plane 0(x,y). The instantaneous state of the element is determined by the velocity and the angular velocities. This article aims to build a mathematical model of a coupling shaft to calculate spectral and modal properties of the connecting shaft with respect to the field of centrifugal forces that is causing the addition of natural frequencies of bending vibrations relative to the angular velocity of the shafts rotation.

2. Formulation of the problem

Propeller shafts are in a steady state stressed by excitation bending moments harmonic, and their vectors are perpendicular to the rotating plane of a relevant fork Hook´s joints (Figure 1).

A model was built on an assumption of existence of the relative spatial bending vibration in the shaft system , (Figure 2), which rotates at an angular speed $\vec{\varphi}_x$. The dimensionality of the problem can be reduced from 3D to 2D by neglecting the Coriolis force and gyroscopic moments acting on the element of the shaft. Then, one can solve the problem in the rotating plane . The instantaneous state of the element is determined by the angular velocity $\vec{\varphi}_x$, the velocity $\vec{v}_x$ and the angular velocity $\vec{\varphi}_{zs}$. A mathematical model of a coupling shaft was built in order to calculate the spectral and modal properties of the connecting shaft, including the natural frequency of bending oscillations.

3. Physical discretization

The drive shaft, shown in Figure 1 (consider solid bearings), is replaced by a discrete mechanical system with only one degree of freedom. This system is divided into two equal halves, which represent an intangible spring (Figure 3) having the rigidity $\frac{k}{2}$.

* [1]Petr Hruby, [2]Tomas Nahlik, [2]Dana Smetanova
[1]Department of Mechanical Engineering, The Institute of Technology and Business, Ceske Budejovice, Czech Republic
[2]Department of Informatics and Natural Sciences, The Institute of Technology and Business, Ceske Budejovice, Czech Republic
E-mail: smetanova@vstecb.cz

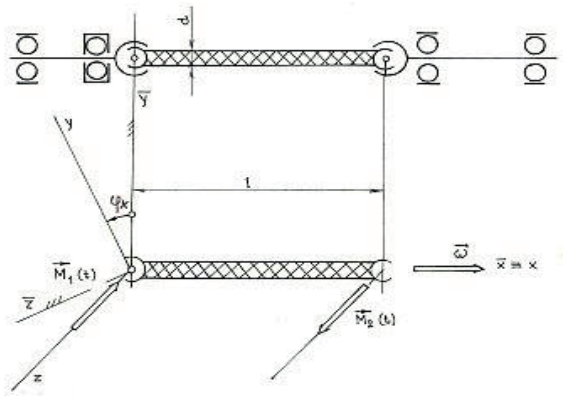

Figure 1 *Model of propeller shafts*

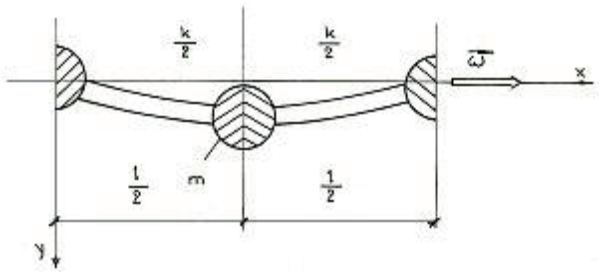

Figure 3 *Replacing of the drive shaft by divided system of one degree of freedom*

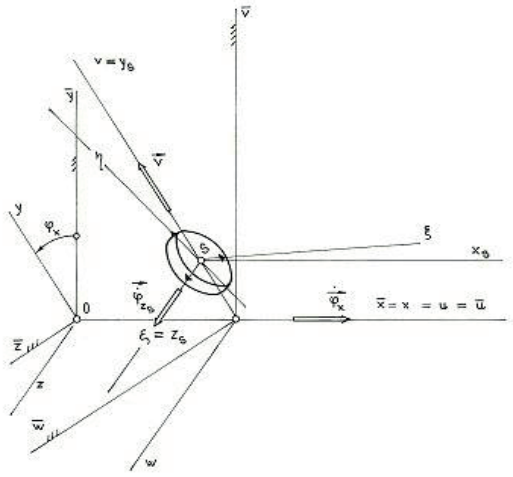

Figure 2 *Coordinate system of the shaft*

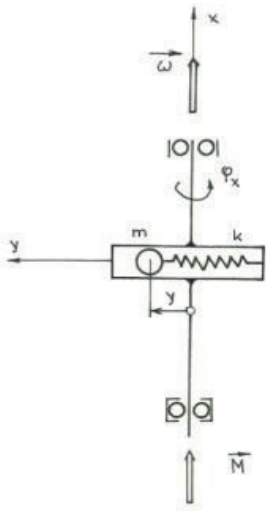

Figure 4 *Modelling of the shaft by the spring*

The mass is concentrated to the endpoints of the springs. This means that the two fixed points belongs to the support and two others fixed points will merge into one in the middle of the shaft. This middle point has the mass of $m = \frac{Sl_p}{2}$, where S is the cross-section area, l is length of the shaft and ρ is density. This model can be simply transformed to model of the spring (Figure 4).

In this case, one can determine the stiffness of this spring as $k = \frac{48EJ}{l^3}$, where E is a modulus of elasticity in tension, J is defined as $J = \frac{\pi}{4}r^4$ and l is length of the shaft. Assuming the constant angular velocity ω it is necessary to introduce the moment $\vec{M}$. Now one can write equations for kinetic and potential energy of the spring, respectively, as:

$$E_k = \frac{1}{2}m\dot{y}^2 + \frac{1}{2}m\left(y\dot{\varphi}_x\right)^2 \quad E_p = \frac{1}{2}ky^2 \tag{1}$$

In addition, equations of motion are written by formulas:

$$m\ddot{y} + \left(k - m\omega^2\right)y = 0,\ M - 2my\dot{y}\omega = 0 \tag{2}$$

Equation of relative oscillating movement in rotating plane can be rewritten in the form:

$$\ddot{y} + \Omega^2 y = 0 \tag{3}$$

where $\Omega = \sqrt{\frac{k}{m} - \omega}$ is the natural frequency of relative undamped oscillations. By modification of this equation one obtains:

$$\Omega^2 + \omega^2 = \frac{k}{m} \tag{4}$$

which is equation of the circle with origin at $O(\omega, \Omega)$ and radius $\frac{k}{m}$.

4. The test model

The test model parameters are chosen of the prototype car – Skoda 781. This choice comes from the cooperation with the industry. Parameter of this test model are: $r = 0.0105m$, $l = 0.65m$, $E = 2.1 \cdot 10^{11}Pa$ and $\rho = 7.8 \cdot 10^3 kg \cdot m^{-3}$. Using these parameters the following was obtained: $J = 9 \cdot 10^{-4}m^4$, $S = 3.46 \cdot 10^{-4}m^2$, $k = 3.3 \cdot 10^5 Nm^{-1}$, $m = 0.88kg$ and $\Omega(0) = 591.9483rad \cdot s^{-1}$ (see Figure 5).

It is also possible to obtain an analytical solution by solving the following equation derived in [5], which is describing the model in Figure 6:

$$\frac{\partial^4 y}{\partial x^4} - \frac{\rho S r^2}{4EJ} \cdot \frac{\partial^4 y}{\partial x^2 \partial t^2} - \frac{\rho S r^2 \omega^2}{4EJ} \cdot \frac{\partial^2 y}{\partial x^2} + \frac{\rho S}{EJ} \cdot \frac{\partial^2 y}{\partial t^2} - \frac{\rho S \omega^2}{EJ} \cdot y = 0 \tag{5}$$

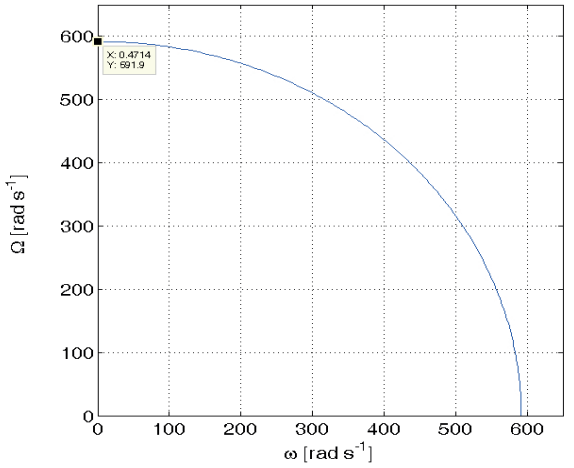

Figure 5 *The natural frequency dependence of discrete model's relative transverse vibrations (shown in Figure 4) on the angular velocity of rotation*

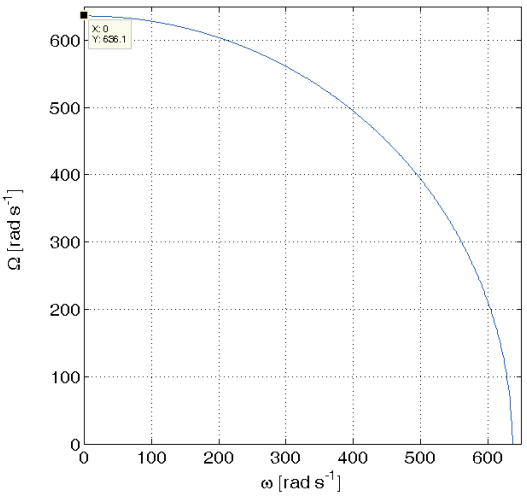

Figure 7 *The graph of functional dependence of the angular frequency (Ω) lateral vibrations in terms of the angular speed of rotation (ω) of the propeller shaft's test model*

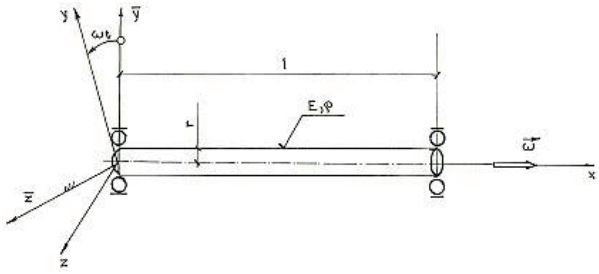

Figure 6 *Test model for calculation of propeller shaft's speed resonance*

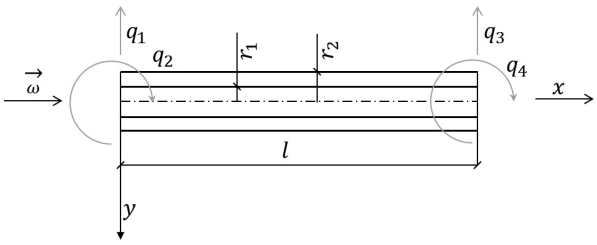

Figure 8 *The element of the propeller shaft in the state of combined bending-gyratory vibrations*

Solution of Equation (5) provides the relation between Ω and ω in form $\frac{\Omega^2}{R^2}+\frac{\omega^2}{R^2}=1$. For the test model, the final analytic solution is: $R=\frac{r}{2}\sqrt{\frac{E}{\rho}}\left(\frac{\pi}{l}\right)^2$.

If one calculates R with given testing parameters, the value $R = 636.1432 rad \cdot s^{-1}$ is obtained and, by parametrizing with ω, the graph in Figure 7.

5. The Finite element method

An element of the shaft in the shape of prismatic section with the circular cross-section is considered (Figure 8).

In this case, the deflection can be described as $y(x,t)=\sum_{i=1}^{4} q_i(t)\Phi_i(x)$, where $\Phi_i(x)$ are the 3rd order polynomials. For more details see [6]. One can take this model and join it multiple times together to create graduated shaft (Figure 9). The graduated shaft means that the shaft is divided into several parts, which are mathematically described separately. These descriptions of part are linked in the model through the boundary conditions of the parts.

Using the finite element method [7], the whole shaft is then described by a matrix and each part as a sub-matrix. For more details see [6], [8], [9], [10].

6. The Transfer-matrix method

For calculation using the transfer-matrix method, the model of the shaft is treated as one dimensional continuum [11] of constant circular cross section. It is defined by:

- Geometrical parameters $l[m]$ - the length of the one dimensional continuum $r[m]$ - radius of cross section of the shaft.
- Material constants $\rho[mkg^{-3}]$ - the material density $E[Pa]$ - the modulus of elasticity in tension or compression.
- Operating parameter $\omega[rads^{-1}]$ - the angular velocity of rotation of the plane $O(x,y)$ around the axis x.

The solution is sought in the form of

$$y(x,t)=Y(x)e^{i\Omega t} \tag{6}$$

The solution of Equation (6) can be arranged to the vector of state $-\mathbf{V}(x)$. This vector is bound by the initial vector state to a coordinate of $x = 0$ by the relationship:

$$\mathbf{V}(x) = \mathbf{H}(x)\mathbf{V}(0) \tag{7}$$

and boundary vectors $\mathbf{V}(0)$, $\mathbf{V}(l)$ of the shaft's condition are bound by the transfer matrix of the continuum section $\mathbf{H}(l)$. This means:

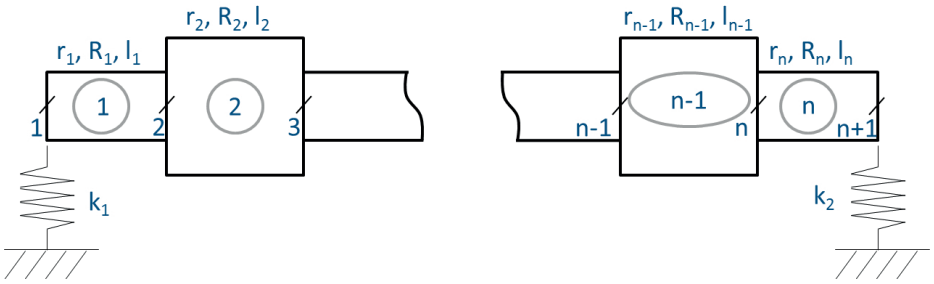

Figure 9 *Dynamic model of graduated shaft*

$$\mathbf{V}(l) = \mathbf{H}(l)\mathbf{V}(0) \tag{8}$$

Where

$$\mathbf{V}(l) = \begin{bmatrix} 0 \\ Y'(l) \\ 0 \\ -Q(l) \end{bmatrix}, \mathbf{V}(0) = \begin{bmatrix} 0 \\ Y'(0) \\ 0 \\ -Q(0) \end{bmatrix} \tag{9}$$

These are boundary vectors for the intended type of the deposit - zero deflection, zero bending moments at the edges. $Y'(0), Y'(l)$ are the amplitudes of the deflection slope line, $Q(0), Q(l)$ are the amplitudes of the shear forces at the edges of the shaft. From Equation 7, Equation 8 and Equation 9 following statements can be derived:

$$\begin{bmatrix} H_{12} & -H_{14} & 0 & 0 \\ H_{22} & -H_{24} & -1 & 0 \\ H_{32} & -H_{34} & 0 & 0 \\ H_{42} & -H_{44} & 0 & 1 \end{bmatrix} \cdot \begin{bmatrix} Y'(0) \\ Q(0) \\ Y'(l) \\ Q(l) \end{bmatrix} = \mathbf{0} \tag{10}$$

The frequency equation can be obtained from the condition of the non-trivial solution.

$$H_{12}H_{34} - H_{14}H_{32} = 0 \tag{11}$$

Based on properties of the shaft and initial condition, the explicit form of the transfer matrices $H_{12}, H_{34}, H_{14}, H_{32}$ can be found. For more details see [12].

7. Conclusion

The mathematical model, based on the physical discretization was defined and used for solving the problem of finding the critical speed of rotations. This model was programmed as a script in the GNU Octave. In addition, there is a possibility of using the analytical solution derived from Equation (6). Both of these solutions give the circular dependency of Ω and ω (Equation (5) and Equation (7)). The use of Finite element method for modelling the propeller shaft and for calculation of critical speed was attempted. However, this needs a little bit more of programming and calculation. The use Transfer-Matrix method was tried, as well. Using this method should enable modeling of a shaft composed of different parts with different properties. The initial goal is to prepare the scripts for testing. After that, the program should be written, which will be more user friendly than the scripts.

Acknowledgement

The work presented in this paper was supported by project TA 04010579 of Technology Agency of the Czech Republic and grant IGS201801 of the Institute of Technology and Business in Ceske Budejovice.

References

[1] EVERNDEN, H. I. F.: The Propeller Shaft or Hooke's Coupling and the Cardan Joint [online]. Proceedings of the Institution of Mechanical Engineers: Automobile Division, 2(1), 100-110, 2006. Available: http://journals.sagepub.com/doi/10.1243/PIME_AUTO_1948_000_013_02 [accessed 2018-07-09]. https://doi.org/10.1243/PIME_AUTO_1948_000_013_02. ISSN 0367-8822

[2] HADDARA, M. R.: On the Transverse Vibration of a Propeller-Tail Shaft System. Ocean Engineering, 15(2), 119-126, 1988. https://doi.org/10.1016/0029-8018(88)90023-6

[3] HAJEK, E., REIF, P., VALENTA, F.: Flexibility and Strength I / Pruznost a Pevnost I (in Czech). State Publishing House of Technical Literature (SNTL), Prague, 1988.

[4] HAJEK, E., REIF, P., VALENTA, F.: Flexibility and strength II / Pruznost a Pevnost II (in Czech). Czech Technical University in Prague (CVUT), Prague, 1985.

[5] HRUBY, P.: Cardan Coupling Shaft Vibrations in the Rotating Plane. PhD. thesis, University of Mechanical and Electrical Engineering (VSSE), Plzen, 1979.

[6] HRUBY, P., NAHLIK, T., SMETANOVA, D.: Proposal Mathematical Model for Calculation of Modal and Spectral Properties. Post-conference proceedings of extended versions of selected papers of conference Mathematics, Information Technologies and Applied Sciences (MITAV 2017), Czech Republic, 131-140, 2017.

[7] REDDY, J. N.: An Introduction to the Finite Element Method, 2nd ed. McGraw-Hill, New York, 1993.

[8] HRUBY, P., HLAVAC, Z., ZIDKOVA, P.: Application of the Finite Element Method in Determination of Modal and Spectral Properties of Propeller Shafts Bending Vibrations. Proceedings of the 5th biannual CER Comparative European Research Conference - international scientific conference for Ph.D. students of EU countries, United Kingdom, 132-135, 2016.

[9] HOSCHL, C.: The Use of Small Computers in the Dynamics of Systems. DT CSVTS Prague, 1983.

[10] HRUBY, P.: Bending-Gyratory Vibrations of Shafts in Drives with Joints. University of Mechanical and Electrical Engineering (VSSE), Plzen, 1981.

[11] ZIDKOVA, P., HRUBY, P.: Mathematical Model of One-Dimensional Continuum in State of Combined Bending-Gyratory Vibration / Matematicky Model Jednorozmerneho Kontinua ve Stavu Kombinovaneho Ohybove-Krouziveho Kmitani (in Czech). Proceedings of International Masaryk Conference for Ph.D. Students and Young Researchers (MMK 2016), Czech Republic, 1804-1813, 2016.

[12] HRUBY, P., HLAVAC, Z., ZIDKOVA, P.: The Transfer-Matrix Method in the Application for an One-Dimensional Linear Continuum Speed Resonance. Proceedings of the 5th biannual CER Comparative European Research Conference - international scientific conference for Ph.D. students of EU countries, United Kingdom, 141-145, 2016.

Petr Jonsta - Zdenek Jonsta - Irena Vlckova - Jaroslav Sojka*

INFLUENCE OF PHYSICAL-METALLURGICAL FACTORS ON RESISTANCE OF API CARBON STEELS TO SULPHIDE STRESS CRACKING

The paper deals with the influence of physical-metallurgical factors on resistance of the X52 and X70 steels in accordance with API 5L to sulphide stress cracking. The resistance against this kind of damage is relatively clearly claimed by usually used approach in this field by the tensile strength of steel, its hardness level, respectively. However, the experimental results had shown that the microstructural parameters are also the significant factors, which affect the resistance of steels to sulphide stress cracking. It was found that the quenching and tempering can significantly increase the resistance to sulphide cracking as in the case of hydrogen induced cracking. It would be appropriate to re-evaluate the material selection process that recommends to use the steels not exceeding approved strength limit in a case of the sulfane environments where the risk of the sulphide stress cracking exists.

Keywords: *carbon steels, microstructure, mechanical properties, heat treatment, sulphide stress cracking*

1. Introduction

Aspects of the hydrogen embrittlement are related to the steel products from their production to their long-time exploitation in working conditions containing hydrogen or in the conditions where the hydrogen release and transition in the metal matrix occur.

Environment containing sulfane, which relates with the mining industry, transport, storage and refining of petroleum and natural gas, belongs to a group of the working conditions, where the hydrogen can penetrate into the material under specific conditions and degrade it. Mechanisms of such a kind of damage are called as Hydrogen Induced Cracking (HIC), Sulphide Stress Cracking (SSC), Stress Oriented Hydrogen Induced Cracking (SOHIC). There is a generally accepted fact that the hydrogen is generated by the corrosion processes on the steel surface and that it diffuses inside the material in a form of the atoms or the protons. The theories of Hydrogen Enhanced Decohesion (HEDE) [1], [2], [3], Hydrogen Enhanced Localized Plasticity (HELP) [4], [5], [6] and Adsorption Induced Dislocation Emission (AIDE) [7], [8] are quoted today.

Increasing the share of the steel products with higher added value is one of the priority interests of the Czech steel industry. One of the possible ways is to increase the production of thermo-mechanically rolled sheets used for welded the pipelines for transportation of petroleum and natural gas to long distances. Those sheets are made of C-Mn steels with carbon content within 0.05 to 0.1 wt. % and micro-alloyed by Niobium, Titanium and Vanadium. In combination with controlled rolling and accelerated cooling is then possible to obtain the steels with high yield strength and good ductility, which are known as the High Strength Low Alloy Steels (HSLA). These steel grades are sorted in petrochemical industry in accordance with API 5L standard, e.g. X52, X60, X70, X80 etc., where the number expresses the yield strength value in imperial units ksi. Due to increased global demand for energy consumption and building of the pipelines for severe climatic working conditions a pressure in the pipelines increases and thus it makes higher requests for mechanical properties and resistance to the corrosion cracking of the HSLA steels [9], [10], [11].

Resistance of the materials to the degradation in conditions containing sulphane is related to various physical-metallurgical factors, which are of different importance. It is a matter of chemical composition, tensile strength level and microstructural parameters. According to the worldwide accepted standard NACE MR0175/ISO 15156 [12] the strength and the hardness of the steel, respectively, one can regard as a reference parameters. Limit values, valid for carbon and low alloyed steels (above them the steel is susceptible to the SCC) are set at 690 MPa and 22 HRC, respectively. The microstructure is taken into account only indirectly - within the limits given by the heat treatment process - although the steels mentioned above are normally available as-rolled, as-normalized or as-quenched. The aspects of segregation phenomenon, amount, distribution and shape of the non-metallic inclusions, are not explicitly reflected. The usually applied approach for selection of material being resistant against the SSC based on only strength or hardness criterion could not be sufficient in some cases; that is documented by various research works [13], [14], [15] and this paper also reflects this fact.

Due to the situation that the petrochemical industry represents the most demanding application from a view of a resistance against the influence of the hydrogen, it is necessary to take care of suitable precautions for the steel producers and also for the

* [1]Petr Jonsta, [1]Zdenek Jonsta, [2]Irena Vlckova, [1]Jaroslav Sojka
[1]Faculty of Metallurgy and Materials Engineering, VSB-TU Ostrava, Ostrava-Poruba, Czech Republic
[2]RMTSC, Material & Metallurgical Research Ltd., Remote Site Ostrava, VUHZ a. s., Dobra, Czech Republic
Email: petr.jonsta@vsb.cz

Table 1 *The chemical composition of the steels (wt. %)*

Steel	C	Mn	Si	P	S	Cr	Ni	Mo	V	Nb	Ti	Al
X52	0.09	0.92	0.28	0.007	0.01	0.02	0.01	-	0.004	0.03	0.01	-
X70	0.10	1.51	0.35	0.019	0.004	0.07	0.02	0.01	0.05	0.04	0.01	0.03

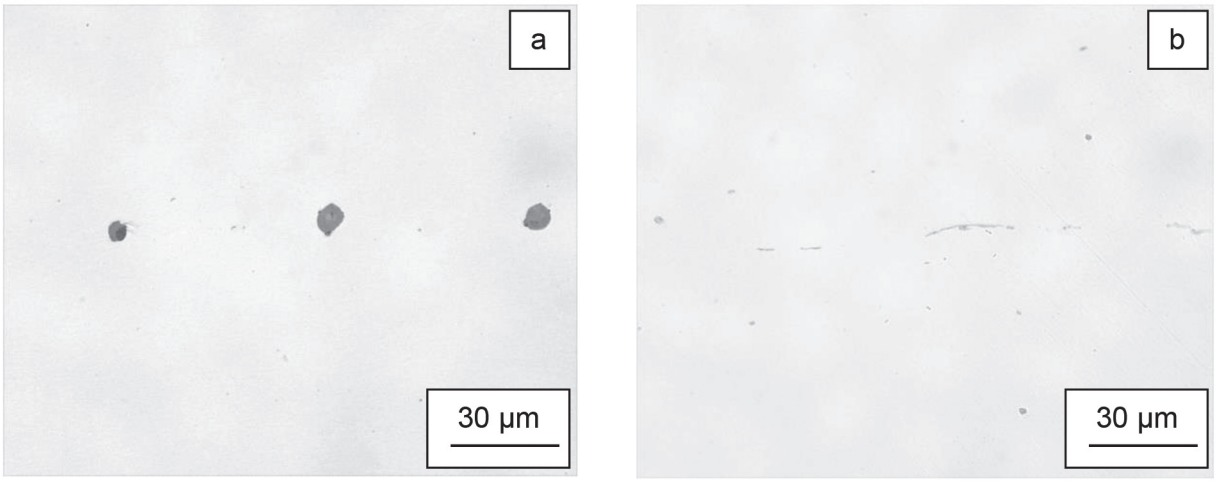

Figure 1 *Examples of non-metallic inclusions in the X52 steel*

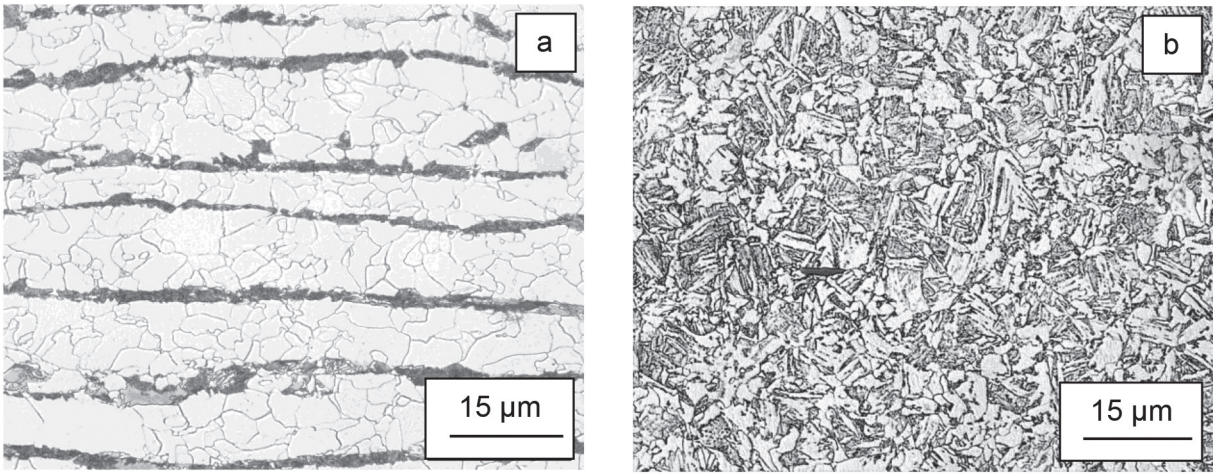

Figure 2 *Microstructure of the X52 steel in the mid-thickness*

final operators of the steel construction, to reduce the formation of the hydrogen embrittlement to a minimum.

This paper deals with the influence of physical-metallurgical factors on resistance of the high strength micro-alloyed steels X52 and X70 to the SSC.

2. Materials and experimental procedure

Tube made of the X52 (559/30 mm) steel and sheet made of the X70 (12 mm) steel, both in accordance with API 5L standard, were used. The chemical composition of the steels is given in Table 1. The X52 steel was studied after rolling, in the as-received state (X52/AR) and after laboratory quenching and tempering at 870 °C/40 min/water + 600 °C/90 min/air (X52/QT). The X70 steel was tested after the rolling, in the as-received state (X70/AR).

Structural analysis was performed by the optical metallography. Tensile properties were determined with using of the MTS 100 kN testing machine on cylindrical specimens with a diameter of 5 mm and a gauge length 25 mm, which were taken from the mid-thickness of the materials in the longitudinal direction.

Resistance to the SSC was tested in accordance with the NACE TM 0177 Standard, Method A [16]. The testing solution was a water solution containing 5.0 wt. % NaCl and 0.5 wt. % of glacial acetic acid saturated by H_2S. The constant load tests were performed on sub-sized cylindrical specimens with a diameter of 3.81 mm and a gauge length of 25.4 mm, which were taken from the mid-thickness of the materials in the longitudinal direction. The applied load varied from 0.5 to 0.9 of the yield strength of the materials being tested. Based on the test results, a critical stress could be evaluated for each of the steels and states that were tested. The fracture surface appearance of the ruptured specimens was observed by use of the scanning electron microscopy (SEM).

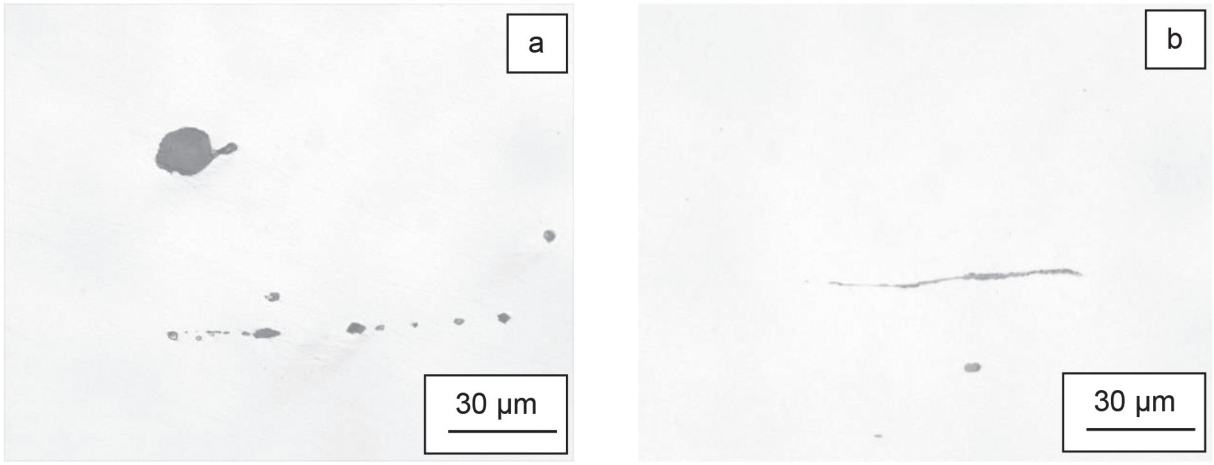

Figure 3 *Examples of non-metallic inclusions in the X70/AR steel*

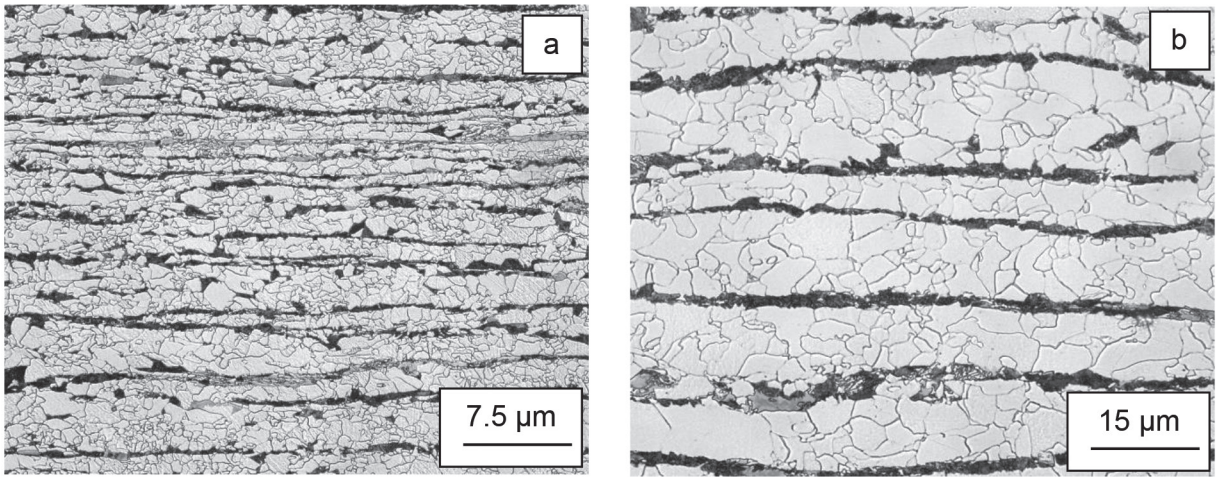

Figure 4 *Microstructure of the X70/AR steel in the mid-thickness of the sheet*

3. Results and discussion

Evaluation of a micro-cleanliness of the X52 steel relieved a presence of relatively high amount of formed manganese sulphides that relate with higher sulphur content in the steel (Figure 1b). In addition, the globular oxide inclusions were found (Figure 1a).

The microstructure of the X52/AR steel is ferritic with narrow pearlite lines where the occurrence of not-tempered martensite is observed in some areas (Figure 2a). The microstructure of the X52/QT steel consists of bainite and ferrite (Figure 2b).

The micro-cleanliness of the X70 steel being examined was very good. Mostly globular complex oxidic or oxi-sulphidic inclusions were observed. Due to the low sulphur content the formed manganese sulphidic inclusions were occasionally detected and they did not play a significant role during the initiation of the defects (Figure 3a and Figure 3b) [17].

The surface microstructure of the X70/AR steel consisted of a fine grained ferrite and narrow lines of pearlite. Between the pearlite lines the lines of not-tempered martensite in the mid-thickness of the sheet were observed (Figure 4a and Figure 4b).

The mechanical properties of the steels are summarized in Table 2. The laboratory heat treatment of the steel X52 caused a significant increasing of the yield and tensile strength (approx. about 100 MPa) with preserving of very good plastic properties.

The results of the SSC tests, performed at constant loads, according to the NACE TM0177, Method A are presented in Figure 5.

The specimens made of the X52/AR steel passed the loading corresponding only to 58 % of the $R_{p0.2}$ that equals to 226 MPa. Thus, the X52/AR steel shown an insufficient resistance to the SSC. However, the X52/QT steel, after the quenching and tempering, passed the loading equal to 92 % of the $R_{p0.2}$ what corresponds to 447 MPa and thus it fully passed the request given for the steels being resistant to the SSC. In this particular case a favorable influence of the heat treatment was confirmed when the tempered hardened structures increased the resistance of the steel X52 to the SSC. Therefore, it was confirmed that one of the key factors, from a view of the resistance to the SSC, was the microstructure. Ruptured specimens were subjected to the fractographical analysis. The specimens were ultrasonically cleaned in a weak solution of phosphoric acid due to the high contamination of its fracture surfaces.

Most probably the lines of not-tempered martensite in the microstructure of the X52/AR steel resulted in a formation of longitudinally oriented cracks on the fracture surfaces (Figure 6). The round-shaped quasi-brittle areas looking like „fisheye“, [18], were also observed on the fracture surfaces (Figure 7). The fracture surface consisted mostly of transcrystalline, brittle, quasi-cleavage character. Zones of the ductile fracture occurred to

Table 2 *Mechanical properties of the steels*

Steel/state	Yield Strength 0.2 % offset (MPa)	Tensile Strength (MPa)	Elongation in 50 mm (%)
X52/AR	390	515	24.5
X52/QT	486	610	22.5
X70/AR	500	600	30.5

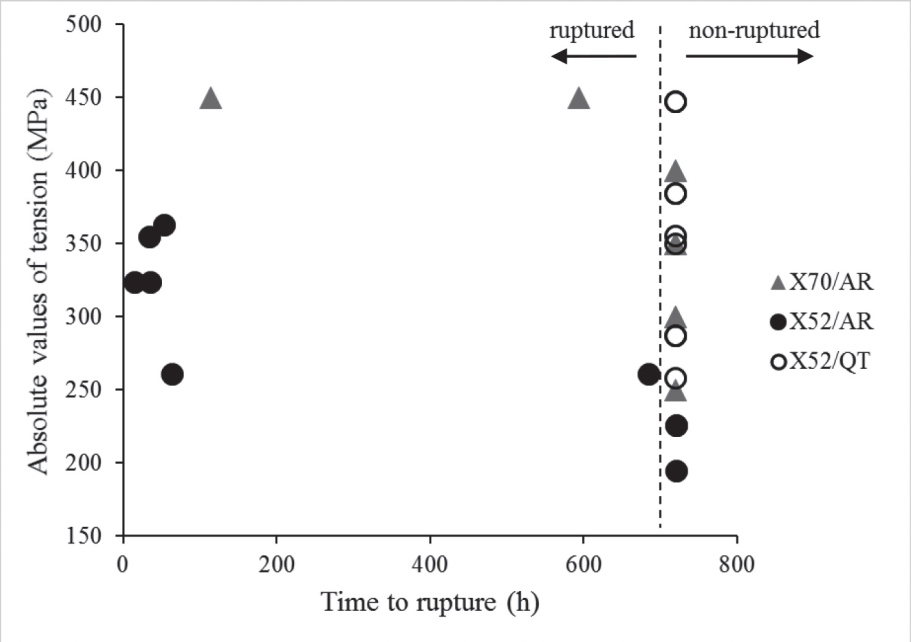

Note: 720 hours is the standard duration of the test
Figure 5 *The results of the SSC tests*

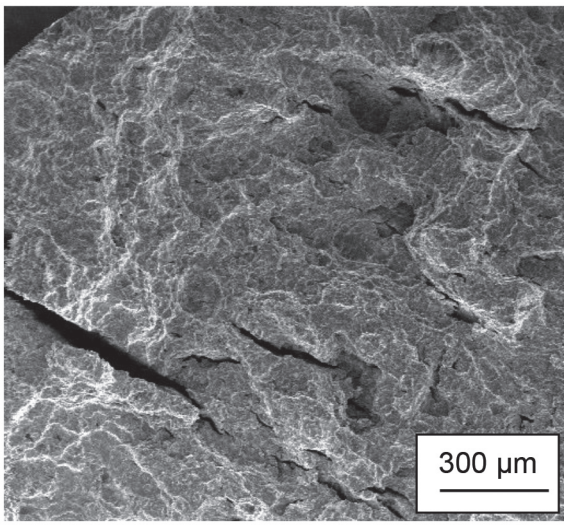

Figure 6 *Fracture surface of the X52/AR steel, 67 % $R_{p0.2}$ (261 MPa), 63 hours*

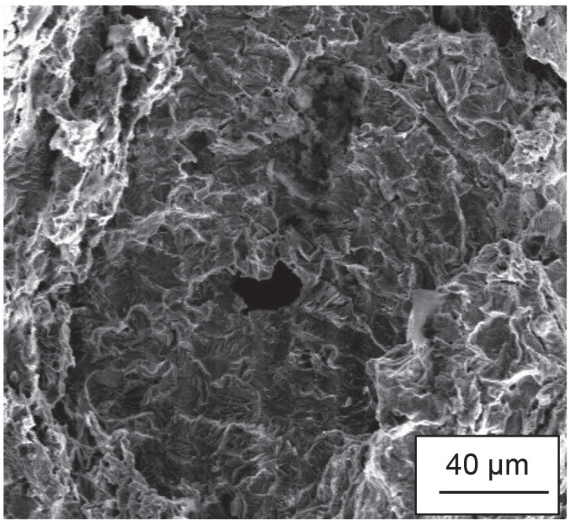

Figure 7 *Fracture surface of the X52/AR steel, 91 % $R_{p0.2}$ (355 MPa), 40 hours*

a limited extent. The next example of the fracture surface is shown in Figure 8. The specimens after the laboratory quenching (X52/QT) were not subjected to the fractographic analysis because none of the specimens ruptured during the SCC test.

The specimens made of the X70/AR steel loaded by 80 % of the $R_{p0.2}$ and less did not rupture after the prescribed test duration, but some longitudinal cracks were found on its surface by visual examination (Figure 9); most probably they were initiated by the lines of not-tempered martensite, which were detected in the mid-thickness of the sheet. The cracks were parallelly oriented with the applied loading force and thus its origin can be attributed to the HIC). Though the cracks did not lead to the final rupture of the specimens, it is possible to declare that the steel was not resistant to the SSC. The damaged specimens were subjected to the fractographic analysis that confirmed the key role of the not-tempered martensite lines in the microstructure when the SCC occurred (Figure 10). Similar to the case of the X52/AR steel, the

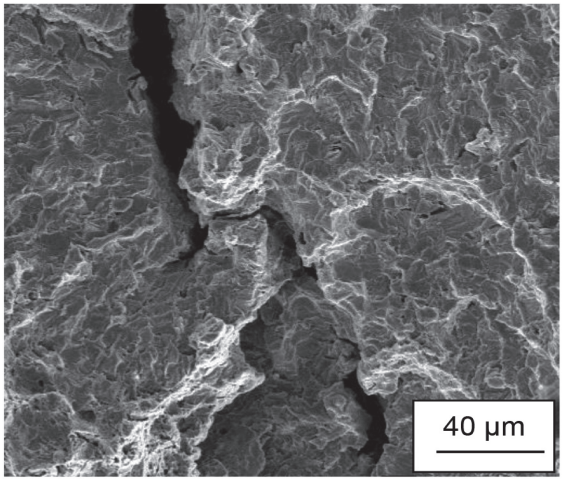

Figure 8 *Fracture surface of the X52/AR steel, 67% $R_{p0.2}$ (261 MPa), 63 hours*

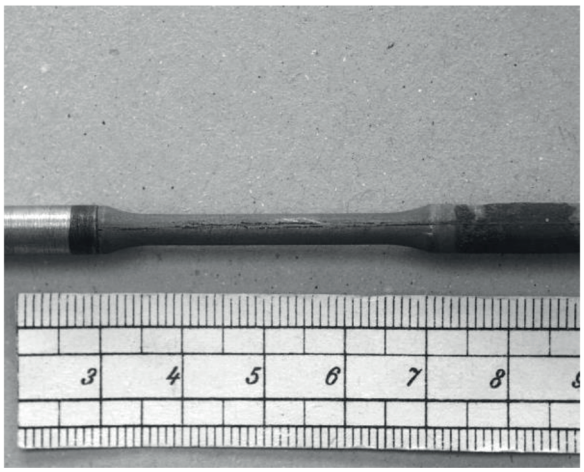

Figure 9 *Longitudinal cracks on the X52/AR steel specimen*

round-shaped zones of the quasi-cleavage damage were observed; in their centers were found the non-metallic inclusions.

Comparison of the SSC testing results between the as-rolled and the as-quenched and tempered states brings up a very important finding that the quenched and tempered state shows much higher resistance to the SSC. Even the generally applied approach, published in NACE MR0175/ISO 15156, is based on the fact that the resistance to the SSC is decreasing with increasing strength of the steel. The standard also allows to use the unalloyed (carbon) steels in as-rolled and as-quenched and tempered states, as well, if the actual hardness does not exceed 22 HRC, without any need to perform the SSC test. However, the results obtained in this paper show that the steels being regarded as the SCC resistant in accordance with NACE MR0175/ISO 15156 do not pass the tests in accordance with NACE TM 0177. It is the problem that needs to pay attention to, since the use of unsuitable material can cause a serious failure. A reference criterion about the SCC resistance of the steel is not only strength level but the microstructural properties and micro-cleanliness, as well. Due to the fact that the SCC belongs to the hydrogen embrittlement demonstration, there must be the same patterns as in the other cases, i.e. HIC or in the case of the Slow Strain Rate Test (SSRT) of hydrogen charged specimens. The presence of the not-tempered martensitic lines in the microstructure is completely

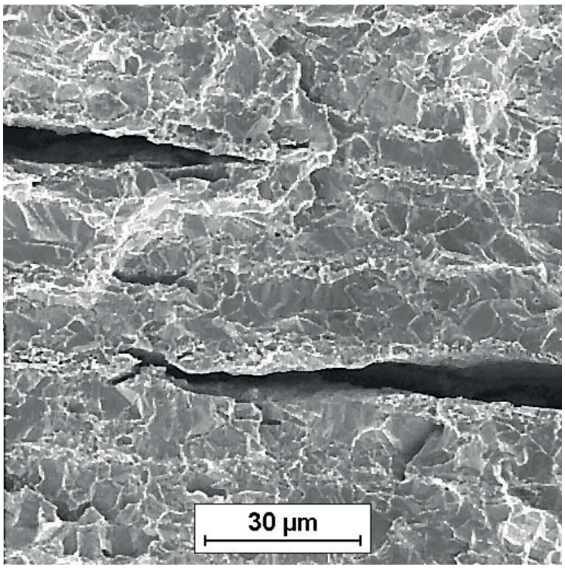

Figure 10 *Fracture surface of the X70/AR steel, 90% $R_{p0.2}$ (450 MPa), 593 hours*

unsatisfactory from a view of the SSC resistance; on the other hand, as-quenched and tempered microstructure exhibits the high resistance to the SSC, even under the test loading corresponding to 90 % of the yield strength.

4. Conclusions

Presented paper was mainly focused on the study of influence of the X52 and X70 steels microstructure on the resistance to the SSC.

The resistance of the steel against this kind of the damage was evaluated in accordance with usually used field approach from which the relationship with the tensile strength level or the hardness level, respectively, was clearly predicted. However, the experimental results have shown that the microstructural parameters are important factors too; they do have the influence on the steel resistance against the SSC. It was found that the resistance to the SSC can be significantly increased by quenching and tempering - similarly as for the HIC. In the case of the as-rolled (as-delivered) steels, the damage mechanism was a superposition of the HIC and the SSC. The cracks located in the segregation lines, caused by the HIC, led to significant reduction of time to rupture, despite the fact that they were longitudinally oriented in the direction of applied loading during the SSC test. This negative phenomenon was not observed after the quenching and tempering. Even though the quenched and tempered steel has the higher tensile strength level in comparison to the as-delivered state, a substantially higher resistance against the SSC was achieved.

It means that the steel selection process for sulfane working conditions, where the SSC risk exists - based on using the steels not exceeding the limited tensile strength level, should be re-evaluated. The influence of the microstructure should not be excluded since it could lead to selection of the material with the low resistance to the SSC that can cause a catastrophic service failure.

Acknowledgement

This paper was created at the Faculty of Metallurgy and Materials Engineering as part of the Project No. LO1203 "Regional Materials and Technology Centre – Feasibility Programme" funded by the Ministry of Education, Youth and Sports of the Czech Republic.

References

[1] RANGLOFF, R., P.: Comprehensive Structural Integrity: Hydrogen Assisted Cracking of High Strength Alloys. MILNE, I., RITCHIE, R., O., KARIHALOO, B. (Eds.), Environmentally Assisted Fracture, Elsevier, Amsterdam, 6, 31-101, 2003.

[2] GERBERICH, W. W., MARSH, P. G., HOEHN, J. W.: Hydrogen Induced Cracking Mechanisms - Are There Critical Experiments? THOMPSON, A. W., MOODY, N. R. (Eds.). Hydrogen Effects in Materials, TMS, Warrendale, PA, 539-553, 1996.

[3] McMAHON, C. J. Jr.: Hydrogen Induced Intergranular Fracture of Steels. Engineering Fracture Mechanics, 68(6), 773-788, 2001. https://doi.org/10.1016/S0013-7944(00)00124-7

[4] BIRNBAUM, H. K., SOFRONIS, P.: Hydrogen-Enhanced Localized Plasticity - A Mechanism for Hydrogen-Related Fracture. Materials Science and Engineering: A, 176(1-2), 191-202, 1994. https://doi.org/10.1016/0921-5093(94)90975-X

[5] LU, G., ZHANG, Q., KIOUSSIS, N., KAXIRAS, E.: Hydrogen Enhanced Local Plasticity in Aluminium: An Ab Initio study. Physical Review Letters 87(9), 095501, 2001. https://doi.org/10.1103/PhysRevLett.87.095501

[6] ROBERTSON, I. M.: The Effect of Hydrogen on Dislocation Dynamics. Engineering Fracture Mechanics, 68(6), 671-692, 2001. https://doi.org/10.1016/S0013-7944(01)00011-X

[7] LYNCH, S. P.: Mechanisms of Hydrogen Assisted Cracking - A Review. MOODY, N. R. et al. (Eds.), Hydrogen Effects on Material Behavior and Corrosion Deformation Interactions. TMS, Warrendale, PA, 449-466, 2003.

[8] LYNCH, S. P.: Comments on „A Unified Model of Environment-Assisted Cracking". Scripta Materialia, 61(3), 331-334, 2009. https://doi.org/10.1016/j.scriptamat.2009.02.031

[9] MAES, M. A., DANNA, M., SALAMA, M. M.: Influence of Grade on the Reliability of Corroding Pipelines. Reliab. Reliability Engineering & System Safety, 93(3), 447-455, 2008. https://doi.org/10.1016/j.ress.2006.12.009

[10] CORBETT, K. T., BOWEN, R. R., PETERSEN, C. W.: High - Strength Steel Pipeline Economics. Offshore and Polar Engineers, 14, 75-80, 2004.

[11] BRONCEK, J., JANKEJECH, P., FABIAN, P., RADEK, N.: Influence of Mechanical Anisotropy in Low Carbon Microalloyed Steel. Communications - Scientific Letters of the University of Zilina, 17(3), 25-30, 2015.

[12] NACE MR0175-2015/ISO 15156 Petroleum and Natural Gas Industries - Materials for use in H_2S-Containing Environments in Oil and Gas Production. NACE Int. Houston, Texas, USA, 2015.

[13] AL-MANSOUR, M., ALFANTAZI, A., M., EL-BOUJDAINI, M.: Sulfide Stress Cracking Resistance of API-X100 High Strength Low Alloy Steel. Materials and Design. 30(10), 4088-4094, 2009. https://doi.org/10.1016/j.matdes.2009.05.025

[14] CARNEIRO, R. A., RATNAPULI, R. C., LINS, V. F. C.: The Influence of Chemical Composition and Microstructure of API Linepipe Steels on Hydrogen Induced Cracking and Sulfide Stress Cracking. Materials Science & Engineering A, 357(1-2), 104-110, 2003. https://doi.org/10.1016/S0921-5093(03)00217-X

[15] ALBARRAN, J. L., MARTINEZ, L., LOPEZ, H. F.: Effect of Heat Treatment on the Stress Corrosion Resistance of a Microalloyed Pipeline Steel. Corrosion Science, 41(6), 1037-1049, 1999. https://doi.org/10.1016/S0010-938X(98)00139-5

[16] NACE Standard TM 0177-05 Laboratory Testing of Metals for Resistance to Sulfide Stress Cracking in H_2S Environments. NACE Int., Houston, Texas, USA, 2005.

[17] BURSAK, M., BOKUVKA, O.: Influence of Technological Factors on Fatigue Properties of Steel Sheets. Communications - Scientific Letters of the University of Zilina, 8(4), 34-37, 2006.

[18] JONSTA, P., VLCKOVA, I., JONSTA, Z., HEIDE, R.: Material Analysis of Degradated Steam Turbine Rotor. Communications - Scientific Letters of the University of Zilina, 18(3), 78-83, 2016.

Nada Bojic - Ruzica Nikolic - Milan Banic - Branislav Hadzima*

EVALUATION OF MECHANICAL PROPERTIES OF THE TWO PVC CONVEYOR BELTS

Conveyor belts with woven plastic belts, aimed for general applications, are very economical transporting means for longer distances. During the operation, the conveyor belts are subjected to various mechanical loadings. The consequences of those loadings are increased stretching of the belt and change of its tensile strength, which negatively affect the proper functioning of the transporter. To avoid the irregularities in the conveyor belt's operation, the tensile properties of the two plastic woven belts were tested (maximal force, maximal extension, breaking force and extension at break). In that way the conditions of the two belts were established. Based on performed experiments the belt that is more suitable for application in the transporter was defined.

Keywords: *woven plastic belt, extension, tensile strength, conveyor belt*

1. Introduction

Modern exploitation technology has determined the importance and role of the continuous transport, especially of the conveyor belts, as their main representatives. Transport by conveyor belts enabled application of the complex technology during the exploitation of various types of the raw materials and achieving the high productivity. Application of the conveyor belts provides for organizing the continuous and completely automated production process.

The bulk materials handling operations are the key functions in a great number of industries. The nature of the handling tasks and scale of their operations vary from one industry to another. However, the relative costs of storing and transporting bulk materials are generally quite significant. Thus, it is important for the transportation systems to be designed and operating in such a manner that the maximum efficiency and reliability are secured [1].

Out of various modes of the bulk solids transporting, the belt conveyors are considered as the most important, mainly due to their widespread use and reliability. Though their use was in the past largely confined to the in-plant transport of materials, they are now dominantly applied in transportation systems for moving various minerals, both in open pits and underground mines, as well.

The belt conveyors can have the load carrying capacity up to 30000 t/h and can be used for transporting the materials along the large length of conveying paths of up to 3-4 km. They are of relatively simple design, easily maintained and highly reliable in operation. The belt conveyor systems are used in various industries, such as in the foundry shop for supply and distributing the molding sand, molds and removal of waste, in coal and mining industry, sugar industry, agricultural and bagasse industry, fuel industry etc. [2].

These applications are made possible through the development of steel cord conveyor belting and the high potentials for broader applications has appeared due to application of the new lightweight belt materials, which also possess the high strength, like for instance those reinforced with Aramid fibers.

The transport task of the belt conveyors can be defined as a process of transporting the set quantity of the bulk material, within a defined time, between the set uploading and unloading locations. This determines the capacity of the conveyor, as well as the route profile and layout. The conveyor belt designer must select the right belt speed and width and to determine the basic parameters of the conveyor's functioning [3]. The belt conveyors are generally of the modular structure, so the designer has to correctly select the prefabricated subassemblies and combine them into a machine system, which will then execute the set transport task. Today, the modern belt conveyors use the belts that are manufactured by the state-of-the-art technologies. Their drives are equipped by the advanced and complex control systems, while the belt support systems are optimized according to the criteria of cutting the costs and increased durability. The belt conveyors are now accompanied by equipment for tensioning the belt as a function of the conveyor's driving system load.

In the past, the belt conveyor systems were often designed using the static analysis, which was based on manufacturers' handbooks and recommendations or the concurrent design standards. It was generally assumed that they are loaded as in the steady state and the belt tensions were calculated solely based on the drive requirements and the need to limit the belt sag. The unknown dynamic effects and uncertain belt splice efficiencies were "taken into account" through extremely high safety factors of the order of 7:1. However, today the dynamic behavior of belts during the starting, stoppings and operation are being properly considered, what leads to resonance free designs, lower and more realistic safety factors and increased reliability [1].

* [1]Nada Bojic, [2,3]Ruzica Nikolic, [4]Milan Banic, [2]Branislav Hadzima
[1]Factory of Sieves and Bearings "FASIL" A.D., Arilje, Serbia
[2]Research Center, University of Zilina, Slovakia
[3]Faculty of Engineering, University of Kragujevac, Serbia
[4]Faculty of Mechanical Engineering, University of Nis, Serbia
E-mail: ruzicarnikolic@yahoo.com

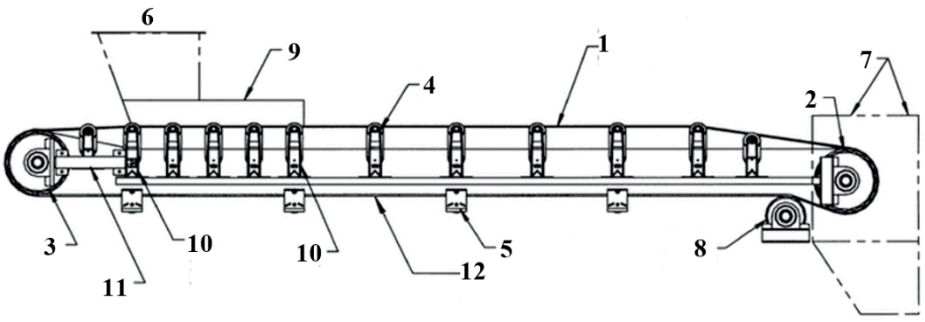

Figure 1 *The scheme of the conveyor belt*
1 - Troughed conveyor belt; 2 - Head pulley and drive; 3 - Tail pulley; 4 - Troughing carrying idlers; 5 - Return idlers; 6 - Feed chute; 7 - Discharge chute; 8 - Snub pulley; 9 - Loading skirts; 10 - Idlers at loading point; 11 - Horizontal screw take-up; 12 - Stringer (conveyor structure) [9].

Figure 2 *Appearance of the conveyor belt*

For instance, the impact process analysis, performed in [4], is based on the hypothesis that the movement of an object, falling onto the conveyor belt and then bouncing on it, is similar to the damped harmonic motion. This is done since the detailed examination of conveyor belts in practice indicated a strong influence of the wear and damage, caused by the dynamic and impact loading, on the conveyor belt service life.

During the conveyor belt operation, the belt is gradually worn out and damaged as a result of deterministic and stochastic stresses, which may not act simultaneously, but in certain time intervals. The risk factors include the multiaxial impact compressive stress, bending and shear stresses, caused by the impact forces, producing wear of the cover layers and often even punctures of the entire conveyor belt. The economic significance of the costs caused by the wear is enormous.

In [5] authors were analyzing the failure of the textile rubber conveyor belt damaged by the dynamic wear. During the operation, the conveyor belt is exposed to working conditions, which are causing the wear and/or damage. The wear on conveyor belts is characterized by almost evenly distributed abrasion of the covers and by the local damage, like tears, nicks in the cover, penetration of the belt and longitudinal slitting. The conveyor belting is the most exposed to damage at the loading station. The objective of that research was to obtain knowledge about the damage process, which is required for the correct regulation of the conveyor belt's operation conditions. The aim was to determine the conditions that caused this type of damages - the height of the material pieces impact and their weight. They used the non-destructive method of the computer metro-tomography to study the changes in the construction of the conveyor belt.

Authors of [6] presented experimental measurements of selected properties of the pipe conveyor belts, which were dynamically damaged. The "popularity" of the pipe conveyors lies in their ability to ensure the protection of environment through which they are passing. They are also proven to be the cost-effective, producing the low labor and operating costs. The pipe conveyors can overcome the problems like integration into the existing industrial system, limited or obstructed space and a difficult terrain. The essential design feature of the pipe conveyors is their tubular shape that is more stable over the straight distances when it comes to belt operation/torsion.

The plastic conveyor belts are elastic and flexible and can be used for various types of transport of the bulk materials, both horizontally or inclined [7]. The conveyor belts importance is often neglected, since they are usually planned as the part of the manufacturing equipment that does not cause any problems and can operate without failures for long times [8]. The best method to determine the state of the belt is to control its stretching (extension) and the tensile strength. This would guarantee that the conveyor belt is fully operational to properly execute the task in the manufacturing process. The conveyor belt transporter consists of the driving element, clutch and axle, electromotor and the belt. Figure 1 presents the scheme of the conveyor belt and its actual appearance is shown in Figure 2. The material discharge is done into the discharge chute at the transporter's head.

The objective of this paper was to establish the state of the two plastic woven belts of the transporter system from the aspect of the mechanical properties reliability and to determine which one is more suitable for application in the particular conveyor belt transporter.

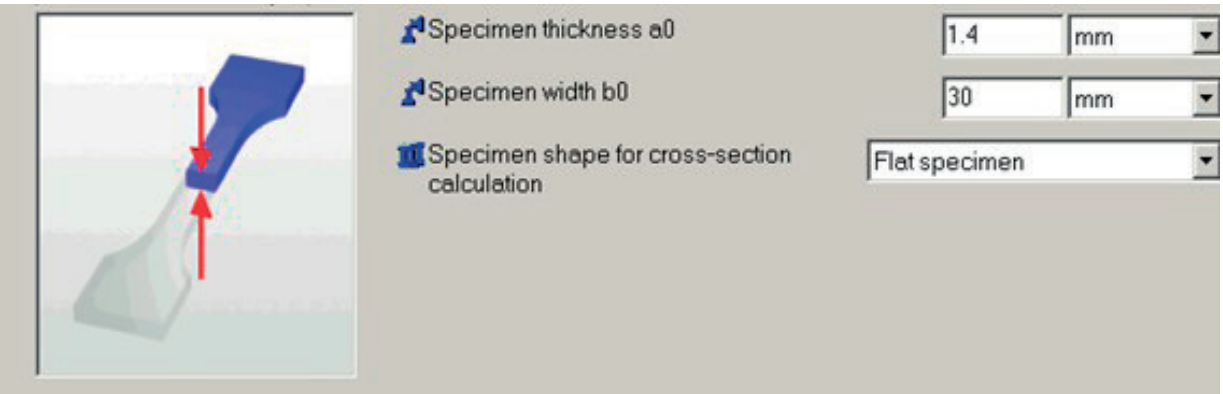

Figure 3 *Geometry of the plastic belts' samples*

Table 1 *Construction of the sieve made from 22BY*

Base wire	Number	18	*/cm*
	Diameter	0.36x0.67	*mm*
	Material	Hydrolysis-resistant polyester	
Weft wire - sieve's face	Number	7.5	*/cm*
	Diameter	0.50	*mm*
	Material	Hydrolysis-resistant polyester	
Weft wire - sieve's back	Number	7.5	*/cm*
	Diameter	0.60	*mm*
	Material	Hydrolysis-resistant polyester	

Table 2 *Construction of the sieve made from 31BY*

Base wire	Number	9	*/cm*
	Diameter	0.36x0.67	*mm*
	Material	Hydrolysis-resistant polyester	
Weft wire - sieve's face	Number	9	*/cm*
	Diameter	0.36x0.67	*mm*
	Material	Hydrolysis-resistant polyester	
Weft wire - sieve's back	Number	6.4	*/cm*
	Diameter	0.70 and 0.80	*mm*
	Material	Hydrolysis-resistant polyester	

2. Transporting belt

The basic and the most important part of the conveyor belt is the endless belt, made of the steel sieve, which is carrying the load. The belt is usually the most expensive part of the transporting system. The belts can be made of different materials, depending on the needs and requirements of the buyer. The usual materials are rubber, textile, steel tape, steels sieve covered by the woven plastic tape, etc. The belt is being driven over at least two rollers, one driving and one tightening, which are placed at the ends of the carrying structure. The transporting distance is defined by the axial distance between those two rollers. The belt, both the top (carrying) and the return (pulley) portion, is supported by the regularly placed idlers. As can be seen from Figure 1, in the loading section there are larger number of the closely spaced idlers, which must accept the incoming impact load on the belt.

The belt must fulfill several conditions to be fully operational- to be flexible, to have certain tensile strength and to be resistant to impact and wear. The subject of this research was the plastic belt (sieve), which transports the sawdust. The sieve represents an intertwined wire, which is formed by weaving of the two sets of wires, namely alternative weaving of the base wire and the weft wire, at a right angle. The base wires are parallel to the motion direction of the sieve (belt) and the weft wires are perpendicular to them [10], [11], [12]. The inner dimensions of the sieve represent the combination of the wire diameters and their distances; the opening between the wires is called the "eyelet". The variables that make the inner dimensions of the sieve are the wire diameter (mm), the opening size, the step, number of wires per cm and the illuminated-through area.

The belts are being delivered in different sizes, widths and lengths. They can be delivered as connected or the connecting can be done directly on the conveyor. For the plastic belt, the cover is made of the PVC, polyamide or some other plastics [13]. The plastic belts are resistant to humidity, oils, grease, chemicals and sea-water. They are manufactured in standardized widths

from 200 to 4500 mm. In the case of the bulk material with larger pieces, the belt width must be expressed as a function of the piece's largest dimension (a_{max}) as

$$B \geq 3a_{max} + 0.2m \quad (1)$$

where: B - is the belt's width.

In the case of the piece load, the belt's width calculation is done according to:

$$B \geq a_{max} + 0.2m \quad (2)$$

where a_{max} is the size of the largest piece.

3. Experimental setup

Two experiments were performed on samples from the two types of woven plastic belts, 22BY and 31BY. The data for constructions of sieves made from these two plastic materials are given in Table 1 and Table 2. Their geometry is shown in Figure 3.

Tests were executed in Laboratory for Mechanical testing in Factory "FASIL". The universal testing machine ZWICK ROELL Z100 was used for tensile test, with recordings of the load and extension. One of the hydraulic jaws was serving for the sample fastening, connected to the fixed part of the machine, while the other was connected to the moving part. The hydraulic jaws were so fixed that when the load changes they would automatically take the position in such a way that the longitudinal axis of the sample coincides with the machine axis. The maximum distance between the jaws was 590 *mm*. The sample was properly fixed so no slippage from the jaws would occur during the tension. The mechanism was without inertia at the prescribed test rate. The recorded extension had accuracy of 1 %. The maximum tensile force was 10 000 N. During the test, the maximum distance between the hydraulic jaws was 150 *mm*. The tension rate was 400 *mm*/*min*. The test rate was 20 *mm*/*min*.

The parameters of the conveyor belt transporter, for which the belts were tested, were the following: transporting distance 295 *m*, efficiency 145 *t*/*h*, the transported material cross-section 0.0105 m^2, the driving pulley diameter 60 *mm*, driving rpms 45 min^{-1}, engine power 40 *kW*, puling force on the driving pulley perimeter 13.025 *N*.

4. Results and discussion

Results of experiments are presented in Figure 4 and Figure 5 and in Table 3 and Table 4. The variables in tables are:

a_0 - sieve's sample thickness
b_0 - sieve's sample width
L_0 - sieve's sample length
F_{max} - maximal force
F_{Break} - breaking force
ε_{Break} - extension at break
ε_{Fmax} - maximal extension.

5. Conclusions

- Based on the conducted tests, it was established that the woven plastic belt of the 22BY type has the lower extension in % and the higher breaking force, with respect to the plastic belt of the 31BY type. Allowed extension of the sieve for this application is 33 %. Extensions of 25.78 % and 28.02% will not lead to increased friction between the carrying idler and the belt, thus, it will not cause the conveyor belt wear.
- Obtained results do not exceed the limit values of 2550 -3300 *N*, so it is concluded that the additional maintaining system need not to be activated. These values are provided by the belts manufacturer. The characteristics of the 22BY belt is the air permeability of 125 Pa at 350 CFM and at 100 Pa - 5700 $m^3/m^2/h$, what additionally increases elasticity of this belt and thus extends its applications field, as well. The 22BY belts enable application in various industrial processes, since due to their construction and characteristics they possess high reliability and long exploitation life.
- "A Conveyor is only as good as the belt that's on it" [14].

Example 1. Belt type 22BY: $N_b = 18N_w = 7.5$
(N_b is the number of the base and N_w is the number of the weft)

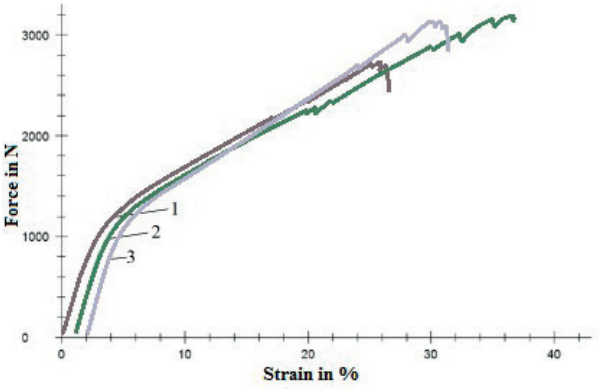

Figure 4 *Force - strain diagram for the belt type 22BY sample*

Example 2. Belt type 31BY: Nb = 9Nw = 9

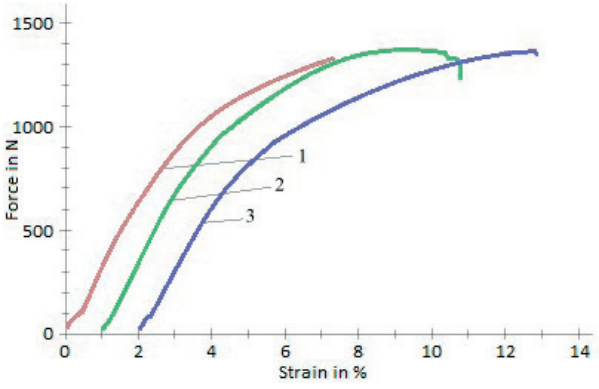

Figure 5 *Force - strain diagram for the belt type 31BY sample*

Table 3 *Results of the tensile test for the belt type 22BY sample*

No.	a_0	b_0	L_0	F_{max}	F_{Break}	e_{Break}	e_{Fmax}
	mm	mm	mm	N	N	%	%
1	1.4	30	150.46	2732.42	2439.67	26.58	25.78
2	1.4	30	150.49	3189.34	3127.55	35.72	35.68
3	1.4	30	150.50	3143.50	2827.67	29.48	28.02

Table 4 *Results of the tensile test for the belt type 31BY sample*

No	a_0	b_0	L_0	F_{max}	F_{Break}	e_{Break}	e_{Fmax}
	mm	mm	mm	N	N	%	%
1	1.5	30	150.45	1328.46	1326.36	7.32	7.27
2	1.5	30	150.33	1373.56	1229.47	9.80	8.68
3	1.5	30	150.32	1369.63	1350.36	10.86	10.73

Acknowledgement

This research was financially supported by European regional development fund and Slovak state budget by the project "Research Centre of the University of Zilina" and by the Ministry of Education, Science and Technological Development of Republic of Serbia through grant TR 35024.

References

[1] ROBERTS, A. W., HARRISON, A.: Recent Research in Belt Conveyor Technology. Proceedings of the "Belcon 5", 1-24, 1989.

[2] MANE, S. P, MANE, P. A., HARAGE, C. G., PRAJAPATI, R. R.: Trials and Analysis on Belt System used for Cooling of casting Mould. International Journal of Current Engineering and Technology, 5(2), 762-767, 2015.

[3] KULINOWSKI, P.: Simulation Studies as the Part of an Integrated Design Process Dealing with Belt Conveyor Operation. Maintenance and Reliability, 15(1), 83-88, 2013.

[4] GRINCOVA, A., ANDREJIOVA, M., MARASOVA, D.: Failure Analysis of Conveyor Belt in Terms of Impact Loading by Means of the Damping Coefficient. Engineering Failure Analysis, 68, 210-221, 2016.https://doi.org/10.1016/j.engfailanal.2016.06.006

[5] FEDORENKO, G., MOLNAR, V., GRINCOVA, A., DOVICA, M., TOTH, T., HUSAKOVA, N., TARABA, V., KELEMEN, M.: Failure Analysis of Irreversible Changes in the Construction of Rubber-Textile Conveyor Belt Damaged by Sharp-Edge Material Impact. Engineering Failure Analysis, 39, 135-148, 2014.https://doi.org/10.1016/j.engfailanal.2014.01.022

[6] FEDORENKO, G., MOLNAR, V., ZIVCAK, J., DOVICA, M., HUSAKOVA, N.: Failure Analysis of Textile Rubber Conveyor Belt Damaged by Dynamic Wear. Engineering Failure Analysis, 28, 103-114, 2013.https://doi.org/10.1016/j.engfailanal. 2012.10.014

[7] TOLMAC, D., PRVULOVIC, S.: Transportation Systems(In Serbian). University of Novi Sad, Technical Faculty in Zrenjanin, 2012.

[8] DROBNJAKOVIC, B., MILANOVIC, D., DROBNJAKOVIC, V.: Selection of a Belt Feeder Drive Group of Crushing Plant for Ore/Waste at the Open Pit of Veliki Krivelj Mine. Mining Engineering, 6(1), 133-138, 2012.https://doi.org/10.5937/rudrad1201133D

[9] High Speed Conveyor Systems[online]. Available: http://essexengineering.com/parts-conveyor-section-9.html [accessed 2018-04-03].

[10] Bojic, N. V., Nikolic, R. R., Jugovic, B. Z., Jugovic, Z. S., Gvozdenovic, M. M.: Uniaxial Tension of Drying Sieves. Chemical Industry, 67(4), 655-662, 2013.

[11] BOJIC, N., JUGOVIC, Z., DRAGICEVIC, S., SLAVKOVIC, R.: Comparative Study of the Tensile Stress of Diagonal Sieves Produced by Plasma Welding and Hard Soldering Process. Metalurgia International, 17(5), 25-29, 2012.

[12] BOJIC, N., JUGOVIC, Z., NIKOLIC, R., LAZIC, V., CUKIC, R.: Determination of Optimal Way for the Diagonal Sieves Joining. Proceedings of "IRMES-2011", Serbia, 573-578, 2011.

[13] Fenner-Dunlop: Conveyor Handbook. Conveyor Belting, Australia, 2009.

[14] Bastian Solutions [online]. Available: https://www.bastiansolutions.com [accessed 2018-02-18].

Martin Frkan - Radomila Konecna - Gianni Nicoletto*

INFLUENCE OF THE HEAT TREATMENT ON THE MICROSTRUCTURE, MECHANICAL PROPERTIES AND FATIGUE BEHAVIOR OF ADDITIVELY MANUFACTURED Ti6AL4V ALLOY

This contribution deals with the selective laser melting (SLM), which is one of the additive manufacturing (AM) technologies enabling the production of complex parts from metal powder, layer-by-layer wise. This technology uses laser as source of energy to melt a powder to compact state. Properties of final products can be significantly influenced by the process parameters and post-fabricated heat treatments. The purpose of this study is to determine the effect of a heat treatment on properties of the Ti6Al4V alloy specimens manufactured by Eosint M280 machine by the SLM. Three sets of specimens, treated at different temperatures (730 ˚C, 900 ˚C, 1200 ˚C), resulting in a different structure, associated mechanical and fatigue properties, were investigated.

Keywords: *SLM, Ti6Al4V, heat treatments, fatigue, microstructure*

1. Introduction

Nowadays, the most widely used technology for metal powder additive manufacturing is the selective laser melting (SLM) that allows production of the near-net shape parts not producible by conventional procedures. This technology is considered to be one of the upcoming techniques to manufacture very complex components for industry like aerospace, automobile, biomedical, prototyping and other. Production of components of complex shapes is possible due to the layer-by-layer building approach. In this process, the 3D digital model is imported to the SLM operating software and it is sliced into two-dimensional layers, each one corresponding to a slice of the model. Layers are scanned with a laser beam according to the shape defined by the SLM software. The energy of the laser beam melts the powder to near-full density. This technology offers several advantages compared to conventional production, thanks to low material waste and high production flexibility that allows an extraordinary freedom regarding the part geometry [1], [2], [3].

Actual developments of fiber optics and high-power laser have enabled the SLM to process different metallic materials, such as aluminum, nickel, titanium alloys and steels. Similarly, this has also opened research opportunities for the SLM of ceramic and composite materials. A review is given in [2]. However, manufacturing of functional parts by the SLM process, requires extensive research of optimum process parameters to obtain fully dense metal components with good mechanical properties. Influence of these parameters is discussed in [4], [5], [6].

The Ti6Al4V alloy is an established SLM material received by aerospace and biomedical industries for a good balance of strength, ductility, fracture toughness, creep characteristics, weldability and very good corrosion resistance [7]. This study investigates influence of the heat treatments on the basic mechanical properties, structure and on fatigue properties, as well.

Microstructure of the Ti6Al4V prepared by the SLM is a result of very high cooling rate during the crystallization (10^6 K/s) and it is formed by an acicular α' hexagonal martensitic phase. The formation and decomposition of α' martensite in additively manufactured Ti6Al4V was studied in [8]. Due to the high cooling rate residual stresses arise, which affect the mechanical behavior of parts [9], [10]. To minimize the influence of residual stresses, parts are heat treated by the stress relieving heat treatment before separation from the substrate. Optimization of mechanical properties via the heat treatment of parts produced by the SLM is discussed in [11].

2. Material and methods

Specimens manufactured from titanium alloy Ti6Al4V powder, supplied by EOS GmbH, were used. The powder particles are spherical, predominantly with a diameter range 25 to 45 μm with chemical composition given in Table 1.

The specimens were manufactured by the SLM on EOS M280 machine. This system uses Yb fiber laser unit with a wavelength of 1075 nm, which is able to supply the laser power of 200 W or 400 W. The EOS M280 machine is equipped with building chamber filled by argon gas to avoid oxidation of titanium powder. A 400 W laser power, with a process chamber temperature of 80 °C and 60 μm layer thickness, was used in the manufacturing process of the specimens. The scan strategy was based on a shell and core concept, where the internal part of the layer is first melted by raster laser motion then the contour of the layer is melted. The scanning of a successive layer is performed after rotation of the

* [1]Martin Frkan, [1]Radomila Konecna, [2]Gianni Nicoletto
[1]Department of Materials Engineering, Faculty of Mechanical Engineering, University of Zilina, Slovakia
[2]Department of Engineering and Architecture, University of Parma, Italy
E-mail: Martin.Frkan@fstroj.uniza.sk

Table 1 *Chemical composition of the Ti6Al4V powder*

	Al	V	O	N	H	Fe	C	Ti
[wt. %]	6.08	3.9	0.085	0.005	0.002	0.25	0.007	Bal.

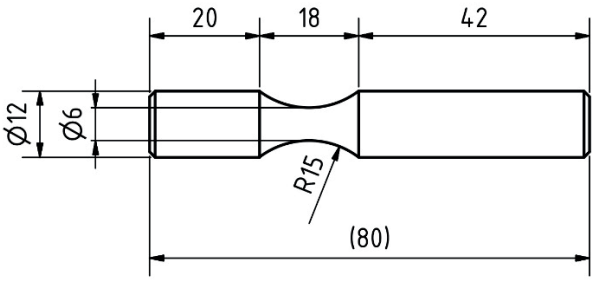

Figure 1 *Rotating bending smooth specimens*

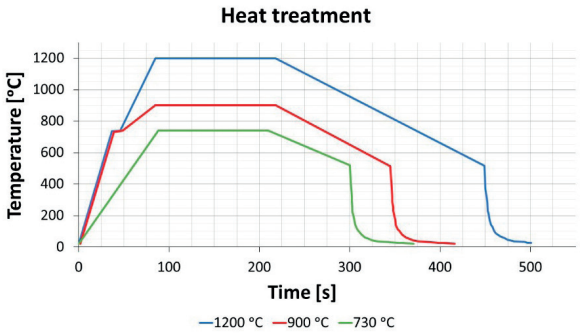

Figure 2 *Graph of different heat treatments*

scanning pattern for a 30-deg angle. All the specimens were built with their long axes parallel to the build direction (i.e. Z-axis).

Microstructure of specimens was observed using a light optical microscope Zeiss Axio Observer Z1M on polished and etched (10% HF for 10 s) specimens that were cut from broken fatigue testing samples. The metallographic specimens have been prepared by the standard procedure of metallographic preparation for the Ti alloys. Observation of structure was made in order to characterize the material anisotropy, which arises due to the typical process conditions, (i.e. layer by layer generative principle, short interactions, high temperature gradients and the high localization of this manufacturing process).

Tensile tests were carried out on specimens fabricated in horizontal orientations (C orientation) on servo-hydraulic MTS 810 machine according to the ASTM 8/E 8M-08 standard at the company BEAM-IT [12].

Vickers hardness tests were performed on metallographically prepared specimens in polished state using HPO 250/AQ machine with a load of 10 N and 10 s of loading time. The average hardness was calculated from 10 measurements.

Fatigue testing was performed at room temperature on a rotating bending fatigue testing machine at the University of Parma [12]. A loading cycle was sinusoidal with a frequency f = 50 Hz. A fully reversal load was applied with the loading cycle asymmetry R = -1 for all the tests. The shape and dimensions of fatigue specimens are shown in Figure 1. The diameter of the minimum cross-section is 6.0 mm. The specimens were tested in as-built state. The tests were run up to failure or they were interrupted at 1 x 10^7 cycles (run-outs). The experimental data were plotted in terms of the S-N diagram, i.e. the number of cycles to failure, N, in dependence on the stress amplitude σ_a.

Heat treatment. During the SLM process considerable thermal-related internal stresses develop in the parts. For this reason the suitable stress relieving heat treatment is an important step in production of parts by the SLM. To investigate the effect of subsequent heat treatment on the microstructure, mechanical properties and fatigue life, three different heat treatments were performed on the Ti6-Al-4V SLM fatigue specimens. To protect against the oxidization of the surface, heat treatment was undertaken in a vacuum furnace, (TAV Vacuum Furnaces). The heat treatment (Figure 2) consists of heating to a maximum temperature (730 °C, 900 °C, 1200 °C), with soaking period of about 2 hours, followed by a control cooling to a temperature 520 °C. The last stage consists of fast cooling from a temperature 520 °C to a room temperature by argon gas, injected to a hot temperature chamber under pressure.

3. Results and discussion

3.1 Structure

Investigation of the microstructure of specimens prepared from the Ti6Al4V alloy powder by the SLM was aimed at the characterization of the microstructure depending on the temperature of the heat treatment. In cases of specimens heat treated at 730 °C and 900 °C, the macrostructure of specimens show characteristic texture (Figure 3a and Figure 4a), which is similar for the lateral planes and differs from orthogonal planes. In Figure 3a are typical dark hot spots corresponding to the thermal history of the SLM production. During the material processing, the primary β-phase grains grow parallel to the build direction as a consequence of the thermal history experienced by the layer-wise fabrication. They are much longer than the layer thickness, which makes of about 60 μm. The microstructure of orthogonal planes shows a cross-section of the primary β columnar grains, which are observed as polyhedral grains. The size of these grains corresponds to the width of the primary β columnar grains. In the case of specimens heat treated at 1200 °C, the structure (Figure 5a) does not show the typical texture for the SLM technologies. The structure is the same for the lateral and orthogonal planes, characterized by large polyhedral grains because of the high temperature of the heat treatment.

The specimens heat treated at 730 °C show a detailed microstructure characterized by a fine needless of α′/α-phase in β matrix (Figure 3b). Black spots, generated by the local intense laser energy distribution, were locally observed as darker places. These localities are characterized by a finer microstructure. The average hardness for this microstructure is 392 HV 10.

Microstructure of specimens heat treated at 900 °C (Figure 4b) is characterized by the coarse needles of the α-phase in the β matrix, arranged in the Widmanstätten form. The thickness of the

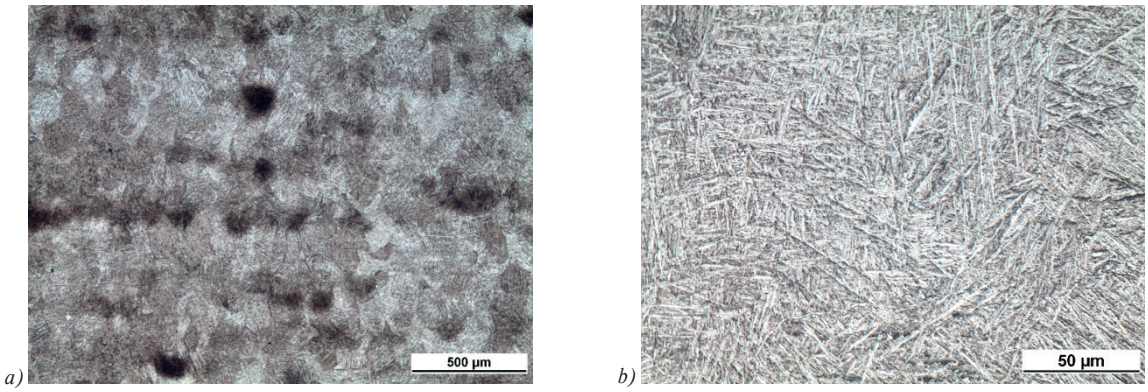

Figure 3 *Ti6Al4V HT 730 °C a) columnar grains, b) acicular microstructure, etchant 10% HF*

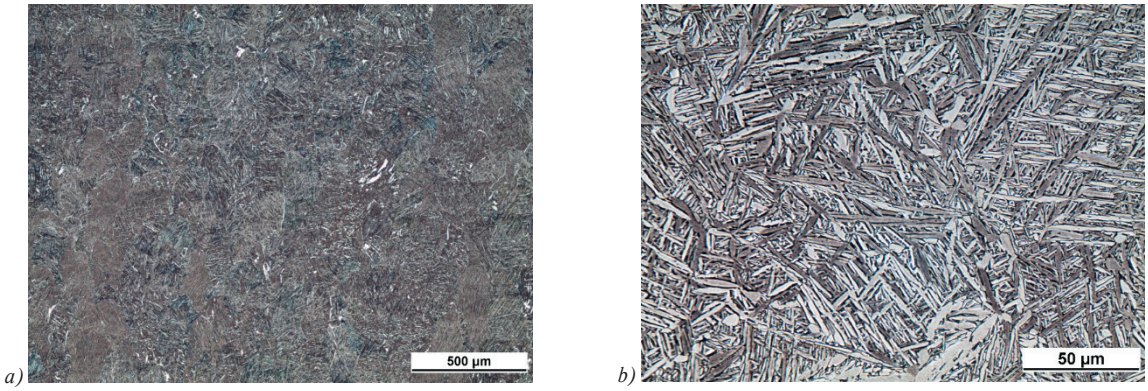

Figure 4 *Ti6Al4V HT 900 °C a) columnar grains, b) coarse needles, etchant 10% HF*

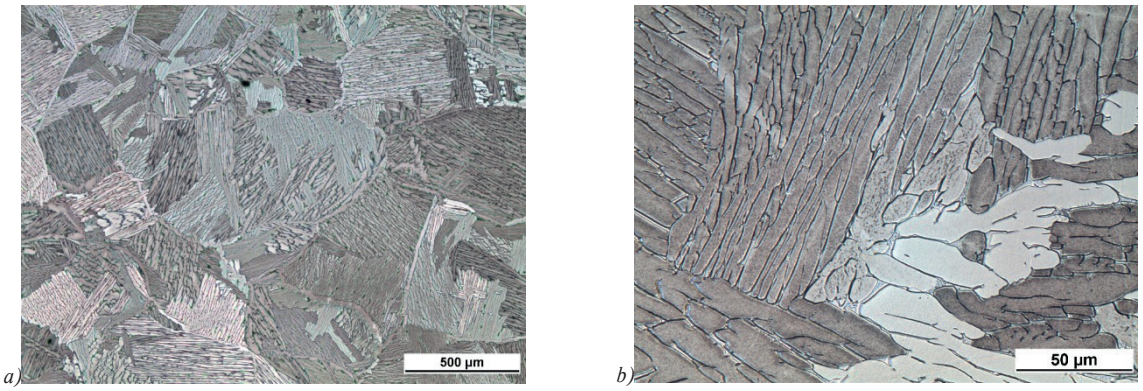

Figure 5 *Ti6Al4V HT 1200 °C, a) polyhedral grains, b) coarse lamellas of α+β phase, etch. 10% HF*

α-needles is different and it depended on the orientation of the lamellas to the metallographic cross section. Due to a different stress relieving temperature, they showed homogeneous structure without black spots compared to the heat treated specimens at 730 °C. The average hardness is corresponding to the coarser structure and is 347 HV 10.

The microstructure of specimens heat treated at 1200 °C is characterized by the coarse lamellas of the α+β phase (Figure 5b). The polyhedral grains show colonies of lamellas with the same orientation. Grain growth occurred due to the high temperature 1200 °C (β transus is~ 995 °C), when α´-martensite (as-fabricated structure) is completely replaced by grains of the β-phase. These large grains of the β-phase transform to coarse lamellas of the α+β phase during the cooling. The average hardness for this structure is the lowest (315 HV 10) due to the high content of β-phase.

3.2 Tensile tests

The tensile tests were carried out on specimens in as-built state, fabricated in horizontal orientations (axis of specimens coincides with axis of the building direction) by the BEAM-IT [12]. The average room-temperature mechanical properties of the Ti6Al4V alloy under different conditions are given in Table 2. The yield strength, ultimate tensile strength and percentage strain were obtained as direct output from the tensile testing machine. The tensile properties (ultimate tensile strength, yield strength) are comparable to the standard Ti6Al4V annealed material [13]. Specimens heat treated at 730 °C have comparable tensile properties as standard solution treated and aged material. Specimens heat treated at 900 °C have comparable tensile properties as duplex annealed material. The lowest tensile

Table 2 Material condition and mechanical properties

Condition	Yield strength MPa	Ultimate tensile strength MPa	Elongation %
Mill annealed	945	1069	10
Duplex annealed	917	965	18
Solution treated and aged	1103	1151	13
SLM Ti6Al4V + HT 730	1104	1176	13
SLM Ti6Al4V + HT 900	990	1078	18
SLM Ti6Al4V + HT 1200	837	928	12

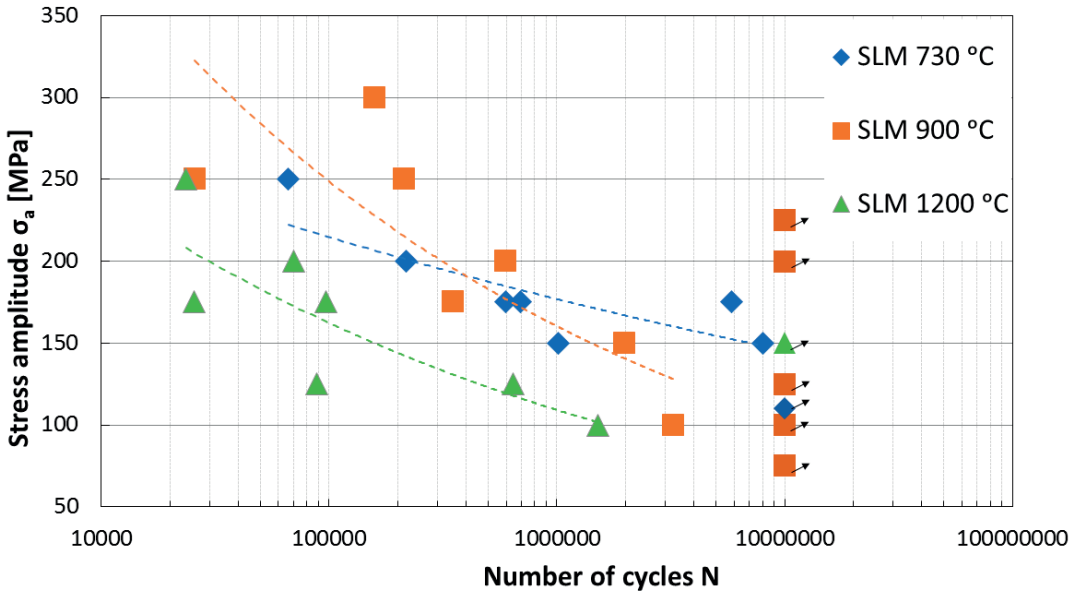

***Figure 6** Influence of the heat treatment on S-N curves of as-built DMLS Ti6Al4V*

properties have specimens heat treated at 1200 °C, which was also reflected to the fatigue behavior. From comparison of the SLM specimens, it can be said, that finer structure is resulting in the higher yield and ultimate tensile strengths. Relationship between the structure and elongation is not clearly defined. Elongation was the highest for specimen heat treated at 900 °C.

3.3 Fatigue

Results of the fatigue tests are shown as S-N curves (Figure 6) [12]. All specimens had the same orientation with respect to the build direction. Their surfaces were left in the as-built state after heat treatment. The structure, which also affects the fatigue lifetime [14], is similar for temperatures 730 and 900 °C, however, for specimens heat treated at 1200 °C it different (see microstructures). The different heat treatments therefore affect the fatigue behavior. From the fatigue data of Figure. 6 it can be stated that specimens heat treated at 730° C and 900° C show similar fatigue behavior in terms of the regression curves. On the other hand, fatigue data of specimens heat treated at 730 °C exhibit smaller scatter, probably due to the finer microstructure. The worst fatigue behavior is for the specimens that were heat treated at 1200 °C due to the coarse lamellar structure. The influence of lamellar thickness on the fatigue behavior have been investigated in [13], where it was found that the fatigue behavior is strongly affected by the width of the alpha lamellae in fully lamellar microstructures.

Although the structure is different (thickness of α-phase lamellas, primary β grain size, texture), differences in the fatigue life are small. The fatigue strength at 1 x 10^7 can be estimated as less than 150 MPa. This low fatigue strength is caused by the rough surface, which significantly affects the fatigue strength, due to the high fatigue notch sensitivity of Ti-alloys [15], [16].

The specimens in as-built state produced by the SLM technology have a rough surface [17], caused by un-melted particles and layer-by-layer manufacturing method used by additive manufacturing technology.

The role of the surface quality on fatigue life is discussed based on Figure 7, where data published by Janecek et al. [18], of Ti6Al4V alloy specimens tested in rotating bending (R = -1) in the range from 10^4 to 10^7 cycles at the testing frequency of 30 Hz are presented. Janecek et al. tested specimens, electro-polished in their gage section, compared to the present as-built SLM specimens. The fatigue strength at 10^7 cycles is rather high, about 400 MPa, for Janecek et al. This result is confirmed by previously published rotating bending test results obtained with SLM Ti6Al4V specimens having machined surfaces and heat treated similarly to the present case (i.e. maximum temperature 740 °C instead of 730 °C) [19].

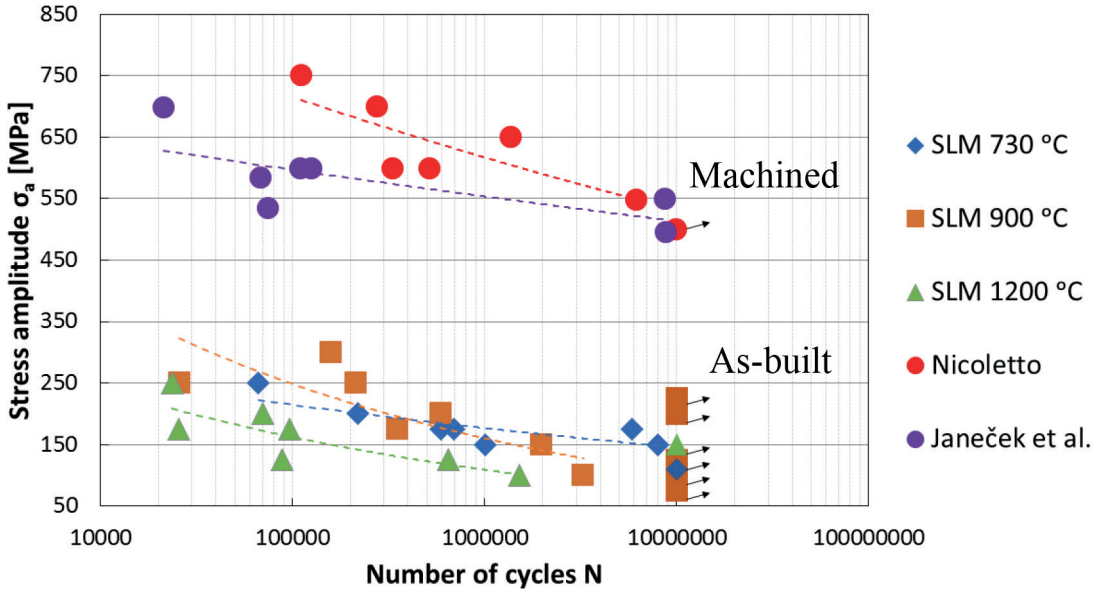

***Figure** 7 S-N curves for as-built and machined DMLS Ti6Al4V*

In the case of Janecek et al. [18], the material was subjected to the following heat treatment: annealing at 980 °C for 1 h, followed by water quenching; annealed at 800 °C for 1 h followed by air cooling; final aging at 500 °C for 24 h. It resulted in a bi-modal microstructure, with ultimate tensile strength of 1050 MPa and yield strength of 950 MPa. Generally, the bi-modal microstructure guarantees good fatigue endurance of the Ti6Al4V alloy. On the other hand, the present material, heat treated at 730 °C reached even higher fatigue strength.

The data by Janecek et al. [18] and Nicoletto [19] demonstrate that the specimens manufactured by the SLM technology and machined surfaces have higher fatigue strength compared to the conventional alloy tested by Janecek et al. [18]. The difference in the fatigue life is especially visible in the low-cycle fatigue region, where the higher load amplitudes are used. This increase in fatigue life is probably due to the very fine microstructure of specimens produced by the SLM method.

4. Conclusion

The aim of this study was to discuss the influence of the heat treatment temperature on the microstructure, mechanical properties and fatigue behavior of the Ti6Al4V alloy produced by the SLM technology. This study leads to the following conclusions:

- The microstructure of the Ti6Al4V specimens prepared by the SLM and then heat treated is characterized by primary β columnar grains that are filled with fine needles of α´/α-phase in the case of the heat treatment at 730 °C or the coarse needles of the α phase in the β matrix in the case of the heat treatment 900 °C or coarse lamellas of the α+β at 1200 °C.
- The mechanical properties, obtained from the tensile test for Ti6Al4V alloys produced by the SLM technology and subsequently heat treated, are comparable to mechanical properties of the wrought Ti6Al4V.
- For the best heat treatment, the fatigue strength at 1 x 10^7 for as-built Ti6Al4V was estimated at 150 MPa. In the case of machined surfaces, the fatigue strength at 1 x 10^7 was estimated to be 500 MPa, similar to what is reported for the wrought Ti6Al4V. The surface quality has therefore a fundamental role in the future application of the SLM technology.

Acknowledgment

The research was supported by the Slovak VEGA grant No. 1/0685/2015. Cooperation with Beam-It, Fornovo Taro (Italy) is gratefully acknowledged.

References

[1] GIBSON, I., ROSEN, D., STUCKER, B.: Additive Manufacturing Technologies: 3D Printing, Rapid Prototyping and Direct Digital Manufacturing. Springer, New York, p. 498, 2015.

[2] YAP, C. Y., CHUA, C. K., DONG, Z. L., LIU, Z. H., ZHANG, D. Q., LOH, L. E., SING, S. L.: Review of Selective Laser Melting: Materials and Applications. Applied Physics Reviews, 2(4), 041101, 2015. https://doi.org/10.1063/1.4935926

[3] HORN, T. J., HARRYSSON, O. L. A.: Overview of Current Additive Manufacturing Technologies and Selected Applications. Science Progress, 95(3), 255-282, 2012. https://doi.org/10.3184/003685012X13420984463047

[4] SUN, J., YANG, Y., WANG, D.: Parametric Optimization of Selective Laser Melting for Forming Ti6Al4V Samples by Taguchi Method. Optics & Laser Technology, 49, 118-124, 2013. https://doi.org/10.1016/j.optlastec.2012.12.002

[5] ZHANG, S., WEI, Q., CHENG, L., LI, S., SHI, Y.: Effects of Scan Line Spacing on Pore Characteristics and Mechanical Properties of Porous Ti6Al4V Implants Fabricated by Selective Laser Melting. Materials & Design, 63, 185-193, 2014. https://doi.org/10.1016/j.matdes.2014.05.021

[6] YADROITSEV, I., BERTRAND, P., SMUROV, I.: Parametric Analysis of the Selective Laser Melting Process. Applied Surface Science, 253(19), 8064-8069, 2007. https://doi.org/10.1016/j.apsusc.2007.02.088}

[7] WELSCH, G., BOYER, R., COLLINGS, E. W.: Materials Properties Handbook: Titanium Alloys. ASM International, p. 1176, 1994.

[8] XU, W., BRANDT, M., SUN, S., ELAMBASSERIL, J., LIU, Q., LATHAM, K., XIA, K., QIAN, M.: Additive Manufacturing of Strong and Ductile Ti-6Al-4V by Selective Laser Melting Via In Situ Martensite Decomposition. Acta Materialia, 85, 74-84, 2015. https://doi.org/10.1016/j.actamat.2014.11.028

[9] ROBERTS, I. A.: Investigation of Residual Stresses in the Laser Melting of Metal Powders in Additive Layer Manufacturing [online]. PhD. Thesis, University of Wolverhampton, 2012. Available: https://core.ac.uk/download/pdf/9559670.pdf.

[10] SHIOMI, M., OSAKADA, K., NAKAMURA, K., YAMASHITA, T., ABE, F.: Residual Stress within Metallic Model Made by Selective Laser Melting Process. CIRP Annals - Manufacturing technology, 53(1), 195-198, 2004. https://doi.org/10.1016/S0007-8506(07)60677-5

[11] VRANCKEN, B., THIJS, L., KRUTH, J. P., HUMBEECK, J. V.: Heat Treatment of Ti6Al4V Produced by Selective Laser Melting: Microstructure and Mechanical Properties. Journal of Alloys and Compounds, 541, 177-185, 2012. https://doi.org/10.1016/j.jallcom.2012.07.022

[12] NICOLETTO, G., MAISANO, S., ANTOLOTTI, M., DALL´AGLIO, F.: Influence of Post Fabrication Heat Treatments on the Fatigue Behavior of Ti-6al-4v Produced by Selective Laser Melting. Procedia Structural Integrity, 7, 133-140, 2017. https://doi.org/10.1016/j.prostr.2017.11.070

[13] DONACHIE, M. J.: Titanium: A Technical Guide, 2nd ed. ASM International, 2000.

[14] FRKAN, M., KONECNA, R., NICOLETTO, G.: Surface Quality and Fabrication Directionality Effects on the Fatigue Behavior of DMLS Ti6Al4V. Proceedings of 26th International Conference on Metallurgy and Materials (METAL 2017), Czech Republic, 1567-1572, 2017.

[15] KAHLIN, M., ANSELL, H., MOVERARE, J. J.: Fatigue Behaviour of Notched Additive Manufactured Ti6Al4V with As-Built Surfaces. International Journal of Fatigue, 101(P1), 51-60, 2017. https://doi.org/10.1016/j.ijfatigue.2017.04.009

[16] BOYER, H. E.: Atlas of Fatigue Curves. ASM International, p. 518, 1986.

[17] NICOLETTO, G., KONECNA, R., KUNZ. L., FRKAN. M.: Influence of As-Built Surface on Fatigue Strength and Notch Sensitivity of Ti6Al4V Alloy Produced by DMLS. MATEC Web of Conferences, 165, 02002, 2018. https://doi.org/10.1051/matecconf/201816502002

[18] JANECEK. M., NOVY, F., HARCUBA, P., STRASKY, J., TRSKO, L., MHAEDE, M.: The Very High Cycle Fatigue Behavior of Ti-6al-4v Alloy. Acta Physica Polonica A, Proceedings of the International Symposium on Physics of Materials (ISPMA13), 128, 4, 2015. https://doi.org/10.12693/APhysPolA.128.497

[19] NICOLETTO, G.: Efficient Determination of Influence Factors in Fatigue of Additive Manufactured Metals. Procedia Structural Integrity, 8, 184-191, 2018. https://doi.org/10.1016/j.prostr.2017.12.020

Jan Dizo - Miroslav Blatnicky - Jozef Harusinec - Alfred Pavlik - Lukas Smetanka*

STRENGTH ANALYSIS OF A FREIGHT BOGIE FRAME UNDER THE DEFINED LOAD CASES

This work presents results of strength analyses of a modified freight wagon bogie frame. It consists of two main parts. The first part is addressed to introduction of the structure of a freight wagon bogie frame. It is a modified frame structure, which reflects current requirements of modern railway transport means. The conditions for rail vehicles approval and the main load cases, which every bogie frame must meet for commissioning, are described. The next part deals with computer modelling and analyses of this bogie frame. Strength analyses were performed using the FE method and they were focused on the assessment of stresses in the frame structure. Loads definition and the method of calculation were based on valid norms and standards.

Keywords: *freight wagon bogie frame, modified structure, strength analysis, finite element method*

1. Introduction

The transport of goods by railways represents an important element of a transport service. It is the environmentally friendly kind of goods transport, which is mainly obvious in international and intermodal transport. Therefore, the railway transport is nowadays an inseparable part of the transport system.

The railway transport allows an efficient way to move large quantities of goods over longer distances [1], [2], [3]. Nowadays, the design of rail vehicles has to satisfy conflicting requirements. On one hand it is the rail vehicles weight reducing and on the other hand all the railway transport means must meet the strict safety criteria, standards and norms. Every new designed railway vehicles and also construction units, such as bogies must meet before commissioning satisfy the terms set out in codes [4], [5].

2. Modified structure of a freight wagon bogie

By reason that mainly in the region of the Central Europe (Slovak Republic, Czech Republic, Poland, Hungary, Baltic countries, etc.) the freight railway transport makes use of the same railway tracks as passenger railway transport, the question about the stronger depreciation of this infrastructure arises [6], [7], [8]. These negative outcomes strongly relate among other things with the much higher axle load of freight wagons and with different design of freight wagons bogies [9], [10].

The Y25 bogie is the most commonly used bogie for freight wagons. In comparison to bogies for passenger wagons, it features the relatively stiff structure. On one hand there are solutions allowing steering wheelsets in curves by releasing the wheelsets in guidance, but on the other hand such a design meets problems when a freight wagon passes straight sections of tracks [11], [12], [13], [14]. These facts have led engineers to the modification of the original Y25 bogie design. Basis of the modification of the bogie consists of removing the buffer beams and in partial modifications of some other parts (increasing thicknesses of same sheets in structure) [15], [16]. Such a modified bogie cannot any longer use standard block brake acting on both side of a wheel, but it is equipped with the integrated block brake unit acting on one side of a wheel or with a disc brake [17]. The decreasing of the bogie mass is another important advantage of such a technical solution. When one compares the original Y25 bogie, equipped with the standard block brake, to the modified Y25 bogie design, equipped with the block brake unit, it can save up to 250 kg [15] and as standard freight wagons use two bogies, the mass of wagons is not longer negligible. Both bogie designs are shown in Figure 1.

From the operation point of view, reducing of the wagon unloaded mass means increasing the wagon capacity weight, lower operating costs when a wagon is transported in an unloaded state by saving energy consumption [18], and from the production point of view, one can save in material costs and partly reduce the needed production time.

The bogie frame is the main carrying part of the bogie. Therefore it is not possible to perform such an essential modification of the frame without adequate analyses. They come out and rely on strict requirements embedded in relevant standards and regulations. In the European standard the considered analysed bogie is classified in the category B-V: bogies freight rolling stock with single-stage suspensions [4].

3. Prescribed loads for freight wagon bogies

Freight bogies are loaded in real operational conditions by a wide spectrum of loads, which depends on actual level of loading, quality of a track expressed by variations from its geometrically

* [1]Jan Dizo, [1]Miroslav Blatnicky, [1]Jozef Harusinec, [1]Alfred Pavlik, [2]Lukas Smetanka
[1]Department of Transport and Handling Machines, Faculty of Mechanical Engineering, University of Zilina, Slovakia
[2]Department of Design and Mechanical Elements, Faculty of Mechanical Engineering, University of Zilina, Slovakia
E-mail: jan.dizo@fstroj.uniza.sk

Figure 1 *The original Y25 bogie (left) and the modified Y25 bogie (right)*

ideal position load or an eventual buckling of the track in the given track section and various others factors. Therefore, for the load of bogie frames the replacement load spectrum was determined according to which new developed bogies are tested [19]. In this work the modified bogie frame was tested using virtual models.

Generally, various load cases of bogies frames can be divided into external and internal. The external load of bogies represents the load relevant to the bogie running on the track, when it has to carry gravitational forces, as well as dynamic forces acting in the vertical and lateral directions. The internal load is caused by the presence and operation of the bogie equipment, such as the brake system, system of suspension with dampers, anti-roll bars system, traction motors and also by masses attached to the bogie frame (inertia effects) etc. [4], [19].

3.1 Combinations of individual loads

In reality, loads described above do not occur individually, but they act concurrently in various combinations and in various intensities. For needs of the strength and dynamic design of a bogie frame, the European standards submit several selected load combinations. They are compiled in such a manner, that the designed bogie frame will withstand the possible combined operational loads. In the European standard two combinations of loads are defined, the static load combination and the dynamic load combination. Based on the static load combination and the removal of the static load, the permanent deformations must not occur in the frame structure. In exceptional cases and based on agreement with the vehicle operator, the permanent deformations are compared to the permissible values [4], [19].

Bogie structures are loaded by the very high number of the varying dynamic loads. Effects of such a load are concentrated in critical locations of the analysed bogie frame (e.g. points of action forces, geometry changes, welded joints etc.). The objective of the fatigue tests is verification, if a bogie frame has sufficient fatigue strength, i.e. if a cyclic operational load does not result in initiation of fatigue cracks or fractures. Fatigue stresses are possible to be determined by the two methods, i.e. the fatigue resistance, if the fatigue lifetime is known (stress value, in which under load by determined number of cycles the fatigue damage not occur) and the cumulative damage, if the stress is constantly under the fatigue lifetime level for all the determined load combinations [4], [19].

In this work, only the static load combinations are considered.

4. Stress analyses of a modified bogie frame

Ride properties of rail vehicles significantly influence their dynamic behaviour [20]. One can theoretically predict the movement of the wheelset on a track by means of the wheelset and track geometrical characteristics analysis. Geometrical characteristics define the rail/wheel profiles contact couple geometrical relationship. The shape of the contact couple crucially influences the size of the contact patch and contact stress between the wheel and rail value. This creates loading and excitation forces acting inside the vehicle and track systems [21], [22], [23]. The analysis of the mechanical systems dynamics may be conducted using various methods [24].

4.1 Determination of the loads

Formulations for determination of the loads are prescribed in the European standard [4]. For these calculations the freight wagon bogie parameters were as follows: the total weight of the bogie was m = 4.25 t, wheelbase b = 1.8 m and the total weight of the wagon M_W = 90 t, (Figure 2).

The bogie is loaded in the vertical direction by the force:

$$F_Z = \left(\frac{M_W}{2} - m\right) \cdot g \tag{1}$$

where g represents the gravitational acceleration of 9.81 m.s^{-2}. For the vertical direction the value of the exceptional load is given by following formulas:

- if vertical forces act only in the centre pivot:

$$F_{ZP_{max}} = 2 \cdot F_Z \tag{2}$$

- if vertical forces act in the centre pivot and on one side-bearer:

$$F_{Z1\,max}\left(or\ F_{Z2\,max}\right) = 1.5 \cdot F_Z \cdot \alpha \tag{3}$$

$$F_{ZP} = 1.5 \cdot F_Z\left(1 - \alpha\right) \tag{4}$$

where F_Z is the total vertical load on a bogie, F_{ZP} is the vertical force acting in the centre pivot, F_{Z1} and F_{Z2} are vertical forces act on side-bearers, α is coefficient for the body swinging. In this case, the value α = 0.3 was considered.

For the lateral force of the exceptional load, acting on every wheelset, the following formulation is applied:

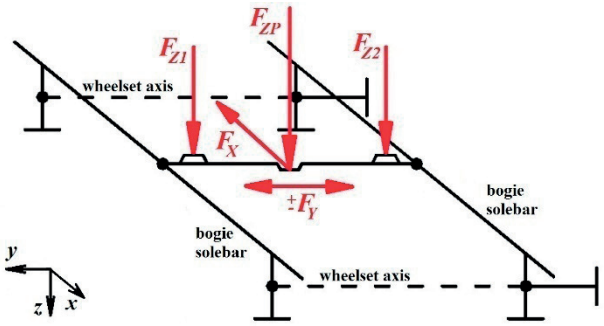

Figure 2 *Distribution of loads on a frame*

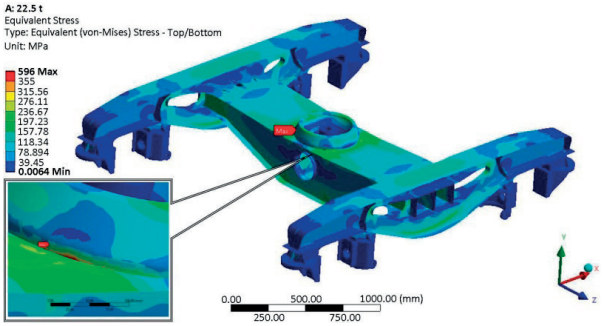

Figure 3 *Results of the strength analysis for the 1st load case*

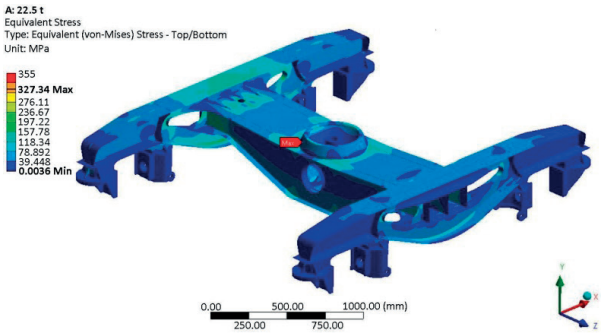

Figure 4 *Results of the strength analysis for the 2nd load case*

Table 1 *Values of the calculated loads*

Load	Value [kN]	Formula
F_Z	399.760	(1)
F_{ZPmax}	799.520	(2)
F_{Z1max}	179.892	(3)
F_{ZP}	419.750	(4)
F_{Y1max}	100.074	(5)
F_{X1max}	44.145	(6)

$$F_{Y1\max} = F_{Y2\max} = \frac{F_{Y\max}}{2} = 10^4 + \frac{F_Z + m \cdot g}{6} \tag{5}$$

The longitudinal force straining bogie frame is given by:

$$F_{X1\max} = 0.1\left(F_Z + m \cdot g\right) \tag{6}$$

The load involved in the case of the wagon impact can be substituted by the static longitudinal forces acting in places where the equipment is connected to the bogie. Its value is determined from the mass of individual elements and maximum acceleration acting on them during wagon impact.

4.2 Simulation calculations and results

The Ansys software was used for the strength analyses. It allows engineers to create computer models of structures, machine components or whole systems, to apply operating load and other design criteria and to study physical responses [25], [26], [27], such as stress levels, pressure, deformations, etc.

The bogie frame is generally made of the combination S235 and S355 steels, which minimal yield strength is of 340-440 MPa and 520-630 MPa, respectively. The S355 steel is used for the centre pivot and axle guides. The material is defined as homogenous, isotropic, linear and elastic with the Young's modulus of elasticity $E = 2.1 \cdot 10^{11}$ Pa and Poisson's ratio $\mu = 0.3$.

Next are presented results from computer analyses of the modified bogie frame, which was subjected to four load cases corresponding to the exceptional loads described in section 4.1. Table 1 contains calculated data, which are needed to apply as loads on the bogie. The third column indicates which formula from section 4.1 was used for calculation.

The structure of a bogie frame is acceptable, when it withstands required loads without deflecting to an extent that would impair functionality under the application of the loads or without suffering permanent deformation after removal of the loads [19]. It practically means that for all the load cases, stresses in the whole structure have to be under the yield strength of used material.

Figure 3, Figure 4, Figure 5 and Figure 6 show results from strength analyses of the modified freight wagon bogie frame under prescribed four load cases. Stresses were evaluated according to the HMH hypothesis.

Consider now Figure 3. For the first load case the highest value of the exceptional load (F_{ZPmax} = 799.520 kN) acts only in the centre pivot. Under this load the highest values of the stresses arise in the middle part of the frame. The maximum calculated stress is 596 MPa. It is located in the area of the centre pivot and the cross girder connection. This value is else over the yield strength of the material, but it occurs only locally. One has to consider important facts related to the numerical properties of the FE mesh, so this value can be neglected. Other values are safely below the yield strength. Therefore, the structure complies with given limits for the first load case.

In the second exceptional load case (Figure 4) the frame was loaded by forces acting in the centre pivot and on one side-bearer (F_{ZP} = 419.750 kN and F_{Z1max} = 179.892 kN). Such the load model simulates a wagon body swinging. From results (Figure 4) one can see, that the maximum stress is in the loaded side-bearer area and it reaches value of 327.34 MPa. In the structure there are no stresses, which could be dangerous for the operation under these analysed load conditions.

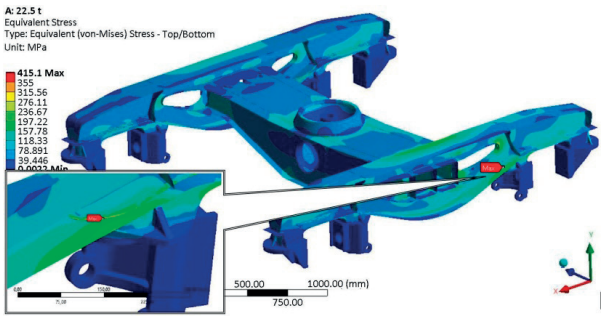

Figure 5 *Results of the strength analysis for the 3rd load case*

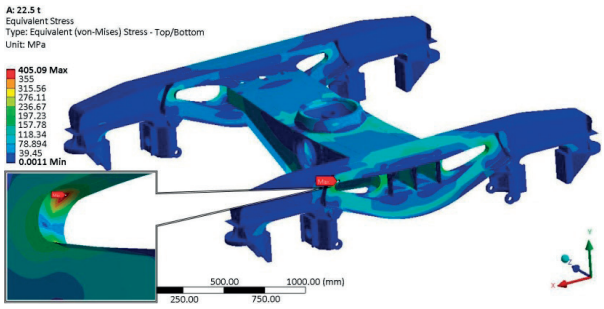

Figure 6 *Results of the strength analysis for the 4th load case*

In the third load case (Figure 5) the exceptional load is formed by two vertical forces (F_{ZP} = 419.750 kN and F_{Z1max} = 179.892 kN) and one lateral force (F_{Y1max} = 100.0774 kN). As one can see in Figure 2, the vertical forces act in the centre pivot and the lateral force acts on the side-bearer. The maximum equivalent stress is 415.10 MPa in the area of the axle guide and the bogie solebar connection (Figure 5). This stress is identified only locally again. In this area two different types of FE mesh are used. The connection of these meshes causes calculation errors. In reality, the calculated stresses do not appear in the structure and the frame structure meets the prescribed criterion.

Finally, the fourth load case (Figure 6), was evaluated. In comparison to the previous case, vertical loads are the same (F_{ZP} = 419.750 kN and F_{Z1max} = 179.892 kN), but instead of the lateral force, the longitudinal force acts in the centre pivot (F_{X1max} = 44.145 kN). This force simulates the dynamic effects caused by traction and braking forces, etc. The maximum stress value (Figure 6) is slightly smaller in comparison to the third load case and it is of 405.1 MPa. It is calculated in the bogie solebar, specifically in the area of the longitudinal girder flange with the upper sheet. This local concentrator is formed due to the reasons described above. The frame structure is able to withstand the fourth load case, as well.

The future research will be focused on investigation of mechanical properties and dynamic behaviour of the entire modified bogie. A mechanical system of the modified bogie in a multibody software will be created and this just analysed FE model will serve as an important input for setting up a multibody system with a flexible body [28], [29] in order to study its dynamic properties and to compare to the original bogie for the detection of possible problems in terms of long-term operation.

5. Conclusion

The three-dimensional model of a modified freight wagon bogie frame was created. Since this is a relatively new design of a freight wagon bogie, the objective was to find out if this new frame structure is able to meet strict criteria for all the new designed rail vehicles and their components, mainly the bogies. From the whole scale of load cases, four cases included as exceptional loads, were chosen. The numerical analyses of the bogie frame structure were performed and based on results it was found out that the structure meets requirements prescribed in the standard. For making the clear conclusions it would be necessary to compare results from numerical calculations and measurements to each other. This is the intention for further research in this area.

Acknowledgement

This work was supported by the Slovak Research and Development Agency of the Ministry of Education, Science, Research and Sport of the Slovak Republic within the project No. VEGA 1/5058/18 “Research of the interaction of a braked railway wheelset and track in simulated operational conditions of a vehicle running in a track on the test bench”.

The work was also supported by the Cultural and Educational Grant Agency of the Ministry of Education of the Slovak Republic within the project No. KEGA 077ZU-4/2017- “Modernization of the Vehicles and engines study program”.

References

1. MASEK, J., KENDRA, M., MILINKOVIC, S., VESKOVIC, S., BARTA, D.: Proposal and Application of Methodology of Revitalisation of Regional Railway Track in Slovakia and Serbia. Part 1: Theoretical Approach and Proposal of Methodology for Revitalisation of Regional Railways. Transport Problems, 10, 85-95, 2015. https://doi/10.21307/tp-2015-064
2. DVORAK, Z., LEITNER, B., NOVAK, L.: Software Support for Railway Traffic Simulation under Restricted Conditions of the Rail Section. Procedia Engineering, 134, 245-255, 2016. https://doi.org/10.1016/j.proeng.2016.01.066
3. LENDEL, V., PANCIKOVA, L., FALAT, L., MARCEK, D.: Intelligent Modelling with Alternative Approach: Application of Advanced Artificial Intelligence into Traffic Management. Communications - Scientific Letters of the University of Zilina, 19(4), 36-42, 2017.
4. EN 13749, Railway Applications - Wheelsets and Bogies - Method of Specifying the Structural Requirements of Bogie Frames. European Committee for Standardization, Brussels, 2011.
5. UIC 566, Loading of Coaches Bodies and their Components. 1994.

6. KOSTRZEWSKI, M., CHUDZIKIEWICZ, A.: Rail-Track Quality Indicator towards Rail Driving Dynamics. Proceedings of the 14th Mini Conference on Vehicle System Dynamics, Identification and Anomalies (VSDIA 2014), Hungary, 211-218, 2014.
7. LUNYS, O., DAILYDKA, S., STEISUNAS, S., BUREIKA, G.: Analysis of Freight Wagon Wheel Failure Detection in Lithuanian Railways. Procedia Engineering, 134, 64-71, 2016. https://doi.org/10.1016/j.proeng.2016.01.040
8. HAUSER, V., NOZHENKO, O., KRAVCHENKO, K., LOULOVA, M., GERLICI, J., LACK, T. : Impact of Three Axle Boxes Bogie to the Tram Behavior when Passing Curved Track. Procedia Engineering, 192, 295-300, 2017. https://doi.org/10.1016/j.proeng.2017.06.051
9. CHUDZIKIEWICZ, A., MELNIK, R.: Statistical Analysis of Vibration for the Rail Vehicle Suspension Monitoring System. Proceedings of the 13th Mini Conference on Vehicle System Dynamics, Identification and Anomalies (VSDIA 2012), Hungary, 149-155, 2012.
10. STEISUNAS, S., BUREIKA, G.: Study of Freight Wagon Running Dynamic Stability Taking into Account the Track Stiffness Variation. Transport Problems, 9(4), 131-143, 2014.
11. LACK, T., GERLICI, J., MANUROVA, M.: Freight Car Bogie Properties Analysis by Means of Simulation Computations. Manufacturing Technology, 16(4), 733-739, 2016.
12. SOUKUP, J., SKOCILAS, J., SKOCILASOVA, B.: Assessment of Railway Wagon Suspension Characteristics. Mechanical Systems and Signal Processing, 89, 67-77, 2017. https://doi.org/10.1016/j.ymssp.2016.08.022
13. KLIMENDA, F., SVOBODA, M., RYCHLIKOVA, L., PETRENKO, A.: Investigation of Vertical Vibration of a Vehicle Model Driving Through a Horizontal Curve. Manufacturing Technology, 15(2), 143-148, 2015.
14. MANUROVA, M., SUCHANEK, A.: Determination of Stiffness of Triple Spring Built in a Bogie of a Rail Vehicle. Manufacturing Technology, 16(2), 390-396, 2016.
15. STASTNIAK, P., MORAVCIK, M.: Freight Bogie Prototype Properties Analysis by Means of Simulation Computations. Manufacturing Technology, 17(3), 381-388, 2017.
16. GERLICI, J., GORBUNOV, M., NOZHENKO, O., PISTEK, V., KARA, S., LACK, K., KRAVCHENKO, K.: About Creation of Bogie of the Freight Car. Communications - Scientific Letters of the University of Zilina, 19(2A), 29-35, 2017.
17. GERLICI, J., GORBUNOV, M., KRAVCHENKO, K., PROSVIROVA, O., LACK, T.: The Innovative Design of Rolling Stock Brake Elements. Communications - Scientific Letters of the University of Zilina, 19(2A), 23-28, 2017.
18. FALENDYSH, A., VOLODARETS, M., HATCHENKO, V., VYKHOPEN, I.: Software Analysis for Modeling the Parameters of Shunting Locomotives Chassis. MATEC Web of Conferences, 116, 03003, 2017. https://doi.org/10.1051/matecconf/201711603003
19. KALINCAK, D., JANICEK, F., KORECZ, K., LANG, A.: Rail Vehicles. Solved Tasks (In Slovak). University of Zilina, 2004.
20. LACK, T., GERLICI, J.: Railway Wheel and Rail Roughness Analysis, Communications - Scientific Letters of the University of Zilina, 11(2), 41-48, 2009.
21. LACK, T., GERLICI, J.: Wheel/Rail Tangential Contact Stress Evaluation by Means of Modified Strip Method. Communications - Scientific Letters of the University of Zilina, 16(3A), 33-39, 2014.
22. SAPIETOVA, A., SAGA, M., STANCEKOVA, D., SAPIETA, M.: Contribution to Numerical Study of Vehicle Vertical Stochastic Vibration. MATEC Web of Conferences, 157, 03015, 2018. https://doi.org/10.1051/matecconf/201815703015
23. SAGA, M., VASKO, M., KOPAS, P., JAKUBOVICOVA, L.: Numerical Algorithm for Beam Residual Stress Identification. Communications - Scientific Letters of the University of Zilina, 16(3A), 13-18, 2014.
24. KULHAVY, P., KOVALOVA, N., VOSAHLO, J.: Methods of Creating a Numerical Model of a Real Seam Based on Experimental Data. Proceedings of the 53rd International Conference on Experimental Stress Analysis (EAN 2015), Czech Republic, 195-202, 2015.
25. BREZANI, M., BARAN, P., LABUDA, R.: Proposal of the Combined Exhaust Gas Heat Exchanger and the Muffler. Diagnostyka, 16(3), 73-78, 2015.
26. VATULIA, G., FALENDYSH, A., OREL, Y., PAVLIUCHENKOV, M.: Structural Improvements in a Tank Wagon with Modern Software Packages. Procedia Engineering, 187, 301-307, 2017. https://doi.org/10.1016/j.proeng.2017.04.379
27. DROPPA, P., HALGAS, P.: Analysis of Hull Protection against Improvised Explosive Devices. Proceedings of the 18th International Conference on Transport Means (Transport Means 2014), Lithuania, 153-156, 2014.
28. DIZO, J., BLATNICKY, M., SKOCILASOVA, B.: Computational Modelling of the Rail Vehicle Multibody System Including Flexible Bodies. Communications - Scientific Letters of the University of Zilina, 17(3), 31-36, 2015.
29. HAUSER, V., NOZHENKO, O., KRAVCHENKO, K., LOULOVA, M., GERLICI, J., LACK., T.: Proposal of a Steering Mechanism for Tram Bogie with Three Axle Boxes. Procedia Engineering, 192, 289-294, 2017. https://doi.org/10.1016/j.proeng.2017.06.050

Jozef Melcer - Jan Kortis - Lubos Daniel - Peter Fabo*

IDENTIFICATION OF MODAL FREQUENCIES FROM THE PRE-STRESSED CONCRETE BRIDGE DYNAMIC RESPONSE TO DIFFERENT SOURCES OF DYNAMIC EXCITATION

The natural frequencies and mode shapes are unique characteristics of each mechanical structure. Their prediction is a crucial part of each dynamic experimental measurement. However, the proper identification of higher natural frequencies and mode shapes can be a problem, especially for big structures such as bridges. The reason is the need to excite the bridge in such a way that it responds in a free-vibrations mode shape. This paper describes three various sources of excitations, which are used to identify the modal characteristics of the pre-stressed concrete bridge. The impulse excitation, traffic load and ambient vibration are used and analyzed. In the case of the loading by a force impulse, modal shapes are also obtained. The study shows that the intensity and kind of the excitation has a noticeable impact on identification of modal frequencies. Finally, the results of the experimental measurements are used to calibrate the numerical model.

Keywords: *dynamic excitation, modal frequencies, free vibrations, moving load, FRF function*

1. Introduction

There is a long tradition in the Czech and Slovak Republic to investigate the effect of moving load on the bridge structures [1], [2]. The theoretical approaches have been also supported with the experimental investigation [3], [4]. The dynamic experimental measurements of real bridge structures are an important source of data that can be used in different ways. Detection of modal characteristics is one of the most important [5]. Knowledge of them is an essential assumption for various applications like model updating, dynamic load identification and health monitoring, or a damage detection problem. There seems to be important to make the right decision on which suitable excitation technique should be used with respect to the conditions that are unique for each bridge structure. From a practical point of view, diagnostic methods, like operational modal analysis (OMA), are preferred because no excitation devices are used and the traffic on the bridge is not limited [6]. Even though that these techniques are useful, it is not clear if they are useful for all conditions.

The main issue in this case is to apply various excitation sources and to analyze effect of them on the obtained modal frequencies of the bridge. The first source of excitation is the impact device, which loads the bridge with an impact impulse (impulse load) in the selected points. In this case, the intensity of impulse is also measured so the techniques of experimental modal analysis (EMA) are used to obtain the modal shapes and frequencies. The second source of excitation is a heavy vehicle passing over the bridge. In that case, the measured dynamic properties of the system vary over time as the vehicle changes its position on the bridge. The advantage is that the weight and position of the vehicle during the measurements are well-known. The ambient vibrations, caused by a train passing over the rail located under the bridge, is the third source of the excitation [7]. This kind of load can be defined as purely random ambient excitation. The speed and weight of the train are not clearly known, as they were not investigated.

The same methodology of transformation of the obtained measured signals into the frequency-domain is chosen for all the three cases (sampling frequencies, filtering, time window, etc.). In the cases when the bridge is excited by an impact device and by the passing train, the frequency response functions (FRF) were also calculated by applying the techniques of OMA and EMA. The article also presents the application of measured data to verify the numerical model of the bridge.

The presented study is focused on the road bridge situated between the two villages, Varin and Mojs, near the city Zilina in the Slovak Republic (Figure 1a). The full length of three span bridge is 87 m. Each span acts independently as a simple supported beam. The main girders 25 I-73 are prefabricated pre-stressed concrete structures with the length 29 m. The girders are placed in the transversal position with the mutual distance 1.44-1.45 m. The cross-section of the bridge contains eight girders. The shapes of the girders and the layers of pavement are showed in the Figure 1b.

2. The excitation of the bridge with impact load

The impulse load is used for experimental modal analysis (EMA) of the bridge. The EMA is a common technique that is used to obtain the frequency response function. Consequently, the modal frequencies and mode shapes of the structure are estimated [8]. The hammer impulse excitation device or electrodynamic shaker are often used as a source of excitation. The choice depends

* [1]Jozef Melcer, [2]Jan Kortis, [2]Lubos Daniel, [2]Peter Fabo
[1]Department of Structural Mechanics and Applied Mathematics, Faculty of Civil Engineering, University of Zilina, Slovakia
[2]Research Center, University of Zilina, Slovakia
E-mail: jan.kortis@fstav.uniza.sk

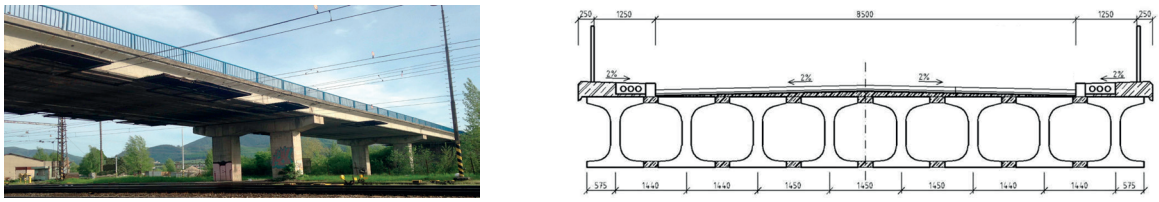

a *b*

Figure 1 *Measured and analyzed concrete bridge, a - photography of actual state, b - the draw of the cross-section*

a *b*

Figure 2 *Modal analysis of the bridge excited by the impact load, a - impact device and its application, b - location of the measurement and loading points*

on the type of structure and what is required to be obtained. In the presented case, the bridge is excited with the impact device with mass that has weight 10 kg and it falls from 1.0 m height (Figure 2a). The sensor that measures the dynamic force is positioned in the contact steel plate. It is a piezoelectric force transducer Kistler 906. The response of the bridge is measured with six piezoelectric accelerometers BK 4508 B002. The analogue signals from the accelerometers and force transducers are amplified and digitalized with the device DEWETRON DEWE-3200.

The location of the accelerometers (ACC) on the bridge and the positions of the excitation points (F_1, F_2) are shown in Figure 2b. The points are situated in the middle and in the quarter of the span, transversally; they are situated on the edge of the pavement. There were seven force impulses generated with the impact device during one measurement. An example of the time series of the measured excitation (impulse at the point F_1) and the bridge response (accelerometer in the point ACC_2) are shown in Figure 3.

Six frequency response functions (FRF) are obtained. The last step is to average them and to obtain a Modal Identification Function (MIF). Figure 4 shows results of the modal analysis for impulse load located at point F_1 (Figure 4a) and at point F_2 (Figure 4b).

The first bending mode shape on the frequency f_1 = 3.906 Hz and the first torsional mode shape on the frequency f_2 = 7.813 Hz were identified in the MIF for point F_1. The second bending mode shape on the frequency f_3 = 14.453 Hz and the second torsional mode shape on the frequency f_4 = 19.953 Hz were identified in the MIF for point F_2. The higher mode shapes were not possible to identify correctly, as there was not sufficient number of measurements points. One of the alternatives, for the same number of accelerometers, seems to be an approach when the measurement is repeated for various locations of measurements points. This has not been applied here.

3. The excitation of the bridge with the moving lorry

The moving lorry T-815 was the second source of excitation. This type of excitation is recommended in the Slovak technical

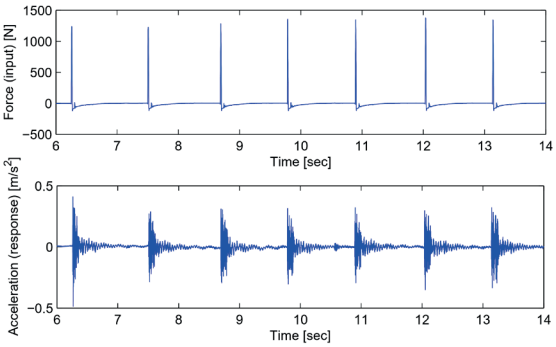

Figure 3 *Example of the measured input (impulse F_1) and output signals (ACC_2)*

standard STN 73 6209 for the dynamic diagnostic tests of the bridges with longer span than 40 m. The obstacle in the middle of the span was used to increase the excitation with the vehicle. The dynamic response of the bridge was measured with the piezoelectric accelerometers BK 8306 (BK1, BK2) located in the middle and quarter of the span. In this case, it is necessary to identify the moment when the vehicle arrives and leaves the bridge. For that purpose, the steel plates with accelerometers BK 4508B 002 (AC1, AC2) are located on the pavement at the beginning and at the end of the span. The situation on the bridge and the positions of the sensors are shown in Figure 5.

During the measurement, 21 passes of the vehicle at different speeds from 5 to 35 km/h were performed with a gross weight of a vehicle of 22.9 t (rear axle 17.45 t, front axle 5.45 t). In Figure 6 there are also results of the FFT that were obtained for the measured signal from accelerometers BK1 and BK2. The function is divided into three parts (t_1 - before the beginning of the test, t_2 - forced vibrations, t_3 - free vibrations). From the measured data, the first two significant frequencies were obtained; the first measured frequency f_1 = 3.91 Hz corresponding to the first bending mode shape and the second frequency f_2 = 7.81 Hz corresponding to the first torsional mode shape.

The results show that the changes in the modal frequencies, while the vehicle is on the bridge, do not vary significantly for the investigated structure. From the free vibrations (t_3) of the

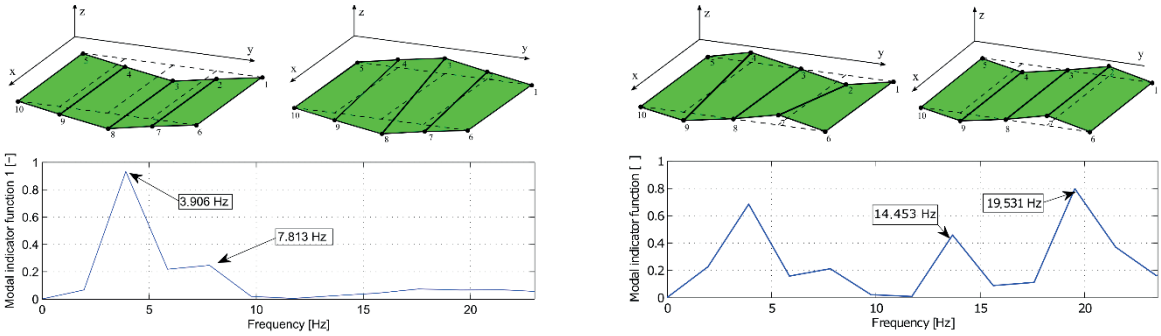

a *b*

Figure 4 *MIF functions and modal shapes of the bridge, a - analysis from impact F_1, b - analysis from impact F_2*

a *b*

Figure 5 *Situation on the bridge by the dynamic measurement, a - situation on the bridge and lorry, b - positions of the sensors*

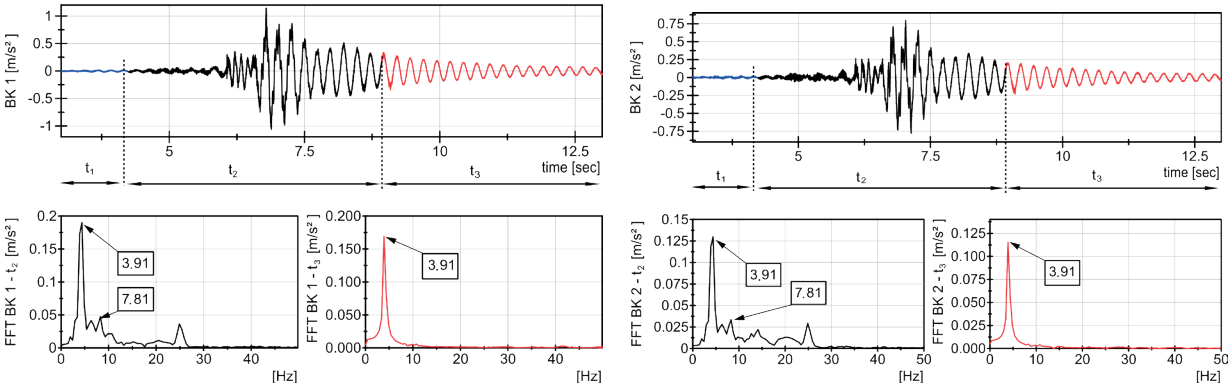

a *b*

Figure 6 *The measured signals and spectrums from accelerometers BK1 (a), BK2 (b)*

structure, it was not possible to recognize the higher mode shapes (frequencies). The reason is the effect of structural damping on the higher mode shapes.

4. The excitation of the bridge with the train moving on the railway near the bridge (ambient vibrations)

The last source of the excitation were the ambient vibrations, generated by the moving train. It was a common passenger train moving at the speed of 80-90 km/h on the rail road, which is crossed under the bridge. The natural bridge frequencies were recognized from the FRF functions that were derived from the response signals and the input signals. The input signal at the ground near to the pillar was measured with the accelerometer BK 8306 (ACC1). The response of the bridge was measured by the two accelerometers BK 8306 positioned in the middle of the span (ACC3) and in the one fourth of the span (ACC2). The whole situation during the experimental measurement is shown in Figure 7.

The example of the measured input (ACC1) and output signals (ACC2, ACC3) are shown in Figure 7c. In the FRF functions, the three modal frequencies are identified (Figure 8). Modal frequencies f_1 = 3.906 Hz and f_3 = 14.650 Hz are also identified in previous measurements. The peak at the frequency f_2 = 9.280 Hz, which is identified in both FRF signals is very interesting as it was not possible to identify it in the previous cases. The following comparison to the numerical model shows that it is also a natural frequency.

5. Calibration of the numerical model of the bridge based on the FEM

The last part in the article is focused on application of the obtained data from the experimental analysis for calibration of the numerical model of the concrete bridge. A model of the whole

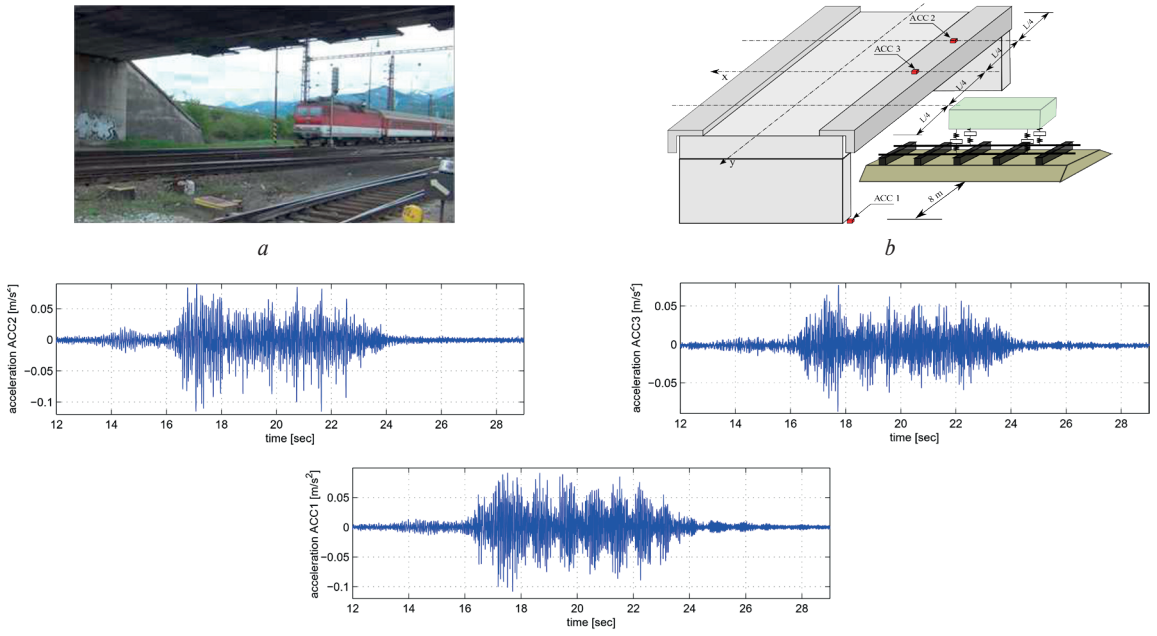

a b c

Figure 7 *Ambient vibration of the bridge generated by the mobbing train, a - passing train, b - positions of the sensors, c - example of the signals*

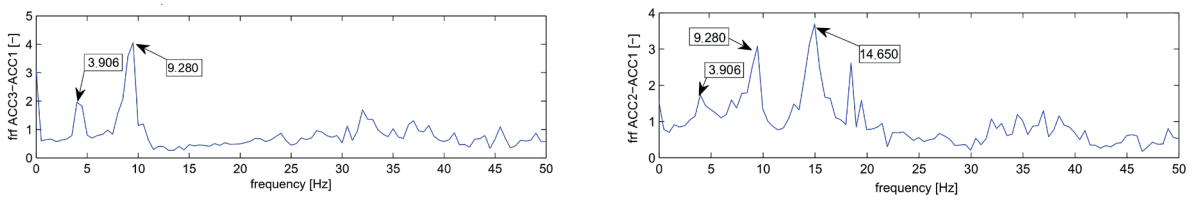

a b

Figure 8 *FRF functions of the structure between sensors ACC3-ACC1 (a), ACC2-ACC1 (b)*

Table 1 *The material characteristics of the structure parts of the bridge*

Construction part	Young modulus [GPa]	Poisson's ratio [-]	Density [kg/m3]
Main girders I	42	0.15	2600
Concrete bridge deck	28	0.25	2400
Concrete cornice	31	0.3	2300
Concrete fills	2	0.3	2300

bridge was not created, but only a model of the middle span. That is enough since the measurements show that each span acts as a single supported beam. The 3D model (3D solid elements) in the commercial software ADINA 9.1 was created, which uses the finite element method for the mathematical definition of the mechanical structures. The numerical model was divided into fourth parts; each part has different linear isotropic material characteristics with respect of the material defined in the plans and technical reports of the bridge values and they are defined in Table 1.

There was only a problem to choose the right characteristics of the concrete fills used between the girders. Their material properties have a significant effect on the global torsional stiffness of the structure and they influence all the calculated modal shapes. Their characteristics were possible to be updated only after the experimental analysis. For surfaces, where girders are placed on bearings, the boundary conditions were defined. The zero translation for the vertical directions and for horizontal direction were defined where there are bearings with restrictions. The geometry of the model with different color for each structural part is shown in Figure 9. The continuous connection of the mesh was created between the elements with different material parameters.

The natural frequencies and mode shapes are computed by application of the Lanczos algorithm. Five natural frequencies and mode shapes were calculated. Figure 10 shows two bending shapes corresponding to the frequencies f_1 = 3.899 Hz and f_4 = 14.510 Hz, two torsional shapes corresponding to frequencies f_2 = 7.856 Hz and f_5 = 20.210 Hz and bending-torsional shape corresponding to the frequency f_3 = 9.281 Hz.

Summary of the calculated natural frequencies and the frequencies obtained from the experimental analysis are

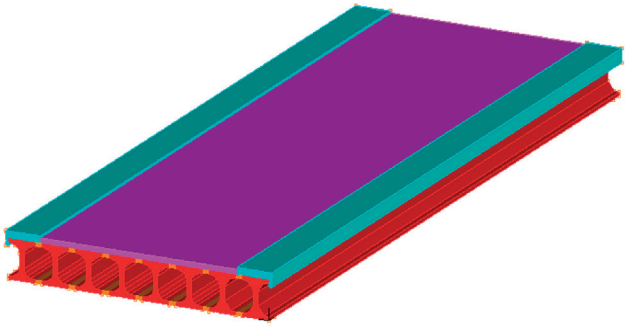

Figure 9 *The 3D FEM model of the bridge in the software ADINA*

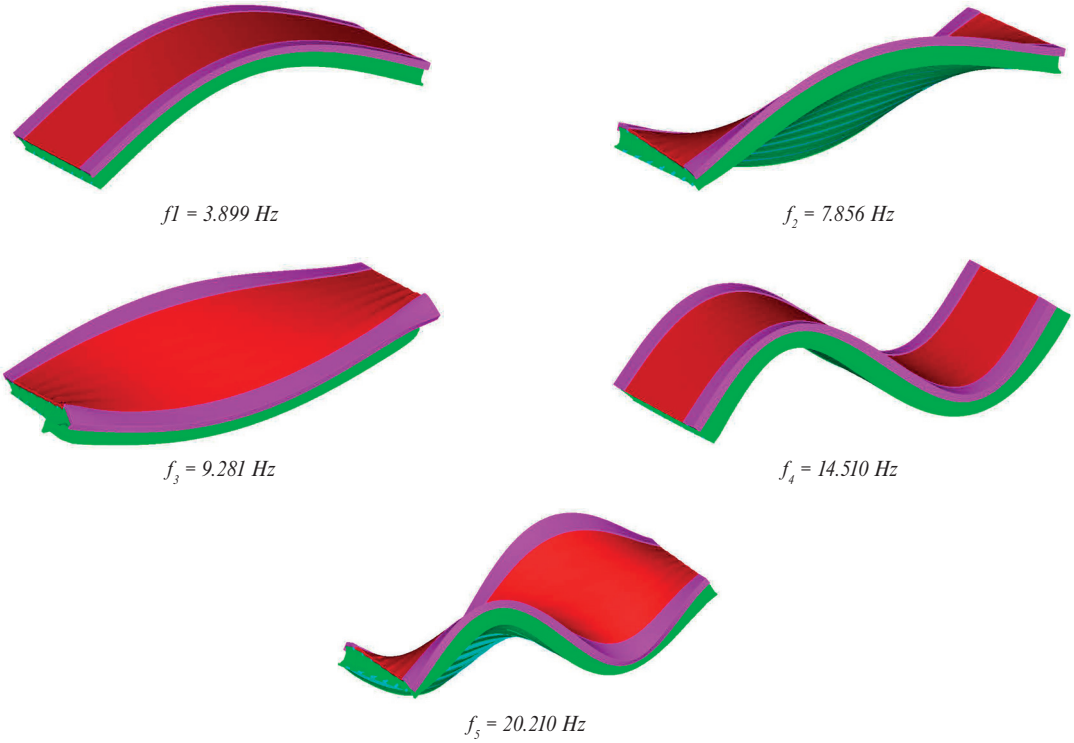

Figure 10 *Modal shapes of the 3D model of the bridge*

Table 2 *Summary of the natural frequencies*

Modal shapes [-]	Identified modal frequencies f_i [Hz]			
	FEM model	Experimental measurements		
		Impulse force	Moving vehicle	Ambient vibration
1. Bending mode	3.899	3.906	3.910	3.906
2. Torsional mode	7.856	7.813	7.810	Indeterminate
3. Torsional-bending mode	9.281	Indeterminate	Indeterminate	9.280
4. Bending mode	14.510	13.687	Indeterminate	14.650
5. Torsional mode	20.210	19.531	Indeterminate	Indeterminate

shown in the Table 2. The results show that all the calculated modal frequencies of the structure are also recognized by the experimental measurements. The frequency of 9.280 Hz is interesting. This frequency was obtained in the model only when the Young modulus of the concrete fills between the girders was changed to the value 2 GPa (Table 1). After the torsional stiffness of the cross-section is reduced, the calculated natural frequencies were reduced to the values comparable to the natural frequencies obtained from the measurements. The second and fourth natural frequencies of the numerical model, after Young modulus of concrete fills was updated, were comparable to the measured frequencies.

The sources of excitation with impulse force and with moving vehicle primarily excited the first torsional mode shape at frequency f_2 = 7.856 Hz. This frequency is very close to the third one f_3 = 9.281 Hz, so the dominant second frequency covers the

third natural frequency. It was possible to be identified only when the structure was excited by the ambient vibrations. As a result, the third natural frequency was not possible to be identified if the bridge was excited by the vertical loading. On the other hand, the first torsional mode shape was not possible to be identified correctly from the response of the bridge to the excitation by the train.

6. Conclusions

The dynamic properties of the concrete bridge were measured and investigated by applying the various types of the excitations. The presented results show that different sources of excitations can lead to identification of different natural frequencies of the structure. For instance, the third torsional-bending mode shape of the investigated bridge can be excited and its frequency can be identified only when the bridge is excited by the ambient vibrations. On the other hand, the first torsional mode shape is excited only by the vertical load, like the impact force or the moving vehicle. In that case, the results of numerical model were crucial to identify the natural frequencies correctly. The combination of measurements of the response to several types of excitations with the results of numerical model seems to be a suitable alternative for proper identification of all the modal characteristics.

Acknowledgments

This paper was supported by the Grant Research Cetnre of The University of Zilina - Second Phase (grant No. 313011D011) and by the Grant National Agency VEGA of the Slovak Republic (grant No. 1/005/16).

References

[1] KOLOUSEK, V., MCLEAN, R. F.: Dynamics in Engineering Structures. Butterworths, 1973.
[2] FRYBA, L.: Vibration of Solids and Structures under Moving Loads. Springer Science & Business Media, 2013.
[3] FISCHER, O., PIRNER, M.: Modal Analysis and Analysis of Forced Vibrations of Multispan Bridges. Acta technica CSAV, 50(2), 167-176, 2005.
[4] FRYBA, L., PIRNER, M.: Load Tests and Modal Analysis of Bridges. Engineering Structures, 23(1), 102-109, 2001. https://doi.org/10.1016/S0141-0296(00)00026-2
[5] TESAR, A., MELCER, J.: Structural Monitoring in Advanced Bridge Engineering. International Journal for Numerical Methods in Engineering, 74(11), 1670-1678, 2008. https://doi.org/10.1002/nme.2224
[6] KORTIS, J., DANIEL, L., FARBAK, M., MALIAR, L., ŠKARUPA, M.: Operational Modal Analysis of the Cable stayed Footbridge. Civil and Environmental Engineering, 13(2), 92-98, 2017. https://doi.org/10.1515/cee-2017-0012
[7] KOUROUSSIS, G., CONNOLLY, D. P., VERLINDEN, O.: Railway-Induced Ground Vibrations - A Review of Vehicle Effects. International Journal of Rail Transportation, 2(2), 69-110, 2014. https://doi.org/10.1080/23248378.2014.897791
[8] CUNHA, A., CAETANO, E.: Experimental Modal Analysis of Civil Engineering Structures. Sound & Vibration, 40(6), 12-20, 2006.

Andrea Kocianova - Eva Pitlova*

CRITICAL GAPS AT UNSIGNALIZED INTERSECTIONS WITH BENDING RIGHT-OF-WAY

The capacity calculation procedure for unsignalized intersections is based on the gap-acceptance theory in most of existing capacity regulations and it relies on one of the important parameters - critical gap. However, the capacity calculation procedure and values of critical gaps according to these regulations are valid only for intersections with standard right-of-way (major street leading straight). Nevertheless, in Slovakia, intersections with bending right-of-way (major street not leading straight, but bending) can be encountered. The specific mode of right-of-way results in different priority ranks of traffic movements (set by traffic rules of driving), more complicated traffic situation and therefore, different driver behaviour characteristics. To examine the gap acceptance behaviour of drivers under these specific conditions, an unsignalized four-leg intersection with bending right-of-way located in an urban area of Zilina, Slovakia, was selected. Three different methods (Raff, Wu, and MLM Troutbeck) were used for critical gap estimation from the field data. In the article, results of critical gaps for three through movements of different priority rank (major-street through movement of Rank 2 and minor-street through movements of Rank 3 and 4) are presented. The results show, that the values of critical gaps differ depending on the method by about 3-5 % only, which is not significant. Troutbeck´s MLM method gives the highest values. The priority rank of movement has the greatest impact on the result. The values of critical gap for major-street through movement of Rank 2 are the smallest; they are approximately 1.3-2.1 s smaller than the values for minor-street through movements of Rank 3 or 4. The highest values of critical gap have been estimated for minor-street through movement of Rank 4 and they are higher compared to the current Slovak regulations TP 102 values for the same priority rank.

Keywords: *critical gap, gap-acceptance behaviour, capacity, unsignalized intersection*

1. Introduction

Unsignalized intersections are the most widely used type of intersections in the road network. The major street is usually the intersecting street with the dominant traffic volume. For this type of unsignalized intersections, capacity calculation procedure based on the gap-acceptance theory and gap-acceptance characteristics of driver behaviour are determined in most of the existing regulations. However, in Slovakia, intersections with bending right-of-way (major street not leading straight, but bending) can be encountered. The specific mode of right-of-way results in different priority ranks of traffic movements (set by traffic rules of driving), more complicated traffic situation, and therefore, different driver behaviour characteristics. The issue is that for this kind of intersection there is no generally known procedure for capacity calculation and no values of critical gaps determined. For this reason, a four-leg unsignalized intersection with bending right-of-way was chosen and gap-acceptance behaviour of drivers characterized by critical gap times was investigated. In the article, critical gaps for the same traffic movements of different priority ranks estimated by three methods (Raff, Wu and MLM Troutbeck) are presented and compared to values of critical gaps in Slovakia valid for standard intersection with straight major street, according to the Slovak regulations TP 102 [1].

2. Description of intersection and data collection

For investigation purposes of the gap-acceptance behaviour of drivers on a specific unsignalized intersection with bending right-of-way, the four-leg intersection located in an urban area of Zilina, Slovakia, was chosen (see Figure 1). Due to the higher load at neighbouring entrances, major street is led in a turn and that causes different redistribution of traffic stream ranks in comparison to traffic management at standard intersection with straight major street. Each traffic stream rank, with its duty to give priority in a specific situation, is shown in Figure 1 and Table 1. However, in practice, for drivers, it is sometimes hard to realize immediately to whom they have to give way [2].

To collect data about traffic load at the investigated intersection, 12-hour traffic survey during a typical working day was performed. The directional distribution and composition of traffic flows were monitored at all the intersection entries. The hourly traffic volumes, with highlighted peak hours in the morning and afternoon, are shown in Figure 2. Traffic patterns during those peak hours, shown in Figure 3, point to a different traffic load redistribution in the morning and in the afternoon. Therefore, the other two 120-minute video recordings during the morning and afternoon peak hours were carried out to collect all the necessary data for critical gap estimation. The total traffic volume on the major street varied from 700 to 1 200 veh/h and 250 to 500 veh/h on the minor street in this observation time. In addition, the waiting time of minor-stream vehicles, queue lengths, and other factors influencing the critical gaps or follow-up

* **Andrea Kocianova, Eva Pitlova**
Department of Highway Engineering, Faculty of Civil Engineering, University of Zilina, Slovakia
E-mail: andrea.kocianova@fstav.uniza.sk

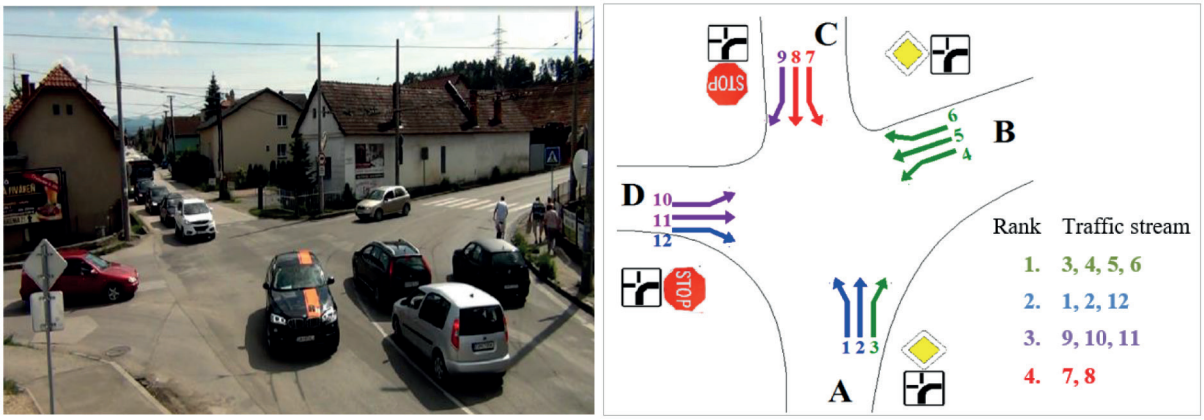

Figure 1 *Intersection with bending right-of-way in Zilina and priority ranks of traffic streams at a four-leg intersection*

Table 1 *Priority rules for traffic streams at the intersection with bending right-of-way*

Rank of priority	Traffic stream	Movement	Gives priority to
2.	1	Major-street left-turn	4, 5
	2	**Major-street through**	**4, 5, 6**
	12	Minor-street right-turn	4
3.	9	Minor-street right-turn	1, 5
	10	Minor-street left-turn	1, 2, 5 ,6
	11	**Minor-street through**	**1, 2, 3, 4**
4.	7	Minor-street left-turn	2, 3, 4, 5, 10,11
	8	**Minor-street through**	**1, 4, 5, 10, 11,12**

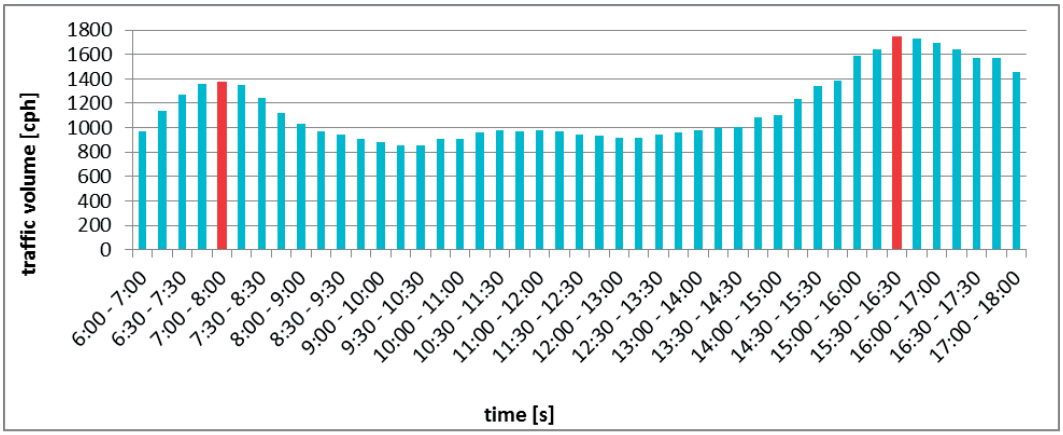

Figure 2 *Traffic volumes during the 12-hour survey and peak hour times*

times (e.g., compliance with road traffic rules, signalling or non-signalling the change of direction of the major-stream vehicles, interruptions by pedestrians, deliberate release of minor-stream vehicles by major-stream vehicles) were monitored.

The video recordings were semi-automatically processed using a special software designed for these purposes. All the necessary data about each minor- and major-stream vehicle were recorded into a database. Each minor-stream vehicle with vehicle type, direction and time of arrival and departure at a specific intersection point was recorded. Each major-stream vehicle, using vehicle type, direction and time of passing a certain cross-line in the intersection, was recorded. These raw data were then used for specifying the major stream gaps for each minor-stream vehicle using a specific tool designed for these purposes. Only gaps between the relevant conflicting-stream vehicles of higher priority according to traffic rules (see Table 1) and only minor-stream vehicles with at least one rejected lag or gap were taken into account. The result was a list of just one accepted and one or more rejected gaps/lags for each minor-stream vehicle together with its waiting time at the first position. An example of these data is presented in Table 2.

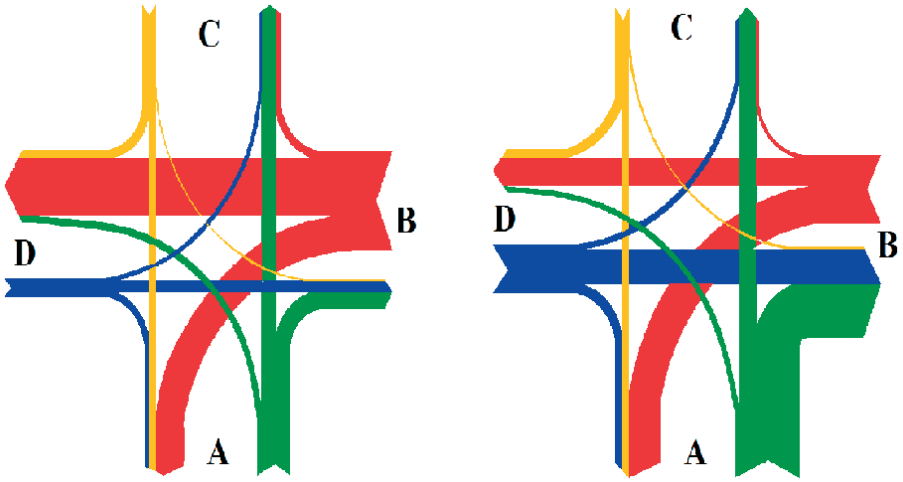

(a) *(b)*

Figure 3 *Pattern of the traffic load redistribution during the morning (a) and afternoon (b) peak hour*

Table 2 *Example of gap-acceptance data at the investigated intersection*

Minor-stream vehicles					Major-stream vehicles				
Traffic stream	Arrival time	Depart. time	Veh. type	Waiting time	Passing time	Traffic stream	Veh. type	Gap/lag time	Type
2	819.20	826.08	Car	6.88	820.72	4	Car	1.52	Rejected lag*
					823.48	4	Car	2.76	Rejected gap
					837.76	5	Car	14.28	Accepted gap
2	834.48	838.36	Car	3.88	837.76	5	Car	3.28	Rejected lag*
					846.96	5	Car	9.20	Accepted gap
11	847.2	860.72	Car	13.52	851.28	1	Car	4.08	Rejected lag*
					857.92	4	Car	6.64	Rejected gap
					859.52	4	Car	1.60	Rejected gap
					871.12	1	Car	11.60	Accepted gap

*lag - the time difference between the arrival time of the minor-stream vehicle and passing time of the first conflicting stream vehicle

3. Estimation of critical gaps

3.1 Critical gap

The critical gap can be defined as the minimum time interval between the major-stream vehicles that is necessary for one minor-stream vehicle to make a maneuver. Values of the critical gaps are different for different drivers and they are dependent on the type of movement, geometry parameters of an intersection and the traffic situation, among others. Due to this variability, the gap acceptance process is considered as a stochastic process and the critical gaps are random variables. Since it is not possible to measure the critical gap time directly, the accepted gap and corresponding largest rejected gap/rejected lag, for each minor-stream vehicle, were used. That means, the data linked to drivers who rejected at least one gap or lag only, were taken into account. Those data were then sorted based on consistent driver behaviour. To obtain the representative sample, the pairs of gaps where drivers had accepted smaller gap than they had rejected, were discarded. Besides that, the other pairs were excluded as well, when accepted or rejected gap had been influenced by other factors such as violation of priority rules or traffic flow interruption by a pedestrian.

The processed and sorted data were used to estimate the critical gaps for three through movements from major and minor street of different priority ranks, highlighted in Table 1. There is a major-street through movement of Rank 2 (traffic stream 2), a minor-street through movement of Rank 3 (traffic stream 11) and a minor-street through movement of Rank 4 (traffic stream 8). The critical gaps were estimated based on two samples - Sample 1 and Sample 2. Sample 1 consists of pairs of the largest rejected gap and its corresponding accepted gap for each minor-stream vehicle. Sample 2 consists of pairs from Sample 1 supplemented by pairs of accepted gap that has only one pertaining rejected lag. Sample 1 for major-street through movement of the traffic stream 2 is shown in Figure 4.

Several methods for the critical gap estimation are presented in literature [3], [4], [5], [6]. In this paper, three methods were used - the Raff´s Method [7], the Troutbeck´s Maximum Likelihood Method [8], and Wu´s Method [9], which are briefly described below.

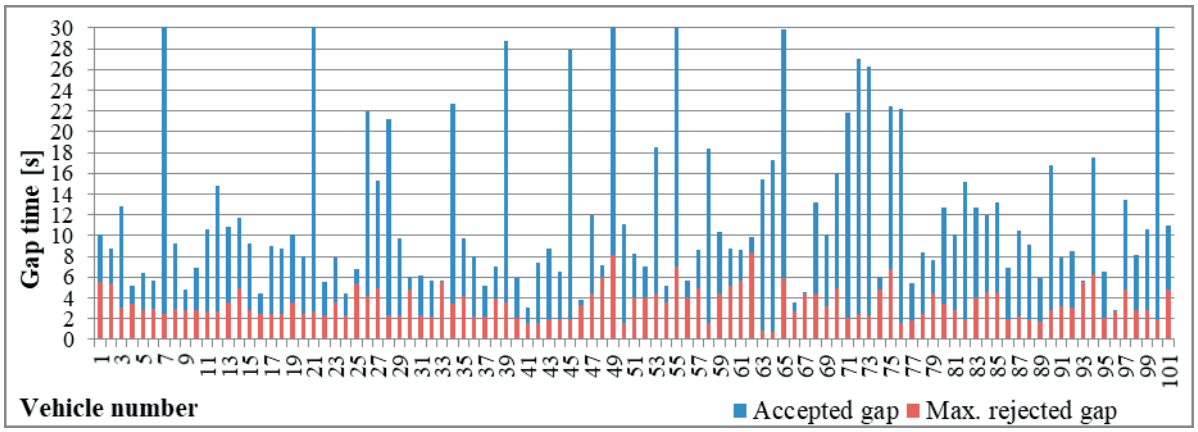

Figure 4 *Maximum rejected and accepted gap times for the traffic stream 2 (Sample 1)*

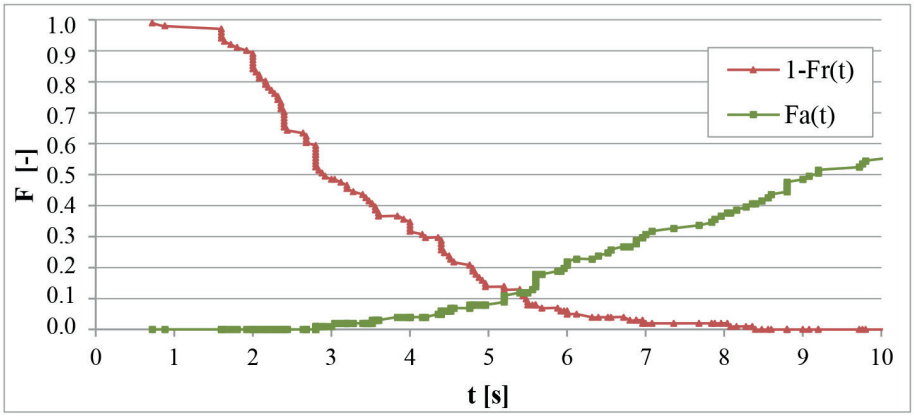

Figure 5 *Example of the critical gap estimation according to Raff´s method for traffic stream 2*

3.2 Raff´s method

The method of Raff [9], is based on macroscopic model and it is the earliest method for estimating the critical gap which is used in many countries because of its simplicity [4]. This method involves the empirical cumulative frequency distributions of accepted gaps $F_a(t)$ and rejected gaps $F_r(t)$. When the sum of cumulative curves of accepted gaps and rejected gaps is equal to 1 then a gap of length t is equal to the critical gap t_c. It means that the number of rejected gaps larger than the critical gap is equal to the number of accepted gaps smaller than critical gap. According to Raff´s method, it is the median value of the critical gap [9].

$$F_a(t) = 1 - F_r(t) \tag{1}$$

Estimation of the critical gap according to Raff´s method for traffic stream 2 is shown in Figure 5. Value of the critical gap is in the cross point of cumulative frequency distribution curves $F_a(t)$ and $1\text{-}F_r(t)$.

3.3 Troutbeck´s MLM method

The model of Troutbeck [8], for the critical gap estimation is based on the Maximum Likelihood Method (MLM) and according to [4] it gives the best results. This microscopic model assumes the log-normal distribution of accepted gaps (a_i) and the corresponding maximum rejected gaps (r_i) for each minor-stream vehicle. The likelihood function is defined as the probability that the critical gap distribution lies between observed distribution of the maximum rejected gaps and the accepted gaps:

$$L^* = \prod_{i=1}^{n} [F(a_i) - F(r_i)] \tag{2}$$

where:

L - maximum likelihood function,
a_i - the logarithm of the accepted gap of vehicle i,
r_i - the logarithm of the maximum rejected gap of vehicle i,
$F(a_i)$, $F(r_i)$ - cumulative distribution functions for the normal distribution.

The logarithm of function (2) is then:

$$L = \sum_{i=1}^{n} \ln[F(a_i) - F(r_i)] \tag{3}$$

The parameters of the critical gap distribution function, the mean μ and variance σ^2, are obtained by maximizing this function. They can be calculated iteratively using the numerical methods. Subsequently, the mean critical gap t_c and the variance s^2 can be computed by equations [8]:

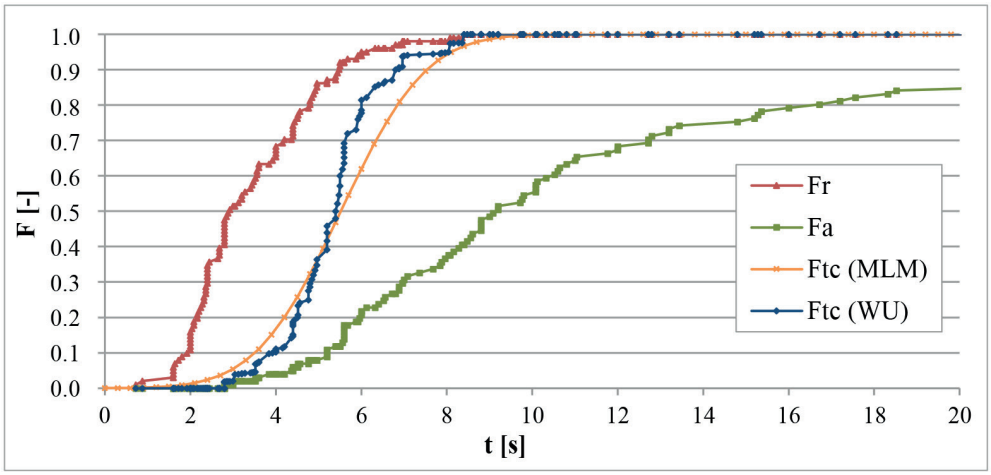

Figure 6 *Distribution functions of the maximum rejected gaps (Fr), accepted gaps (Fa), critical gaps from MLM of Troutbeck (Ftc, MLM) and Wu´s model (Ftc, WU) for the traffic stream 2*

$$t_c = e^{\mu+0.5\cdot\sigma^2} \tag{4}$$

and

$$s^2 = t_c^2 \cdot \left(e^{\sigma^2} - 1\right) \tag{5}$$

respectively.

Distribution functions of the maximum rejected gaps $F_r(t)$, accepted gaps $F_a(t)$ and the estimated critical gaps by Troutbeck´s MLM $F_{tc}(t)$, for the traffic stream number 2, are shown in Figure 6. The likelihood parameters (μ and σ^2) were obtained by the iteration process programmed in MS Excel. The values of mean of the critical gap t_c and variance s^2 were calculated according to Equations (4) and (5).

3.4 Wu´s method

The Wu´s method is quite a recent model for critical gap estimation based on macroscopic probability equilibrium between rejected and accepted gaps [9]. The equilibrium is established macroscopically from the cumulative distribution of the accepted and rejected gaps $F_a(t)$ and $F_r(t)$. This method, unlike Troutbeck´s MLM method, does not require a distribution type of critical gaps and the calculation process is simple without the need of an iteration process. It can be easily implemented into the Excel spreadsheet (detailed calculation procedure step by step is given in [9]). Distribution function of the critical gaps $F_{tc}(t)$ according to Wu´s model is as follows:

$$F_{tc}(t) = \frac{F_a(t)}{F_a(t) + 1 - Fr(t)} = 1 - \frac{1 - F_r(t)}{F_a(t) + 1 - F_r(t)} \tag{6}$$

For comparison, the distribution function of the critical gaps $F_{tc}(t)$ for the traffic stream 2 calculated in accordance with the Wu´s model by Equation (6) is drawn in Figure 6.

4. Results and discussion

In the following Table 3 are listed the critical gaps of the investigated intersection with bending right-of-way for all the three through traffic streams (2, 11 and 8), estimated by three methods (Raff, Wu and Troutbeck´s MLM) from two samples (Sample 1 and Sample 2). The estimated values of the critical gaps from Sample 1 are higher than the values from Sample 2 with the biggest difference in traffic stream 11 estimated by MLM, where the value of the critical gap decreased by *0.6 s*. The comparison of used methods shows small differences for each individual traffic stream. The last two columns in Table 3 show variances of the maximum and minimum values of the critical gaps presented in seconds and percentage. Those differences vary within the range of *3-5 %*. The Troutbeck´s MLM method gives the highest values.

The critical gap value of each individual traffic stream rises with higher priority rank. For the better visual comparison, they are presented in Figure 7. Values of the critical gaps for the traffic stream 2 (major-street through movement of Rank 2) are the smallest (*5.0-5.5 s*). They are about *1.3-2 s* smaller in comparison to the values of traffic streams 11 and 8 (minor-street through movements of Rank 3 and 4). This is due to the traffic stream 2 being the major traffic stream with higher priority with easier traffic situation for its maneuver. Those values also correspond to the critical gap values listed in the current Slovak regulations TP 102 for similar movement - major-street left-turn movement of Rank 2 for conventional rural four-leg unsignalized intersections [1]. A similar situation is with traffic stream 11 (minor-street through movement of Rank 3), where the critical gap values are between *6.2-7.0 s*, depending on the type of sample and estimated method. However, the situation is different for traffic stream 8, which is also minor-street through movement, but with the lowest priority. The values of the critical gap for this traffic stream are in range *7.1-7.4 s*. Values from the field data differ more significantly from the TP 102 values for corresponding priority rank (minor-street left-turn movement of Rank 4). The reason could be more complicated traffic situation and limited familiarity of drivers with this type of intersection on the road network.

Table 3 Critical gaps of through movements of Rank 2, 3, and 4 estimated by three methods compared to values from the Slovak regulations TP 102

Sample	Traffic stream	Priority rank	RAFF	WU	MLM	TP 102	Variance of max - min value	
			[s]	[s]	[s]	[s]	[s]	%
S1	2	2.	5.40	5.35	5.52	5.5 *1	0.17	3.1
	11	3.	6.72	6.78	7.05	6.5 *2	0.33	4.7
	8	4.	7.16	7.19	7.44	6.6 *3	0.28	3.8
S2	2	2.	5.20	4.96	5.17	5.5 *1	0.24	4.6
	11	3.	6.26	6.22	6.45	6.5 *2	0.23	3.6
	8	4.	7.10	7.16	7.26	6.6 *3	0.16	2.2

*1 major-street left-turn movement of Rank 2; *2 minor-street through movement of Rank 3; *3 minor-street left-turn movement of Rank 4

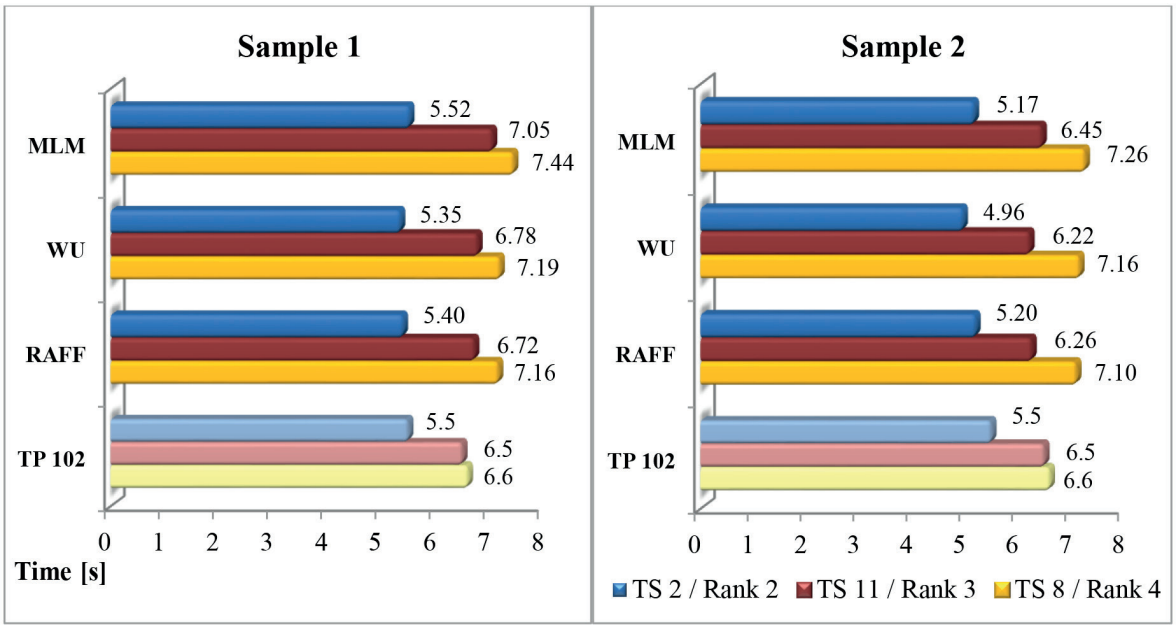

***Figure** 7 Comparison of the critical gaps of through movements of Rank 2, 3 and 4 estimated by three methods (Raff, Wu and MLM) to TP 102 values*

5. Conclusions

Different traffic rules of driving at unsignalized intersections with bending right-of-way in comparison to standard intersections result in a different rank of priority of traffic movements. For such specific redistribution of traffic stream ranks, there is no generally applicable procedure for capacity calculation and, so far, only little research has been focused on investigation of the gap acceptance behavior of drivers.

To find out drivers´ behavior at this type of intersection, the initial study was focused on investigation of the critical gaps. This paper presents the values of the critical gap times for three through movements of different rank of priority estimated for two samples of entering data by three methods (Raff, Wu and Troutbeck). It points to the following:

The values of the critical gaps, estimated by these three methods, do not differ significantly. These differences vary within the range 3-5 %.

The Troutbeck´s MLM method gives the highest values, which were about 0.2 s higher in comparison to Raff or Wu estimation methods.

Values of the critical gaps depend on the sample of entering data of accepted and rejected gaps. These values are higher for Sample 1, where only pairs of accepted and maximum rejected gaps for each minor-stream vehicle were included in the database. The difference is about 0.2-0.6 s.

The values of critical gaps for the same movements, according to major/minor street and rank of priority, differ more significantly. The values of the critical gaps for the major-street through movement of Rank 2 are the smallest. They are about 1.3-1.5 s smaller in comparison to the values for the same through movement from the minor street of Rank 3 and about 1.8-2.1 s smaller in comparison to Rank 4. The values of the critical gap for the minor-street through movement of the lowest priority are the highest and they are also higher in comparison to the Slovak regulations TP 102 value for the same priority rank.

The results of the initial study indicate that it is not correct to use the values of the critical gaps valid for unsignalized

intersections with standard right-of-way in the case of unsignalized intersections with bending right-of-way without verification in practice. This is because the critical gaps for the same traffic movements differ depending on the rank of priority with different traffic situations and therefore, different gap-acceptance behavior of drivers.

While the traffic situation and priority rules are the same for the same movements at a standard four-leg intersection (e.g., minor-street through movements are of the same Rank 3), they are different for each individual inferior traffic stream at the specific four-leg intersection (the same movements are not of the same priority rank). It indicates that values of the critical gaps and the follow-up times should be determined for individual inferior traffic stream separately.

Acknowledgement

This contribution/publication is the result of the project implementation: **Centre of excellence for systems and services of intelligent transport II,** ITMS 26220120050 supported by the Research & Development Operational Programme funded by the ERDF.

References

[1] TP 102 Roads Capacity Calculation. Technical regulations (in Slovak) [online]. Ministry of Transport, Construction and Regional Development, Bratislava, 2015. Available: http://www.ssc.sk/files/documents/technicke-predpisy/tp2015/tp-16_2015.pdf.

[2] PETRU, J., KRIVDA, V., MAHDALOVA, I., SKVAIN, V.: Video Analysis of Conflict Situations at T-Intersection with Cranked Priority. Applied Mechanics and Materials, 719-720, 1000-1004, 2015. https://doi.org/10.4028/www.scientific.net/AMM.719-720.1000

[3] AMIN, H. J., MAURYA, A. K.: A Review of Critical Gap Estimation Approaches at Uncontrolled Intersection in Case of Heterogeneous Traffic Conditions. The Journal of Transport Literature, 9(3), 5-9, 2015. http://dx.doi.org/10.1590/2238-1031.jtl.v9n3a1

[4] BRILON, W., KONIG, R., TROUTBECK, R.: Useful Estimation Procedures for Critical Gaps. Proceedings of the 3rd International Symposium on Intersections without Traffic Signals, USA, 71-87, 1997.

[5] GUO, R.: Estimating Critical Gap of Roundabouts by Different Methods. Proceedings of the 6th Advanced Forum on Transportation of China, China, 84-89, 2010.

[6] VASCONCELOS, A. L. P, SECO, A. J. M. S, SILVA, A. M. C. B.: Comparison of Procedures to Estimate Critical Headways at Roundabouts. Promet - Traffic&Transportation, 25(1), 43-53, 2013. https://doi.org/10.7307/ptt.v25i1.1246

[7] RAFF, M. S., HART, J. W.: A Volume Warrant for Urban Stop Signs (cited in [4]). Eno Foundation for Highway Traffic Control, Saugatuck, Connecticut, 1950.

[8] TROUTBECK, R. J.: Estimating the Critical Acceptance Gap from Traffic Movements. Physical Infrastructure Center Research Report 92-5. Queensland University of Technology, Brisbane, Australia, 1992.

[9] WU, N.: A New Model for Estimating Critical Gap and its Distribution at Unsignalized Intersections Based on the Equilibrium of Probabilities. Proceedings of the 5rd International Symposium on Highway Capacity and Quality of Services, Japan, 2006.

Peter Havaj*

THE QUALITY AND THE COMPLETE EVIDENCE SECURING DURING THE TRAFFIC CRIME SCENE INVESTIGATION AND ITS RELEVANCE FOR EVIDENCE COMPLETION DURING THE TRAFFIC ACCIDENTS

Main purpose of this paper is to point out the problems considering the modern scientific usage of methods, ways and approaches, including the crime investigation of traffic accidents-collisions. We want to show the basic need of experienced traffic crime detective, his/her deep knowledge of the whole issue - the process of the traffic accident perpetrating as a complex process with the direct impact on the traffic crime detective work, which could be used in the process of the clearance the case, the video-record output created by program PC CRASH as the virtual element of legal evidence, enabling deeper knowledge of the whole process.

Keyword: *traffic accident-collision, crime scene investigation, error elimination, process of gaining the legal evidence*

1. Introduction

Traffic accident is an event in the traffic and it represents special, complex and undivided issue from the technical point of view and the next legal considerations. The results are derived directly from the quality and complete evidence securing, which represents crime scene investigation - as the specific method of criminal clearance, based on direct observation, exploring and evaluation of the material environment, its separate objects related to the criminal case with the main objective to clear the case, to seek and to secure the criminal evidence meant to serve as the prodigy to objective truth and to its perpetrator, as the basic need for detective´s next approach [1].

Basic tactical principles of the crime scene investigation (CSI):

- *crime scene investigation is managed by one leader* - CSI is a team work, including the work of police officers, detectives, tech-lab unit, specialists and other partake persons. This group has to set certain objectives and must take the professional responsibility for the whole process and its results.
- *CSI urgency* - it is derived from the time change of the specific criminological trails due to natural aging process and also due to external influence of the environment. The CSI urgently eliminates these changes or contamination of these criminal evidence.
- *CSI non-repeating* - the inadmissibility of the CSI recurrence of result from the fact that the probative crime evidence value could be easily objected in the court. The CSI repeating shows negligence and irresponsible approach. Value of the gained evidence during the repeated CSI is generally lower.
- *CSI cannot be substituted* - it is derived from the significant principle that emerges from the fact that the CSI is separate criminalist methods. Its results cannot be substituted by other means of observation and evaluation.

Traffic criminal scene investigation (TCSI) - meaning, methods, perspective research and error elimination

The TCSI is the first step to achieve adequate investigation efficiency as the final relevant and accurate legal consideration.

The basic principle of the TCSI is to collect facts, which have tactical and legal meaning. The TCSI includes methods and drills as the measuring, which provide the main conclusions.

Meaning of the TCSI is based on seeking, finding, identifying, securing of the criminal evidence or other trails, which have special meaning for identifying the traffic accident reasons.

The results of the TSCI are documented by:

- Photo-document collection or video record
- TSCI statement
- Sketch (graphical description) of the traffic accident site, which serves to prepare a final plan of the traffic accident site.

Within the theory of the forensic tactics, the TSCI uses basis methods of measuring and tracking the position on the crime scene. They can be divided into:

a. Direct methods, which are touchable and untouchable, touchable mean direct measuring by measuring tools and untouchable mean laser scanning, photogrametry etc.
b. Indirect methods (for example digitalization).

Important elements in space characteristic are:

- section shape of the accident road section and terrain
- lengthwise profile of the accident road section and terrain
- cross profile of the accident road section and terrain

2. Other elements that influence the quality of the TCSI result

Besides the equipment, the main predispositions of the high level quality of the TCSI are work experiences, knowledges and responsiblity of investigators. They have to recognize the crime

* **Peter Havaj**
University of Security Management in Kosice, Slovakia
E-mail: peter.havaj@vsbm.sk

evidence, they have to know where it can be found and how to secure and document it. It is necessary to understand, that the TSCI is not a simple act. The TSCI is carried out in different weather and environment conditions, the factor of time is also important. The quick and wise decisions during the TSCI is very important for next steps, on the other hand, an incorrect decision can significantly complicate further investigations. Inexperience and little knowledge of the detectives are the main reasons of spoiling or rather complete destruction of the evidence provided by the TCSI for the following legal process.

The TSCI often follows after the medical emergency or firefighter action. It contains rescuing persons from the damaged vehicle, emergency reviving of the victims, preventing of fire situation, gas loosing, contamination. These actions deteriorate the status of the next TSCI, for example victims are not in their original places, so the detecting of original location has to be done later.

Cleaning the road from the debris, cutting or moving cars could also change the traffic accident site.

Position changes, degradation of crime evidence and other clues, after the medical emergency or firefighter action, change the original status of the TCSI. It can complicate not only the TSCI but later analysis, as well. Minimizing the degradation process due to medical emergency or firefighter action can be realized by preliminary criminal photo collection carried out by rescue services.

3. Error elimination during archiving TCSI

The point of measuring (POM) is chosen by subjective stance of the detective and sometimes it is not specifically precise (beginning of the road curve). In such a case a possibility for great difference in the POM description could be created. Occasionally, the selected POM cannot be found in time, since the object was damaged or removed (e.g. a traffic sign). Problem of "close POM" forces detective to recognize the POM before and after the measuring, which can lead to wrong interpretations. The distant POM can be also a problem (several hundred meters), which decreases the precision of the later measuring. It is helpful to create auxiliary point of measuring (APOM), which is precisely localized with respect to the POM and other measurements can be drafted from this point. The localisation of the whole TCSI site should include the GPS, especially for accidents in the forest or field. Irreplaceable error eliminator is high level crime photo collection, which enables later additional photogrammetric identification of the evidence, that was previously neglected on site. The crime photo collection must be presented for the later process in electronic form with a HD, because the printed form cannot show the high level zoom and details.

The crime photo collection in the highlight quality (resolution 640x480) is not appropriate for photogrammetric examination. The crime photo-documentation must, in particular, show vehicle damage indetail and traces on them and other objects and enable to create the entire image of the accident site, individual shots have to follow. The TCSI also includes the cargo weight, pedestrian, bicycle and motorcycle rider weight and height. Those information should be a part of the medical report of the injured persons, as well as the strict localisation of the injuries (for example broken pedestrian leg focused from heel represents decisive point of the accident process). The TCSI also includes detection of fastening belts and airbags status as well as the status of the vehicle interior (seat deformation, broken and deformed parts of the interior).

Those facts are important for the next clearance, as well as the vehicle technical parameters. Special issue of the TCSI are traffic accidents during the bad weather and poor visibility (fog, snowing, heavy rain etc.), where localisation must be connected with the observatory description, because it is very important to distinguish for example unilluminated person or vehicle lights.

Public lights and their location, intensity and functionality in specific time are very important information for the whole legal process and its results. Error elimination also includes the position of possible unknown vehicle, which obstructed the view of the driver, but which already has left the TCSI. In that case, it is important to localise such a vehicle by statement of each witness. During the collisions of moving and standing vehicles is necessary to localise original position of the stationary vehicle before collision. It is important during the chain crashes.

The next removable imprecision is determination of lights condition at the time of traffic accidents, which can be determined at the time of detectives' arrival. It is obvious that light conditions during a certain day period can be changed within minutes (e.g. sunset) and this fact has to be also taken into account. In addition, the impact of lights of opposing vehicles has to be realistically evaluated, for example determination of the pedestrian, who was illuminated outside the range of the car lights. The crime photo collection of the car lights range and visibility is realized during the night time, without using photo flash or other source of light. It is necessary to point out the difficulty and complexity of the TCSI, which includes mistakes, errors and also necessity to eliminate them in all available ways, where for example could be included the detective's experiences, technical inventory and cooperation with emergency and firefighter units. The training of the traffic detectives should also include audit of quality of special tasks and activities during the TCSI.

Main tool that influences the effectiveness of the traffic accident investigation, is interrogation of participants and witnesses of the traffic accident. Its objectives are:

- clarification of the traffic accident, which was subjectively perceived and observed by the interrogating person.
- collecting other information that have significant influence on the traffic accident (cargo weight, personal motoric skills, height and injuries) from the witness' point of view
- activities of a witness during the crash accident (reaction, reaction after the crash - breaking, turning the wheel)
- finding the specific visual and acoustic perception of the witness ("I´ve seen")
- seeking the circumstances that might have influence on a traffic accident (illumination, covered driver's view, special objects)
- securing such subjective information from the interviewers, which can be confirmed by subsequent evidence or can be excluded
- finding everything

- securing special subjective information from the witness which can exclude intentional changes in later testimony in front of the court

For securing the quality and complete interview, an analysis of the mistakes in this process was created and, therefore, the PC program "Interrogation" was created, which provides that:

- asked questions will be according to the roster of the recommended questions
- it is possible to add questions into the roster according to the specific conditions of the road accident section and other local specifics
- it is possible to add questions based on detective´s experience.

Injuries and death of persons, as a result of the traffic accident, belong to the group of injuries characterized by specific signs and these signs are reflected in the process of documentation, evidence and legal considerations.

One of the signs is that the occurrence of injuries to road accident participants is usually directly related to the movement of vehicles that are complex technical equipment moving on the road (usually the road) and whose movement is fully subject to physical law. Vehicles during the collision leaves traces, they become deformed, they stop in final position, which is objectively documented, measured and detectable. If a vehicle crash does not involve injury and death, it can be considered as a technical problem [2].

Situation is different when the traffic accident involves human or pedestrians. Human has different parameters of movement from the technical point of view, he/she has different body properties, capability of movement, capability of speed change and geometrical shape (fall, inclination etc.). In that case, it is necessary to add the coroner - forensic surgeon considerations to technical considerations. Human body is always severely damaged, which reflects the collision and possible tracks. Forensic exploration then begins at the stage of measuring and documenting of the traces and then proceeds to assess the cause and the way they are generated [2].

The forensic surgeon examination is considered as a special action, which demands special preparation and competence. It is known that most of the MD´s are capable, but less capable in this concrete task. The problem is caused by the absence of technical knowledge resulting to the non complex evaluation or misinformation about the results of technical evidence.

This scientific paper brings a selected range of issues to expand the knowledge and aims which contribute to:

- clarify the possibilities for interdisciplinary procedures, both by technical analysts and by forensic practitioners
- to show value of the physical evidence found on the human body and its meaning during investigation from the specialist point of view and also from the detectives point of view, who coordinate the whole process
- to clarify the value of evidence found on the body and their counterfeit value by the courts for the purposes of legal assessment of the course of a traffic accident.

It is obvious that special forensic procedures and knowledge should be defined according to science discipline - biochemistry, which includes the main procedures.

4. Pedestrian injuries in traffic accident - criminal tracks and evidence

Pedestrian injuries caused by traffic accident can be evaluated by:

I. Legal examination

It is derived from the source of injury and final effect of definition needed for the TCSI, proving the guilt and measure of the caused damage for financial retribution of the affected persons.

II. Medical evaluation

It is derived from the possibility of diagnostics and the following healing process of injuries and from the principle of reducing the health consequences, as well as quantifying the extent of injury for the purpose of compensating the injured person.

III. Forensic surgeon examination

a. Approaches the assessment of injuries for subsequent legal proceedings in the context of an investigation of the facts
b. Evaluates the injuries for interdisciplinary evidence, measures the violence and its impact on the body of the injured, as well as the detailed localization of the places where the violence was inflicted on the body (system FORTIS).

Forensic surgeon examination can be divided into:

- assessing of injuries to persons who have not survived the traffic accident
- assessing of injuries to persons who have survived the traffic accident.

Observation of the injured body (OIB) can be considered as the part of the TSCI not realized on the place of traffic accident. It can be considered as later observation of the injured body (LOIB).

Output of the LOIB is crime photo collection, description and medical documentation.

The traffic accident is a unique action according to physics, unrepeatable system of phenomena, influenced by many factors, absolutely individual for each traffic accident. The best way to get clearance of the TSCI is usage of all available knowledge and relevant actions. Said simple, more information - better results [3].

Traces of victims and injured persons are integral part of an accident and are the main sources of information about its course - especially in the collision phase, and has to be a part of the accident analysis as well as expert evidence. Evaluated criminal traces by forensic surgeons are objectified, localised and parameterized for the traffic specialist. In some cases analysts send the information to forensic surgeons for assessment the circumstances that caused the injuries, [4].

Pedestrian injury can be considered as criminal evidence for the TSCI. For this purpose, the system FORTIS is created, which allows the forensic surgeon assessment to be used for the needs of the accident analysis as an equivalent to the other traces on the vehicle, the roadway or other objects. The evaluation of the FORTIS injury then represents de facto the forensic footprint sophisticated judiciary assessment (see the following definition of a trace from the point of view of general criminal activity). Using

the appropriate methods allows to include injuries occurring during traffic accident between the criminal evidence.

Criminal evidence is every change in material space of criminal relevant action, which can be related by causality, time or place and it can be findable and usable in the process of clearance.

Necessary condition - creation of the criminal evidence in causality with the criminal deed

Need of findability, seekability, securability and usability is derived from the practical need of change as how can criminal evidence be found, kept, distinguished.

Meaning and value of criminal evidence - the criminal trace is useful only in the case that it can be decoded and used. This can be done when one is possible to find, secure and examine the traces by technical means and method.

Each CSI evidence has its value [5]:

- **The criminological-tactical value** of criminal footprints is particularly applicable in assessing the way in which criminalistic relevant events are committed. **Tactical value** of the crime evidence is applied in considerations of the criminal ways of objects related to the TSCI. Information value of the crime evidence enables considering the circumstances of the origin, course and extinction of the relevant criminal events, causes and conditions that enabled it.
- **Technical value** of the crime evidence is related to the possibility of its finding, capturing and later examination
- **Legal value** of the crime evidence means that legally obtained crime evidence has a special place in the legal process and may have the value of proof in criminal proceedings under some conditions.

Evaluation of the person's injuries includes methods of forensic surgeon examination, classification and use for evidence.

Currently, one can divide classification, identification, as well as considerations of injuries as crime evidence, from the forensic point of view, into four basic evolution levels [6], [7]:

The 1st level

Typical examination exercised by descriptive way with the usage of minimal, almost none exact methods, based mostly on the specialist "experiences". The possibility of misconduct by forensic practitioners is mainly related to their technical ignorance of the actual course of the accident and the possibility of proving beyond "convincing" is none and relies primarily on the confidence in the knowledge of the forensic practitioner and the correctness of his judgment.

The 2nd level

Comparison connected with the simple modeling of the damaged body movement, or general consultation with tech specialist without closer explaining of the individual aspects of created injuries. The possibility of erroneous conclusions is partially eliminated, but produced evidence is based mostly on the expert's "experience and belief" and relies on the confidence in the knowledge of the forensic practitioner and on the correctness of his judicial assessment.

The 3rd level

Comparison connected to cooperation with the technical specialist in such a manner, that visually compares the process of the damaged body movement calculated in a simulation program (video calculation of collision).

Possibility of the forensic surgeon wrong results are mostly eliminated, but the crime evidence is still bound to the experience of the specialist, as well as the way of his calculations of the collision, where the exact knowledge about injuries is not used and the way of its creation.

The 4th level

A detailed description of the identified injuries and their localization by using documented traces (measurements, photo-documentation) and defining the findings in a standardized form applicable to a technical expert (e.g. the FORTIS system) as a description of the traces, which has to be taken into account in the calculation of collision and to document their compliance with the judgment finding followed by consultations of the forensic practitioner and technical expert and evaluation of the results of the video presented and review of the contact parameters. The possibility of false conclusions is virtually eliminated and this procedure leads to the fact that the obtained evidence has all the features of accuracy, completeness and controllability in relation to all found traces.

Crime evidence of the 4th level was repeatedly accepted from courts of justice in criminal and civil cases.

5. Forensic surgeon system for parameterization and localisation of injuries by FORTIS and its possibility for crime evidence usage

Nowadays, the forensic surgeon analysis for traffic accident injuries does not always follow a standard line, due to the absence of certain procedures for standardization of injuries.

The classic way of evaluation the injuries is a scale of Abbreviated Injury Scale/Injury Severity Score (hereinafter AIS/ISS) derived from medical considerations [8].

Other systems are GSI (Gadd System Index), HIC (Head Injury Consideration), 3MS, TTI (Chest Injury), VC (Soft Tissue dDamage), EIC (Broader Injuries). These parameterization systems do not provide sufficient information for the crime evidence standard, because they are derived from the effect of the injury, not the cause. Forensic surgeons recognize cause of the violence and divide it into low, medium, and high category (for example low speed of the vehicle) without closer specifications. It is also important to consider the fact that not all the damage to health of a pedestrian is a direct consequence of the degree of violence on his body during the collision and then the question arises if the death has been caused by the direct impact of the collision with the vehicle [4].

Mentioned deficiencies of existing status are solved by a modified system **FORTIS** (Forensic Traumatology Injury Scale), which enables a more comprehensive assessment of the severity in Fortis points (FP) injury and also distinguishes the causes of health damage in the following categories:

BI - basic injuries (direct impact of violence)

Co1 - direct post-traumatic complications (e.g. traumatic shock, hemorrhagic shock, cardiac tamponade, hemothorax, pneumothorax)

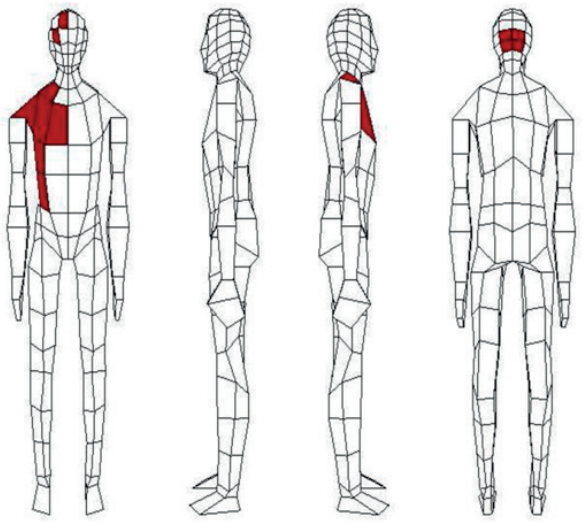

Figure 1 *Visualization of the FORTIS output for injury classification after a real traffic accident according to description X [11]*

Table 1 *Visualisation of FORTIS© - score FORTIS in BF output of every part of the injured body according to medical examination [11]*

	total	ZPZ	Ko1	Ko2
Hull	14.2	14.2	0	0
Pelvic bone	0	0	0	0
Right thigh	0	0	0	0
Right calf	0	0	0	0
Right foot	0	0	0	0
Left thigh	0	0	0	0
Left calf	0	0	0	0
Left foot	0	0	0	0
Left upper arm	0	0	0	0
Left forearm	0	0	0	0
Right upper arm	1	1	0	0
Right forearm	0	0	0	0
Neck	0	0	0	0
Head	7.6	7.6	0	0
Left knee	0	0	0	0
Right knee	0	0	0	0

FORTIS total ZPZ	22.8
FORTIS total Ko1	0
FORTIS total Ko2	0
FORTIS total	22.8

Co2 - associated complications (e.g. inflammatory changes, edema of non-traumatic etiology, thrombosis, conditions after surgery, etc.)

Methodology of parameter standardisation of the pedestrian injuries in traffic accidents (quantification of injuries) requires application of the self-modified system **FORTIS**, which enables (with high level input parameters) to calculate the severity of the underlying health damage, direct post-traumatic complications and associated complications, including more painful treatment and poor quality health care, and in the case of fatal injuries determines the health damage that is the direct cause of death [9].

Mentioned classification of the health damages can be considered significant in legal assessment.

According to the documentation and the TCSI it is ideal to use PC FORTIS, which was designed for easier drills. Except for patient data (age, weight, clothes, diagnosis description), it enables direct localisation the causes of the injuries by saved data.

5.1 PC Fortis in action

X - description of person's injuries [10]:

- bruises and bloody skin existing on the head, chest and abdomen
- *damaged abdomen (mentioned in medical documentation)*
- *serial bone fractures of the 3rd to 8th right ribs*
- *closed bone fracture of clavicula with removed part of the bone at the right*
- *damaged right lung,*
- *damaged brain core in the middle brain area (according to MRI)*
- *diffusional anoxal damage of the brain (according to MRI)*

5.2 Output of the FORTIS

Output of FORTIS is localisation of every injury (see description X), final point value, point value according to cause and creation of the injury and its location on the human body (Figure 1).

Detailed description score according to the FORTIS is compatible to the system PC CRASH, which calculates the physical parameters of the contacts and enable to distinguish the violence during the collision, which has affected individual parts of it, respectively recognizing the consequences of this violence on the pedestrian, which uses the physical parameters [9].

System Fortis represents practically usable tool for replacing medical terminology for the needs of experts and traffic accident analysts, with a description of the injuries expressed in a joint statement by their parameterization with sufficient counter value [8].

Program PC FORTIS can be considered as a guide line for specialist and detective practitioners. System FORTIS in parameterization of injuries enables the direct visualization of the injury display, as a significant information for the road traffic expert, and can be considered as an integral part of the solution of pedestrian injury parameterization. System also allows not only to visualize the location of the injuries but to create an individual characteristics of injury, as well (the ratio of violence acting on individual parts of the body according to its distribution according to the computational model in the PC Crash simulation program used for the accident analysis), for specific collisions and conditions, including o.i. the individual characteristics of the pedestrian's body, its position, movement, type of vehicle, its speed, dynamics at the moment of collision, etc. [9].

Detective must apply coordination of interdisciplinary evidence. Detective has clearly to understand the method of evidence, the value of their outcomes and the overall complexity and usability for the needs of the legal assessment.

The use of the FORTIS system for the needs of an accident analysis provide a procedure for the analysis of a forensic practitioner and a judicial expert, which aims to:

- judicial expert should have, before the whole analysis, forensic practitioner quantification and visual localisation of the injury
- Forensic practitioner should have technical analysis of data, for example video-records of collision between pedestrian and a vehicle, as well as physical parameters - without this documents he cannot prepare the analysis of the injuries and the whole TSCI comprehensively and qualitatively.

The idea of system FORTIS is based on necessity to use program from the first moment - first contact between patient and MD. It is reasonable to use this system for criminalistic methodology, as well as for documentation of a body injury.

6. Conclusion

Only skilled detective can use these methods, ways and approaches during the TCSI and that requires high knowledge of the whole issue.

Detectives should also use video-records of calculations, made in the PC Crash, as part of their accident investigation procedures. These, as "virtual elements" of evidence, enable a deeper understanding of the course of an accident beyond its verbal description. Combination of all the above mentioned facts allows a qualified assessment of the acquired knowledge and technical conclusions. The videos make it possible to "see and adopt" the casual course of an accident already as a whole, or even in the eyes of drivers, witnesses and other participants and provide the opportunity to realistically assess and judge the content of their testimonies, which creates the prerequisites for a good legal assessment of the case.

References

[1] HAVAJ P., MANDELIK J.: Criminalistic Procedures in the Process of Explaining Traffic Accidents (in Slovak). Proceedings Security in the Process of Globalization - Today and Tomorrow, Poland, 2013.

[2] MOSER, A., STEFAN, H., KASANICKY, G.: The Pedestrian Model in PC-Crash -The Introduction of a Multi Body System and its Validation. SAE TRANSACTIONS, 108, 794-802, 1999.

[3] BOBROV, N., MANDELIK, J., HAVAJ, P., RABEK, V., PIWOWARSKI, J.: Possibility of the Evaluation of Injuries of an Unbelted Passenger in a Vehicle and the Need for Special Procedures while Inspecting the Site of the Accident. Security Dimension, International & National Studies, 20, 132-164, 2016. https://doi.org/10.24356/SD/20/7

[4] MANDELIK, J.: Parameterization of pedestrian injuries and possibilities of its use in dealing with accidental (in Slovak). Dissertation thesis, University of Zilina, Institute of Judicial Engineering, 2006

[5] BOBROV, N., LONGAUER, F., MANDELIK, J.: Documentation of Fatal Road Traffic Injuries - A New Approach by FORTEST Method. Proceedings of XXth Congress of International Academy of Legal Medicine, Hungary, 2006.

[6] BOBROV, N., GINELIOVA, A., MANDELIK, J.: Trauma Injury Assessment with Survival (in Slovak). Final report of project VEGA No. 1/0428/11, 2013.

[7] BOBROV, N., GINELIOVA, A., MANDELIK, J., LONGAUER, F., MATYAS, T.: Assessing The Extent of Soft Tissue Damage in Polytrauma during Pedestrian Traffic Accidents (in Slovak). Folia Societatis Medicinae Legalis Slovacae, 2(1), 13 - 17, 2012.

[8] BOBROV, N., LONGAUER, F., SZABO, M., MANDELIK J., MANDELIKOVA, Z.: FORTIS Standardization of Traffic Injury Parameters in Forensic Medicine (in Slovak). Proceedings of scientific and professional works on the 80th anniversary of the founding of the L. Pasteur University Hospital in Kosice, Slovakia, 2004.

[9] HAVAJ, P., MANDELIK, J.: Selected Modern Methods for Solving Extraordinary Events in Road Transport (in Slovak). Monograph, Ostrowiec Swietokszyski, 2016. ISBN 978-83-64557-14-9

[10] BOBROV, N., MANDELIK, J.: Parametrization and Localization of Pedestrian Injuries by Using FORTIS System and Use of PC FORTIS. Soudni inzenyrstvi = Forensic engineering: casopis pro soudni znalectvi v technickych a ekonomickych oborech, 25(4), 227-234, 2014.

[11] BOBROV, N., MANDELIK, J., MACEJ, P.: PC Fortis program©.

COMMUNICATIONS – Scientific Letters of the University of Zilina
Author guidelines

1. Submitted papers must be unpublished and must not be currently under review for any other publication.
2. Submitted manuscripts should not exceed 8 pages including figures and graphs (in Microsoft WORD – format A4, Times Roman size 12, page margins 2.5 cm).
3. Manuscripts written in good English must include abstract and keywords also written in English. The abstract should not exceed 10 lines.
4. Submission should be sent by e-mail – as an attachment – to the following address: komunikacie@uniza.sk.
5. Uncommon abbreviations must be defined the first time they are used in the text.
6. Figures, graphs and diagrams, if not processed in Microsoft WORD, must be sent in electronic form (as JPG, GIF, TIF, TTF or BMP files) or drawn in high contrast on white paper. Photographs for publication must be either contrastive or on a slide.
7. The numbered reference citation within text should be enclosed in square brackets - in numerical order. The reference list should appear at the end of the article (in compliance with ISO 690).
8. The numbered figures and tables must be also included in the text.
9. The author's exact mailing address, full names, E-mail address, telephone or fax number, the name and address of the organization and workplace (also written in English) must be enclosed.
10. The editorial board will assess the submitted paper in its following session. If the manuscript is accepted for publication, it will be sent to peer review and language correction. After reviewing and incorporating the editor's comments, the final draft (before printing) will be sent to authors for final review and minor adjustments.

Errata: Communications – Scientific Letters of the University of Zilina, Vol. 20, No.2, 2018, „Application of a Priori and a Posteriori Estimate on Risk Assessment", pp. 56-61. The proper name of third author should be as follows:
Witalis Pellowski.

komunikácie
COMMUNICATIONS

VEDECKÉ LISTY ŽILINSKEJ UNIVERZITY
SCIENTIFIC LETTERS OF THE UNIVERSITY OF ZILINA
VOLUME 20 Issue 4

https://doi.org/10.26552/com.J.2018.4

Address of the editorial office:
University of Zilina
EDIS – Publishing House
Univerzitna 8215/1
010 26 Zilina
Slovakia

E-mail: komunikacie@uniza.sk

Individual issues of the journal can be found on:
http://www.uniza.sk/komunikacie

Each paper was reviewed by two reviewers.

Journal is excerpted in **SCOPUS, EBSCO** and **COMPENDEX**.

Published quarterly by University of Zilina in EDIS – Publishing House of University of Zilina

Registered No: EV 3672/09

ISSN (print version) 1335-4205
ISSN (online version) 2585-7878

ICO 00397 563

December 2018